Creation of Circumferential Tears in Ovine Lumbar Intervertebral Discs

by

Kurt van Ryswyk

Thesis

Submitted to Flinders University

for the degrees of

Bachelor of Engineering (Mechanical) (Honours),

Master of Engineering (Biomedical)

College of Science and Engineering

Accepted November 6th 2019

Table of Contents

Table of Figures and Tables

GLOSSARY

Aetiopathogenesis	The cause and/or development of a disease or abnormal condition
AF	Annulus Fibrosus
CI	Confidence Interval
CT	Computer Tomography (imaging)
DALY	Disability Adjusted Life Years. The combination of years of life lost (YLL) due to premature mortality, and years lived with disability (YLD).
GAGs	Glycosaminoglycans
GBD	Global Burden of Disease
ILM	Inter-lamellar Matrix
IVD	Inter-Vertebral Disc
LBP	Low Back Pain
MRI	Magnetic Resonance Imaging
Natural Life	the expected span of a persons life or under normal circumstances.
NP	Nucleus Pulposus
Ovine	Of, or related to, sheep
PGs	Proteoglycans
PL	Posterolateral
SEM	Scanning Electron Microscope
Sequelae	a condition which is the consequence of a previous disease or injury.
Silent Nociceptors	Pain receptors that only become sensitised following damage or inflammation
YLD	Years of Life Lived with Disability
YLL	Years of Life Lost (to premature mortality)

Declaration

I hereby declare that this thesis is my own and that; to the best of my knowledge and belief, it contains no material previously produced by another party for a degree or diploma in any university, and that to the best of my knowledge and belief it does not contain any material previously published by another person except where reference is made.

Kurt van Ryswyk

Abstract

Low back pain is a cause of significant impairment, reduced quality of life, lost productivity, and direct medical costs in the global population. Low back pain is strongly correlated to herniation of lumbar intervertebral discs (IVDs) which is also related to disc degeneration and to circumferential tears in the Annulus Fibrosus (AF). The study of annular circumferential tears would be very useful for future spinal research but such studies but have been limited in scope due to the difficulties of inducing such tears in healthy IVDs and the confounding factors involved in studying degenerated IVDs.

The purpose of this project was to develop a low-cost method, capable of reliably creating inner annular delaminations in IVDs. High-pressure fluid injection was selected as the most promising method to induce delaminations. A simple injector device was developed using a syringe adaptor to a commonly available pneumatic fluid dispenser with time control. To test the effectiveness of the injection device, ninety-seven IVDs were harvested from forty-three stored sheep spines, hydrated under a physiological preload, and injected in the anterior annular region

Circumferential delaminations were successfully induced at pressures between 413 and 690 kPa (60 to 100 psi) with a mean success rate of 56%, and a maximum success rate of 86% for 80 psi injections. An analysis of variance (ANOVA) was carried out, but results were highly variable. It was shown that there was a marginally significant relationship between injection duration and delamination length ($P < 0.1$), but no significance was shown for injection pressure vs delamination despite supporting trends.

This study was exploratory and had several challenges and limitations. Spines recruited for the study were mostly specimens rejected from other projects. As such many were smaller discs or came from spines which included some damaged discs and variation in disc quality was inevitable. The injection method was been shown to be successful but highly varied in results. Future work would include performing a study with specimens of uniform age and quality to more accurately establish optimal injection parameters.

Acknowledgements

I hereby express thanks to my supervisor Associate Professor John Costi whose patience and support has made this project possible. I express appreciation for Micheal Russo whose camaraderie and cheerful support, feedback, assistance and advice has been pivotal to success. I would also like to acknowledge Damien Kleiss in Engineering Services, who made key suggestions and insight.

On a personal note, words can not express the importance of the support from my friends and teammates from Flinders Automotive Solar Team, Dr Stuart Wildy and Jade Wildy.

Chapter 1 Introduction

This project builds on from the work of a prior student, Brodie Peek (2016) and of Fazzalari et al. (2001), who used both pressurized injections to create annular circumferential tears in ovine spinal segments. Investigation into intervertebral disc (IVD) injuries is important due to the high prevalence of Lower Back Pain(LBP) in society, and the associated costs and disability. Back pain is a widespread global problem that is a burden for both the sufferers and for society as a whole. The injuries and damage that cause low back pain occur in the soft tissue of the intervertebral disc and accumulate with age, but can occur at any age and may be associated with a range of activities, occupations and physical insults. As a result of the prevalence of LBP, there is a lot of work in the medical science and engineering community investigating the nature and mechanisms of injuries to intervertebral discs. A better understanding of injuries and soft tissue damage within the intervertebral disc is likely to provide a scientific background for treatments, medical procedures, recovery and rehabilitation guidelines, safety standards, and occupational liabilities.

The IVD, the largest avascular organ in the human body, acts to transmit and distribute stresses between neighbouring vertebral bodies while providing a flexible joint. The IVD is composed of a gel-like inner called the Nucleus Pulposus (NP) and the tough outer called the Annulus Fibrosus (AF). The AF is composed of layers of tightly aligned collagen type I fibres. When pressure is applied to the IVD through the vertebral bodies, the NP is compressed against the AF. As such the ability of the IVD to support a load is dependent on the ability of the AF to contain the pressure of the NP. Failure of an IVD normally involves egress of the NP through the AF as a disc herniation.

Key to the understanding of IVD injuries are tears of the AF, which may include radial tears, rim lesions, and circumferential tears. Circumferential tears are by far the most common form of annular tear and are strongly correlated to disc degeneration and the initiation of other tears. Circumferential tears are disc damage related to separations or delamination between the lamellae, extending along the lamellar boundary rather than through the AF. They occur in the inner AF, primarily in the posterior-lateral (PL) region where annular stress is greater.

Herniations have been shown to develop with the progressive occurrence of circumferential tears through the thickness of the AF until the AF suffers structural failure.

The purpose of this project was to induce circumferential delaminations in the inner annulus. It is challenging to induce a circumferential tear for research study purposes. It is important to leave the outer annulus intact while accessing the inner annulus. This should leave the IVD intact with largely unchanged properties so that any changes can be attributed to the induced circumferential tear. The scope of this project is to develop a device or technique with which to induce delaminations. Examination of the properties of circumferential tears was in the scope of future work.

This thesis begins with a review of relevant literature. This is followed with discussion of the design decisions in developing the injection device, and analysis of the experimental results.

Chapter 2 Literature Review

Low Back Pain

Multiple studies have shown that Low Back Pain (LBP) is one of the most common health problems afflictions, affecting some 85% of people in their lives (Tymecka-Woszczerowicz et al., 2015). Interestingly, LBP is a globally important issue, having a similar profile of prevalence and burden across cultures and regions. LBP was shown to be the single greatest contributor to global disability, measured by Years of Life Lived with Disability (YLDs), and 6th globally for total disability, measured in Disability Adjusted Life Years (DALY). (Dario et al., 2015; Hoy et al., 2014; Vos et al., 2017, 2012). The age group most affected by LBP is ages 65-79, with a drastic increase in effect after the age of 35. LBP is a disease with a long period of effect, imposing losses on productivity, quality of life, and financial burden over the course of the subject's natural life. LBP prevalence is estimated at 9.4% in the 2010 Global Burden of Disease (GBD) study (Dario et al., 2015; Hoy et al., 2014). The GBD study 1990-2015 showed that Lower Back pain increased in prevalence by 18.7% from 2005 to 2015. This was associated with an increase of 18.6% in YLDs (Hurwitz et al., 2018), which highlights both the escalating nature of the problem and the need for further research into causes of LBP.

2.2 Anatomy

The human spine provides structural load support for the body superior to the pelvis, while allowing flexibility and movement, as well as protectively encasing the spinal column. “The human spine has 7 cervical, 12 thoracic, 5 lumbar, and 5 fused sacral vertebrae." (Walker et al., 2008). The vertebrae are stacked in a column, 29 high and separated by IVDs, as can be seen in Figure 2-1.

Figure 2-1, The human spine and the lordotic curve, with lumber region in grey (Bogduk, 1997)

2.2.1 Vertebral Bodies

Each vertebra has three primary elements, the vertebral body, posterior elements, and pedicles. Vertebrae and IVDs interface to each other via the vertebral endplates, a layer of hyaline cartilage 0.6-1 mm thick. (Bogduk, 1997; Walker et al., 2008). Hence this is also where forces experienced by the vertebrae are transmitted to the IVDs.

The vertebral body (VB) is separated from the posterior elements via bony processes called the pedicles, leaving a vertical void in the mid-section of the vertebra. When the vertebrae are stacked as a complete spinal column, these voids align to form the vertebral canal. The spine and body are generally are innervated from the spinal cord, running down the vertebral canal., as can be seen in Figure 2-2 (Urban and Roberts, 2003).

The posterior elements are bony processes on the posterior of each vertebra. These include the Transverse Processes, Spinous Processes, Superior Articular Process, and Inferior Articular Processes, which collectively provide attachment points for back muscles, ligament and tendons. The superior and inferior articular processes make it possible for the spine as a whole to articulate. The inferior articular process of the one vertebra interfaces to the superior

articular processes of the next inferior vertebra via a typical synovial joint, the zygapophysial joints, providing resistance to lateral shear forces.

Figure 2-2, a spinal segement, showing the NP, AF, vertebral bodies (VB), the cartilaginous end-plate (CEP). spinal cord (SC), the nerve root (NR), and the apophyseal joints (AJ). (Urban and Roberts, 2003)

2.2.2 Intervertebral Discs

IVDs provide a tough flexible connection between neighbouring vertebral bodies, facilitating movement, and transmitting load between vertebrae (Walker et al., 2008). The IVD is composed of an outer ring called the AF, and a gel-like centre called the Nucleus Pulposus (NP). Human IVDs are 7-10 mm thick and approx. 4cm in diameter in the lumbar region (Walker et al., 2008).

IVDs are primarily composed of the gel-like water holding NP at the core, the tough AF, which surrounds and contains the NP, and the sandwiching bony endplates of the neighbouring vertebrae. IVDs do not receive a blood supply and are the largest avascular organs in the human body. Instead, IVDs are supplied with nutrients via diffusion. (Urban et al., 2004) This means that following an injury, IVDs are slow to heal, and tend to accumulate damage and degeneration over time.

2.2.2.1 Nucleus Pulposus

The NP exhibits viscoelastic properties (Iatridis et al., 1996) which depends on its water content, hence the primary function of the NP is its ability to hold water. It has been shown that an unloaded IVD will absorb water, while an IVD under sufficient load to overcome its osmotic gradient will lose water (Urban and Maroudas, 1981). The NP is composed of Type II collagen and proteoglycans (PGs). PGs comprise approximately 65% of the NP's dry weight, while type II

collagen is about 20% of the NPs dry weight. The central NP contains a matrix of randomly arranged collagen fibres, and radially arranged elastin fibres (Walker et al., 2008). This matrix is embedded in a PG rich gel, called aggrecan. The aggrecan maintains the hydration level of the NP through osmotic pressure (Walker et al., 2008). The Collagen provides a structural matrix, holding in the proteoglycans. The proteoglycans create an osmotic gradient that forces water molecules into the NP. When properly hydrated the NP will be composed of 70-90% water. The water held in the NP is therefore dependent on the balance of hydrophilic osmotic forces drawing water into the NP, and the compressive load squeezing water out of the NP. When compressed, the NP exerts force radially outward, redistributing stress to the AF.

2.2.2.2 Annulus Fibrosus

The AF is a tough outer ring around the circumference of the IVD, comprised of 15-25 concentrically arranged 'lamellae' (Walker et al., 2008). Each lamella is comprised of bundles of highly organised parallel type I collagen fibres, forming a connection between the vertebral endplates (Walker et al., 2008). In each lamella, the fibre direction is highly uniform and angled 65-70° from vertical. The angle direction of the collagen bundles is offset from neighbouring lamella in an alternating fashion, providing the AF high strength 'cross-ply effect', in circumferential directions (Bogduk, 1997). The outer annulus is innervated with silent nociceptors, pain receptors that only become responsive following injury and/or inflammation of the tissue (Botwin et al., 2005).

It should also be noted that while the AF forms a complete ring around the NP, not every lamella completely circles the NP. As the AF varies in thickness, lamella may be terminated where the AF narrows. This is particularly true where the AF becomes thinner in the PL region "In any given quadrant of the annulus, 40% of the lamella are incomplete. In the PL quadrant, some 50% are incomplete." (Bogduk, 1997). It is logical to consider that these discontinuities in the lamella may be a contributing factor to the progression of delaminations, and may help to explain why circumferential tears are far more common in the PL region.

2.2.2.3 The Interlamellar Matrix

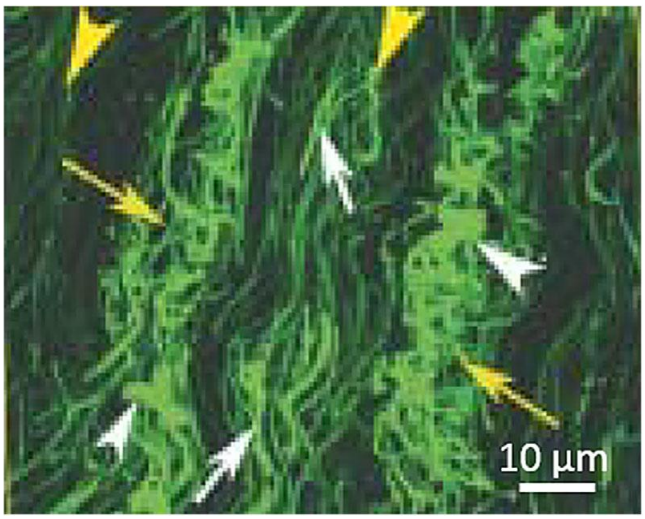

Figure 2-3, , The intra- and inter-lamellar space showing elastic fibre structure in the outer AF of a human L3/L4 disc. Arrowheads show the ILM space including thicker elastin fibres in a coil-like structure. (Tavakoli et al., 2016)

Neighbouring lamellae interface to each other via an interlamellar matrix (ILM). This interface is largely composed of elastic fibres in a well organised orthotropic network. Elastic fibres in the ILM interface tended to form a loose network, composed of larger parallel fibres, interconnected via 'smaller very fine elastic fibres' as can be seen in Figure 2-3 (Tavakoli et al., 2018). The ILM itself is less than 30 µm thick, or 1/8 the thickness of a single lamella (Tavakoli et al., 2016). The ILM is composed primarily of elastic fibres, but also includes type IV collagen fibres, glycoproteins, and ground matrix. The elastic fibres occupy only 2% of the weight fraction of the ILM, but 10% by volume. The non-fibrillar matrix in this region is mostly water, and rich in PGs, including lubricin, aggrecan, GAGs, decorine, biglycan, perlecan, and versican. These PGs provide the interlamellar region with lubrication and hydration (Tavakoli et al., 2016). The ILM exhibits 33% greater peel strength in the outer AF compared to the inner AF, with the result that delaminations are more likely to originate in the inner AF (Gregory et al., 2012).

2.2.3 Vertebral Endplates

The vertebral endplates are the interface between the vertebral bodies and the IVD. The endplates perform the function of fixing the IVD to the vertebral bodies, and of transmitting force between the IVD and the VBs. While technically part of both the VB and the IVD, the endplates are widely discussed as a component of the IVD (Bogduk 1997, p16). The endplate is composed of a layer of hyaline cartilage 0.6-1 mm thick. Degeneration of the endplates is a major indicator of the disc degeneration.

2.3 Disc Degeneration

Figure 2-4 Normal vs a highly degraded IVD (Urban and Roberts, 2003)

In general, the IVD is the tissue in the human body with the earliest onset of degradation (Urban and Roberts, 2003). This can cause a wide range of symptoms. The degeneration process of the intervertebral discs is associated with disc dehydration and desiccation of the nucleus. This process is typically asymptomatic (Walker et al., 2008). "DDD is not necessarily painful and even then, the pain may be variable" (Buenaventura et al., 2007). Correlations have also been found between early-onset DDD, and obesity (Dario et al., 2015).

Early changes related to DDD start in the central NP. Fragmentation of the NPs collagen matrix leads to a loss of PGs and a reduction in hydration level. Degeneration of the endplates accelerates the loss of PGs, further reducing IVD hydration (Walker et al., 2008). A reduction in fluid weight of 10% is correlated to the difference between a healthy IVD and a degraded one (Costi et al., 2002)

2.3.1 IVD Tears

There are three primary types of tear affecting IVDs. Radial tears, concentric or circumferential tears, and transverse tears, also known as rim lesions (Botwin et al., 2005; Vernon-Roberts et al., 2007). Examples of these tear types are presented in Figure 2-5.

A study of human cadaver spine segments (T12-L1), categorised anomalies and found that concentric tears were the most common with an incidence of 74%, compared to radiating tears and rim lesions each with an incidence of 47%. In this study circumferential tears were found to

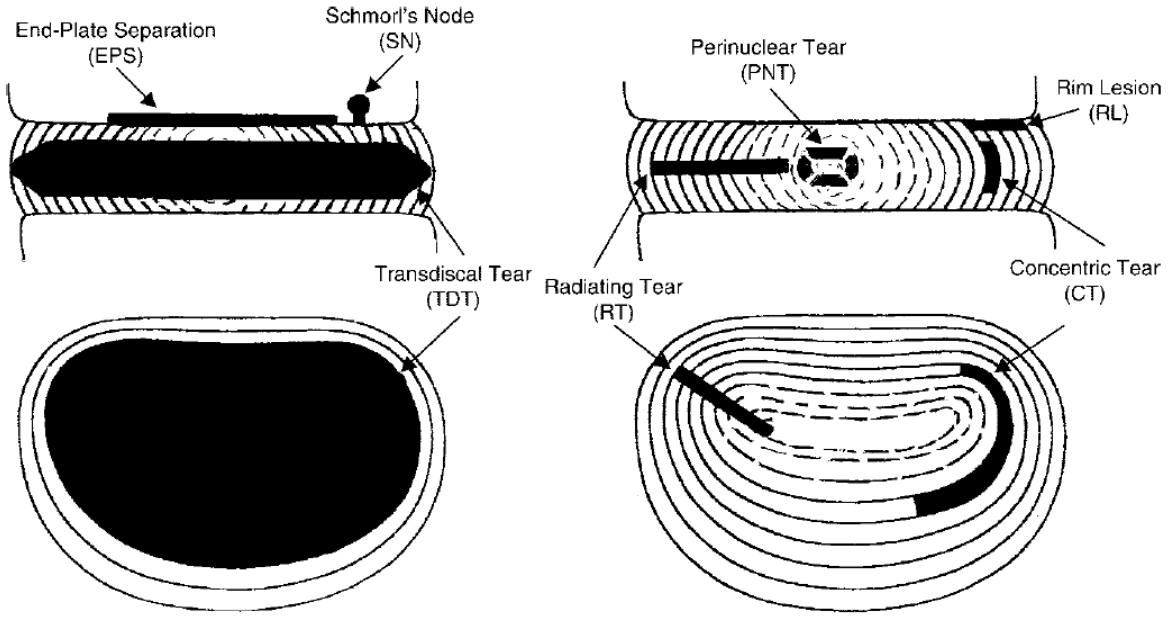

Figure 2-5, Types of annular tear, (Vernon-Roberts et al., 2007)

occur more often in the anterior lateral region and less commonly in the posterolateral region. It was shown that radiating tears did not correlate to propagation of the nucleus material into clefts in the annulus. No correlation was found between the different types of IVD tear but concentric tears were strongly correlated to disc with 10% or more of the AF delaminated. (Vernon-Roberts et al., 1997). A subsequent survey of human L4 -L5 spinal segments by the same authors found that there was a high incidence of tears in specimens below the age of 30 and that concentric tears consistently appeared at younger ages than other tear types(Vernon-Roberts et al., 2007). This indicates that concentric tears have a causal relationship with other subsequent tear types. It was also found that annular tears correlated to the development of vascular tissue and pain-related innervation of the annulus.

Osti et al (1990) performed a study with surgically created radial tears, 2/3 into the AF on live ovine models. The sheep were then left alive to be selected, culled and studied at periodic intervals. This resulted in concentric clefts in the AF, progressive disc (Osti et al., 1990) degeneration and nuclear degeneration after 18 months. (Osti et al., 1990). These results were later confirmed in FEA studies (Natarajaan, 1994). A study by Moore et al (1994) demonstrated that lesioned IVDs would experience disc degeneration even if they were immobilised.

2.3.2 Mechanisms of Degeneration

Iatridis and ap Gwynn (2004) used Scanning Electron Microscope (SEM) data from caudal rat IVDs using lamination theory. It was found that interlaminar shear stress was large, ranging from 0.4 – 1 MPa and that interlaminar stress would increase correlated to lamella layer thickness (Iatridis and ap Gwynn, 2004). It was noted that thickening of the lamella was also associated with disc degeneration, and is hence another variable that correlates to delamination (Iatridis and ap Gwynn, 2004). Iatridis also found that "delaminations near a focal disruption or existing tears in the annulus are likely implicated in annulus damage associated with circumferential tears while propagation of fibre breaks was considered a likely failure mode associated with radial tears under extreme loading conditions or when collagen damage occurs over a reasonably large region as may occur with biological degradation." This study showed that thanks to the composite nature of the AF and the IVD, failure required multiple failure mechanisms to occur at the same time and that multiple cracks and micro failures are required prior to the failure of the macro-structure (Iatridis and ap Gwynn, 2004).

Schollum et al. (2008) performed an optical study of the anterior AF of ovine IVDs, revealing a complex bridging structure within the interlamellar space.

Tavakoli et al. (2018) performed a study with ovine specimens investigating the effects of herniation on the biomechanical properties of the ILM. In the Tavakoli study FSUs

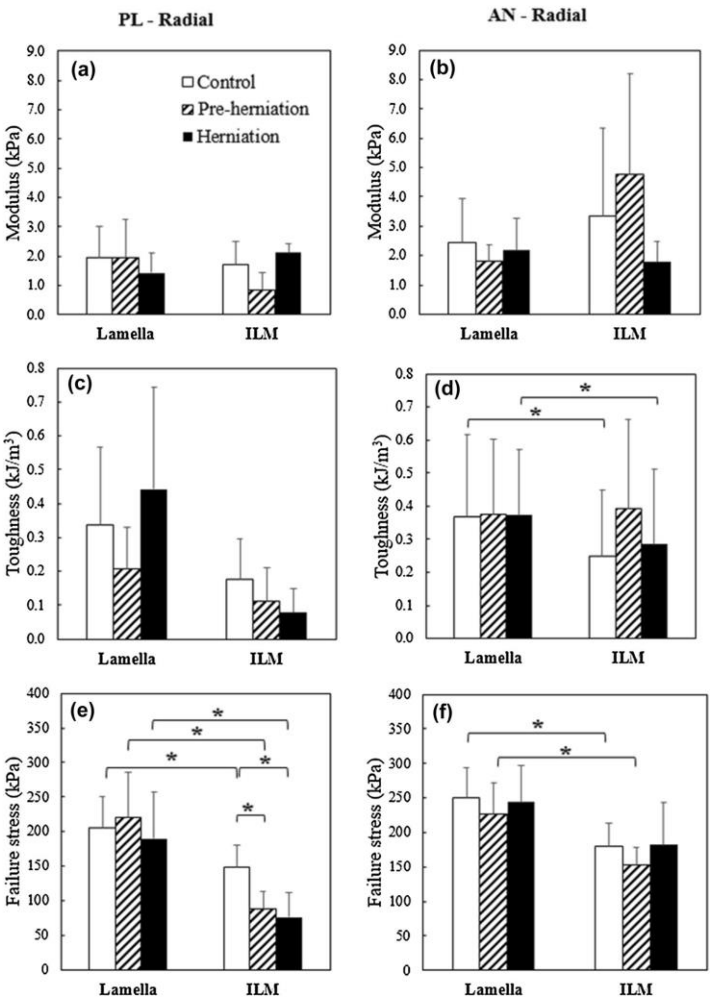

Figure 2-6 Ovine ILM vs lamella mechanical property testing result means (95% CI)(Tavakoli et al., 2018)

were assigned to groups to undergo herniation (via a 3 mm compressive displacement), pre-herniation (via a 1.5 mm compressive displacement) or control (hydration and overnight loading only). Following the compressive insult to the IVDs, specimens representing either single lamellae or a dual lamellae layer were extracted for micro-mechanical testing and microscopic examination. It was found that ILM failure stress was significantly reduced during pre-herniation, but not during herniation itself. This result provided evidence that the threshold for ILM damage is significantly lower than that required to cause a herniation (Tavakoli et al., 2018), as is shown in Figure 2-6 section (e) for the posterolateral region. Interestingly this effect was not noted in the anterior region, shown in section (f) of Figure 2-6. By contrast, the lamella showed no significant reduction in failure stress due to herniation or pre-herniation. This study provides a strong indication that the ILM is an important region of interest for the progression of DDD. This study also showed that pre-herniation caused significant widening of the lamella, caused structural changes including disorganisation of fibre direction in the lamellae, and caused loss of distinction of the Lamellar/ILM boundary, as is shown in Figure 2-7.

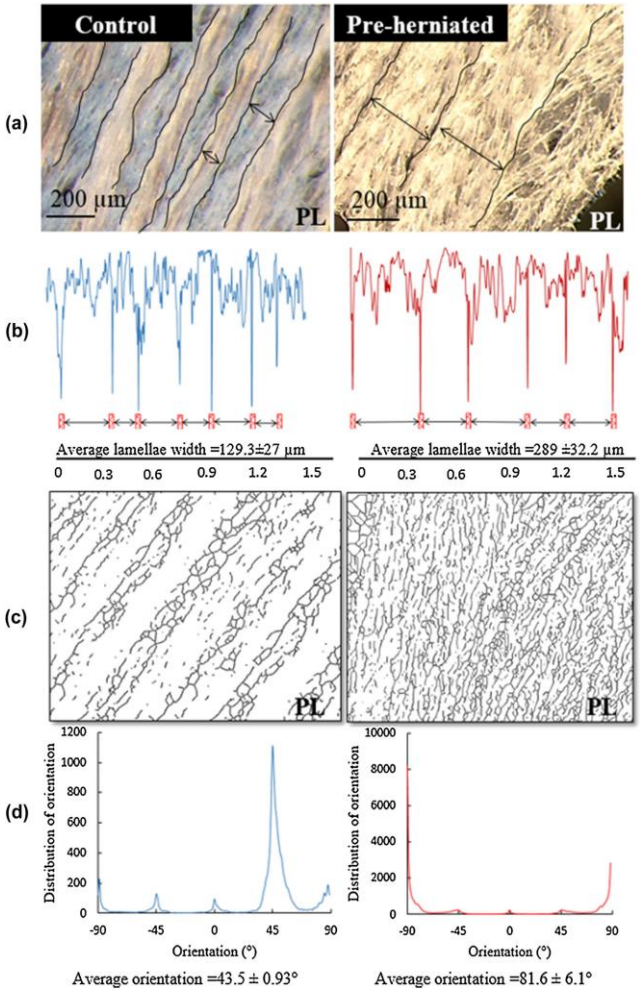

Figure 2-7,Light microscopy images (a) and surface profile plots (b) comparing a control and pre-herniated sample in the outer posterolateral (PL) (Tavakoli et al., 2018)

A study was carried out on ovine IVD, performing injections into the NP through the vertebral endplate until failure of the unconstrained motion segment occurred (Veres et al., 2008). This study showed that even without loads applied, the posterior region was most vulnerable to

failure and suggested that this is due to mechanical factors rather than tissue degeneration. It was also found that intra-lamellar connections tended to fail rather than bridging in the ILM.

Veres et al. (2010) performed a study on ovine IVDs, testing the role of flexion and torsion on IVD with high internal pressure. IVDs were injected into the NP through the vertebral endplate, result in seventeen vertebral failures and eight IVD herniations out of twenty-five tests. It was found both flexion and torsion would reduce the disc walls ability to withstand stress, and that herniation resulting from NP pressurisation tends to result from radial tears.

2.4 Needle Stick Injuries

As this project involves a needle insertions, a review of needle stick injuries to the IVD is of interest.

2.4.1 Discography

An important example of injuries to IVDs via needle penetration is discography, a controversial provocative technique developed by Hirsh in 1948 (Botwin et al., 2005; Cuellar et al., 2016; Tomecek et al., 2002). While it is possible to use non-invasive techniques to diagnose damaged IVDs and DDD, the correlation of such damage to LBP is not clear at all. A damaged or degraded disc may be asymptomatic, and there may be no way to ascertain if a damaged disc is the source of a subjects pain (Buenaventura et al., 2007). Lumbar discography involves puncturing a disc to inject contrast. This allows measurements of pressure in the NP, the pressure required to inject dye, the volume injected, the pressure end-point where the injection ceases due to equalisation of pressure, and the rate at which the pressure bleeds off after an injection. All of these measures may be used to infer disc integrity (Tomecek et al., 2002). The pressure in injection also directly stimulates the disc, provoking the patient's pain response and allowing it to be correlated to particular discs and injected contrast dye may also be of utility with subsequent medical imaging (Tomecek et al., 2002), as is shown in Figure 2-8.

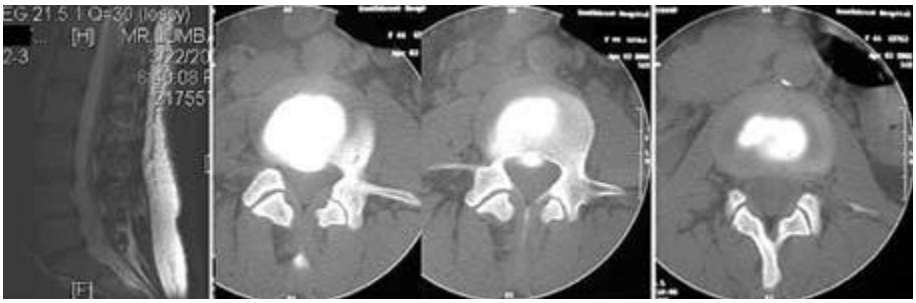

Figure 2-8, Medical imaging from discography.

Left: Sagittal MR image demonstrating a significant collapse of L4–5 and L5–S1 intervertebral discs with degenerative changes of the endplates. Centre: Post-discography CT scan of L3–4 revealing annular tears and internal disc disruption. Right: Post-discography CT scan demonstrating a normal (L2–3) disc. (Tomecek et al., 2002)

A matched cohort study by Carragee et al (2009) compared 75 discography patients to 75 controls over 10 years. After 5 years, reviewers found that the risk of negative outcomes caused by discography procedures was strongly correlated to abnormal combinations of symptoms and radiological results (Tomecek et al., 2002). However, reviews of the data at the 10th year follow up found the discography patients had significant increases in negative outcomes including additional lumbar surgeries, additional MRI and CT imaging, LBP events, LBP related disability, and LBP related medical visits (Cuellar et al., 2016), as is shown in Figure 2-9 and Figure 2-10. It was also found that IVD subjected to discography had significantly greater loss of IVD height(Carragee et al., 2009), an indicator of more advanced DDD compared to control. Studies of discography patient outcomes highlighted concerns that puncture of IVDs may not be as safe as had previously been assumed. Interestingly, both 22G and 25G needles were used in the Carragee study, and even small gauge needles appeared to accelerate DDD (Carragee et al., 2009).

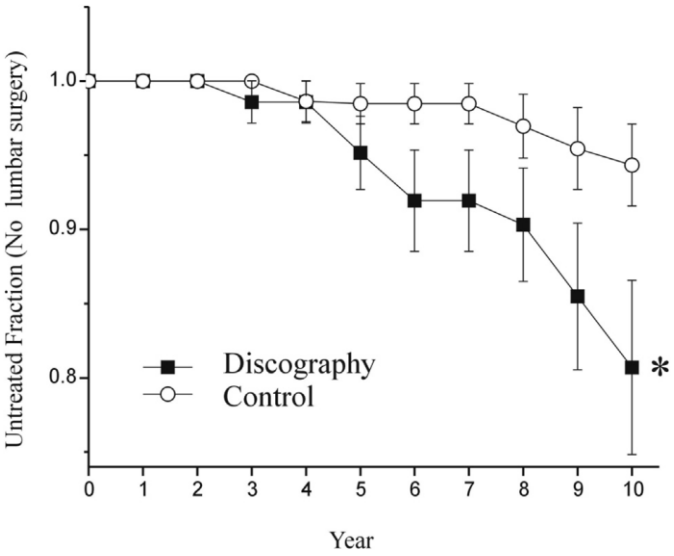

Figure 2-9,The surgery-free survivorship of the discography group vs control cohorts. (Cuellar et al., 2016)

2.4.2 Needlestick Investigations

In 2001 Fazzalari performed a study investigating the effects of circumferential tears on live ovine models. Circumferential tears were induced in the mid-lateral anterior region via 690 kPa saline injection, held for 1 minute. Positive control group discs were treated with a 27 gauge needlestick only, while negative control group discs were completely uninjured (Fazzalari et al., 2001). The study did not induce significant DDD, with no disc progressing beyond grade III (loss of distinction between AF and NP), according to the protocol used by Hansson and Roos (1981). The Fazzalari study did show that delaminations would cause changes in IVD mechanical properties, including significant reductions in disc stiffness compared to negative controls as is shown in Figure 2-11. Figure 2-11 also shows that there was no significant difference between the positive control needle stick group. This study also showed that a needle stick injury alone could accelerate disc degeneration and cause permanent damage, even with a small 27-gauge needle (Fazzalari et al., 2001). Figure 2-12 shows that there were no significant changes in disc grade for different levels of IVD. This supports the idea that tendency to create a concentric tear may not be related to disc level. It was also noted that accurate needle placement was a common issue with small 27G needles.

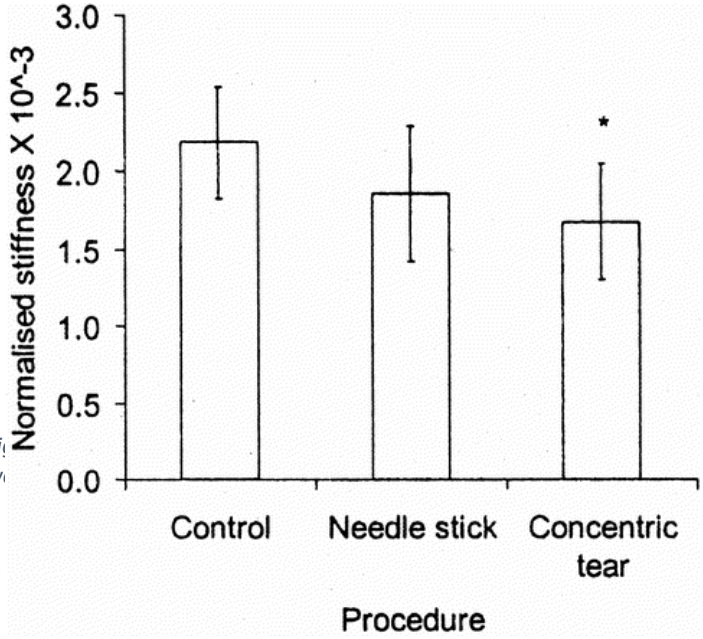

Figure 2-11, Changes in disc stiffness for concentric tears and controls, (Fazzalari et al., 2001)

Korecki et al. (2008) examined the effect of needle punctures on the mechanical properties of bovine caudal IVDs over a period of 6 days. IVDs were posterolaterally punctured and kept in an organ culture for 6 days with a daily compression protocol. This study showed that both large 14G and small 25G needles caused similar mechanical and biological changes in the IVD and

that these changes were due to the needle stick alone. There were no significant differences between large and small needle groups.

Elliott et al. (2008) investigated the effects of needle diameter on changes to IVD properties following saline injections into both rat caudal IVDs and ovine IVDs, and performed a review of studies involving IVD punctures into rat, rabbit, dog, mini-pig, and ovine IVDs. For needle diameters from 25 – 40% of disc height only minor nonsignificant changes to disc mechanical properties were observed. For needle diameter/disc height ratios greater than 40% significant mechanical changes occurred including reduction of internal disc pressure and loss of stiffness.

Martin et al (2013) had similar findings comparing the effects of IVD punctures on an in-vivo mouse model with both large (26G) and small (29G) needles. Martin et al. showed that the large needle puncture caused significant and permanent mechanical changes to the IVD including loss of disc height, NP glycosaminoglycan content reduction, and NP collagen content reduction. Punctures with the small needle did not show significant change. the small needle did not demonstrate a significant change.

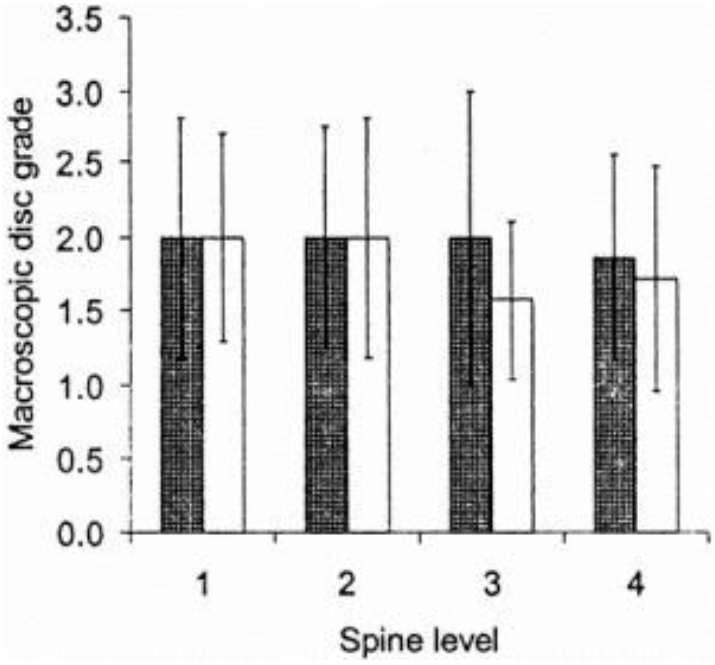

Figure 2-12, Effect by disc level for concentric tears (black) and needle stick (white), (Fazzalari et al., 2001)

2.5 Animal Models

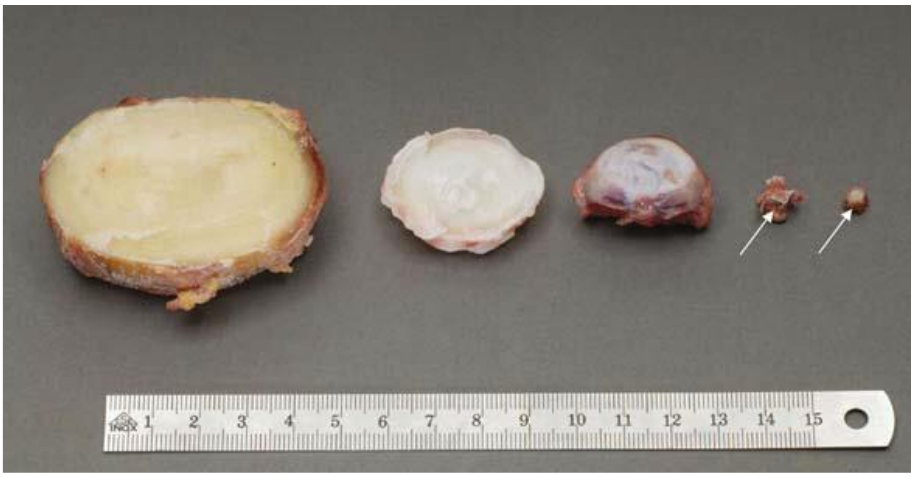

Figure 2-13, Relative sizes of spinal discs from (left to right) human L4-L5, bovine tail C1-C2, ovine thoracic T11-T12, rat lumbar, rat tail, (Alini et al., 2008)

When studies are conducted on a disease or injury that affects humans, from a scientific standpoint it is preferable to be able to study human tissue or human functional units. This allows the researcher to minimize assumptions regarding subtle but complex differences in geometry, biology, structure, and mechanical or material properties. However, acquiring human specimens for in vitro testing is difficult, expensive, and can present additional scientific challenges (Wilke et al., 1997). There is also a significant amount of work and time that must be devoted to acquiring ethics approval for the intended study.

It may also be a challenge to find available human specimens that are normal, i.e. without injury, excessive age or other pathology that may act as confounding factors for biomechanical testing. Even without excessive pathology being present, human samples tend to have widely biological variability, particularly in terms of bone density and quality (Ashman et al., 1989). This variability can mean that an otherwise simple study will require a large number of specimens to "overcome the wide scattering effect associated with biological variability" (Wilke et al., 1997).

In order to overcome the difficulties and costs associated with the use of human tissue in testing, it is common to use animal models. Use of animal models requires a close understanding of the differences in the form, functions and biology between the animal and human tissue in order to identify any potential confounding factors.

The first and most obvious difference to consider is geometry. This is practical, as it may be physically difficult to perform a required procedure on a very small disc or vertebral body, such

as is shown by the very small rat discs in Figure 2-13. It is also important to consider relevant geometry within a particular model. As a result of load distribution in a bipedal human, the diameter and cross-sectional area of the vertebral endplates and IVDs increases as one moves along the spinal column in the caudal direction. By comparison in large quadrupeds, the diameters of vertebra and IVD remains almost constant along the spinal column. (Alini et al., 2008). Similarly, IVD height increases in humans for IVDs towards the caudal end of the spinal column but is relatively constant for large quadrupeds. Hence compared to humans, large quadrupeds have large cervical vertebra, but relatively smaller lumbar vertebra (Alini et al., 2008).

There are also biological differences to consider. Most animals retain notochordal cells in the NP through their adult lives. On the other hand, humans retain a small number of notochordal cells in the NP in infancy only and have no Notochordral cells in the NP at all by 4-10 years of age (Alini et al., 2008). Notochordal cells have a marked effect on the metabolism of PGs, and thus may moderate hydration and IVD mechanical properties. Cattle, sheep and some dog breeds are noted to follow a similar pattern to humans (Alini et al., 2008), which may be important in some study designs.

2.5.1 Ovine Anatomy

It has been shown that ovine IVDs and FSUs have a reasonable similarity to human in terms of geometric ratios, biological factors, and mechanical response, and provide a useful analogue to humans for biomechanical testing (Wilke et al., 1997). "…sheep spines consist of 7 cervical, 12–14 thoracic, and 6–7 lumbar vertebrae" (Wilke et al., 1997). By comparison, a human has seven cervical, twelve thoracic, and five lumbar vertebrae. As was previously mentioned, sheep are quadrupeds and thus discs and vertebrae differ in size pattern compared to humans. A study by

Table 2-1, Relevant Anatomical Parameter Abbreviations (Wilke et al., 1997)

TABLE 1. Anatomical parameters and their abbreviations in this paper

Body part	Abbreviations	Dimension
Vertebral Body	VBH	Vertebral body height
	EPW	End-plate width
	EPD	End-plate depth
Pedicle	PDH	Pedicle height
	PDW	Pedicle width
Spinal canal	SCD	Spinal canal depth
	SCW	Spinal canal width
Spinous and transverse process	SPL	Spinous process length
	SPA	Spinous process angle
	TPL	Transverse process length
	TPA	Transverse process angle
	TPW	Transverse process width
Articular facet	FCH	Facet height
	FCW	Facet width
	IFW	Interfacet width
	CAX*	Card angle about x-axis
	CAY*	Card angle about y-axis
Intervertebral disc	IDH	Intervertebral disc height
Suffices	u	upper or cranial
	l	lower or caudal
	a	anterior
	p	posterior

*The two angles CAX and CAY represent tilting angles of a card, which was tilted relatively to the transversal plane first around the x-axis (CAX) and then around the y-axis (CAY) to have the same orientation of the joint plane.

Wilke et al., (1997) found that ovine vertebral height varied from 56.3 mm (±3.1 SD) at C2, to 26 mm (±1.1 SD) through the mid-thoracic, increasing in height up to 41.6mm (±1.1 SD) at L6. This is a significant difference from the human pattern, which is a constant increase in vertebral body size and width as one moves in the caudal direction. Relevant ovine dimensions are shown in Table 2-2 and Table 2-3. It has been suggested that sheep spines are more suitable for biomechanical testing than deer, as sheep have great similarities to human vertebral shape (Wang et al., 2015).

Table 2-2, Selected Ovine Vertebral Body Dimensions (Wilke et al., 1997)

TABLE 2. Dimensions related to the vertebral body of the sheep (mean ± S.D. in mm)

Vertebra	EPWl	EPWu	EPDl	EPDu	VBHa	VBHp
C2	28.6 ± 1.5	52.6 ± 1.3	25.1 ± 0.5	17.7 ± 0.7	56.3 ± 3.1	46.8 ± 1.9
C3	29.2 ± 1.0	24.7 ± 1.2	25.8 ± 0.8	20.6 ± 0.7	44.6 ± 1.2	45.5 ± 1.9
C4	29.1 ± 1.4	25.8 ± 1.0	26.5 ± 1.2	20.7 ± 1.2	44.3 ± 1.7	43.8 ± 2.1
C5	29.3 ± 1.4	24.4 ± 1.4	24.6 ± 1.3	21.1 ± 1.4	40.3 ± 1.2	39.6 ± 1.5
C6	25.8 ± 1.4	23.4 ± 1.1	23.6 ± 1.1	20.2 ± 1.2	34.2 ± 1.1	33.8 ± 1.6
C7	24.4 ± 1.4	21.8 ± 1.6	21.8 ± 1.0	20.8 ± 1.2	26.6 ± 1.4	27.0 ± 1.1
T1	19.7 ± 0.6	20.7 ± 1.4	20.4 ± 1.4	20.7 ± 1.2	24.0 ± 1.2	26.8 ± 1.0
T2	19.7 ± 1.2	17.8 ± 1.1	19.8 ± 1.2	19.8 ± 0.8	25.1 ± 0.8	26.0 ± 1.2
T3	20.6 ± 0.9	18.9 ± 1.2	19.8 ± 0.8	19.2 ± 0.8	26.1 ± 1.1	26.5 ± 0.8
T4	21.3 ± 0.6	20.5 ± 1.2	19.3 ± 1.0	18.7 ± 0.8	25.6 ± 0.4	26.0 ± 0.9
T5	21.7 ± 0.7	20.4 ± 0.4	19.3 ± 0.8	18.6 ± 0.7	25.0 ± 1.1	26.1 ± 1.1
T6	21.3 ± 1.0	20.6 ± 0.8	19.0 ± 0.8	18.5 ± 0.9	24.3 ± 0.9	25.2 ± 1.0
T7	21.4 ± 0.7	21.1 ± 0.8	18.6 ± 0.7	18.5 ± 0.5	24.3 ± 0.7	25.5 ± 0.6
T8	20.9 ± 0.8	21.2 ± 0.8	19.0 ± 0.8	18.2 ± 0.4	25.2 ± 0.8	26.1 ± 0.4
T9	22.2 ± 0.6	21.2 ± 0.6	18.5 ± 0.7	18.6 ± 0.7	216.2 ± 0.6	27.9 ± 1.1
T10	22.9 ± 0.8	21.9 ± 0.4	18.5 ± 0.7	18.5 ± 0.9	27.1 ± 0.7	28.9 ± 1.0
T11	24.5 ± 0.9	23.4 ± 0.7	18.7 ± 0.4	18.7 ± 0.4	28.9 ± 0.7	30.5 ± 0.6
T12	25.0 ± 1.0	23.9 ± 0.4	18.7 ± 0.8	18.6 ± 0.7	30.1 ± 0.4	31.9 ± 0.4
T13	26.6 ± 0.7	25.2 ± 0.4	19.0 ± 0.5	18.7 ± 0.9	32.4 ± 0.7	34.3 ± 0.8
L1	26.3 ± 1.1	25.0 ± 0.0	20.0- ± 0.0	19.5 ± 0.7	35.0 ± 1.4	37.0 ± 0.7
L2	28.9 ± 1.2	26.5 ± 0.8	20.4 ± 0.5	20.4 ± 0.7	36.5 ± 1.4	38.7 ± 0.8
L3	29.8 ± 1.3	26.5 ± 0.9	20.0 ± 0.6	20.5 ± 0.7	37.2 ± 1.3	40.2 ± 1.2
L4	31.0 ± 0.6	27.4 ± 0.4	20.1 ± 0.7	20.8 ± 0.8	37.6 ± 1.2	41.1 ± 0.8
L5	32.1 ± 1.1	28.7 ± 1.0	19.5 ± 0.6	20.4 ± 0.8	39.7 ± 1.6	41.5 ± 1.3
L6	36.4 ± 1.6	30.5 ± 0.5	18.5 ± 0.5	19.7 ± 0.4	39.4 ± 1.7	41.6 ± 1.1
L7	40.4 ± 2.0	32.7 ± 0.6	17.7 ± 0.9	17.6 ± 0.7	34.4 ± 1.2	36.2 ± 1.6

Table 2-3, Anterior Disc height for Ovine Spinal Discs (Wilke et al., 1997)

TABLE 6. Anterior disc height of the sheep (mean ± S.D. in mm)

Disc	IDHa
C2–3	6.7 ± 0.8
C3–4	6.9 ± 0.8
C4–5	7.2 ± 0.6
C5–6	6.8 ± 0.6
C6–7	7.2 ± 0.8
C7–T1	5.3 ± 0.4
T1–2	4.5 ± 0.8
T2–3	3.3 ± 0.3
T3–4	2.8 ± 0.3
T4–5	2.7 ± 0.3
T5–6	2.6 ± 0.2
T6–7	2.6 ± 0.2
T7–8	2.6 ± 0.2
T8–9	2.7 ± 0.3
T9–10	2.8 ± 0.3
T10–11	3.0 ± 0.4
T11–12	3.2 ± 0.3
T12–13	3.7 ± 0.4
T13–L1	4.3 ± 0.4
L1–2	4.4 ± 0.2
L2–3	4.2 ± 0.4
L3–4	4.5 ± 0.4
L4–5	4.3 ± 0.3
L5–6	4.5 ± 0.5
L6–7	4.5 ± 0.0

2.5.2 Hydration

Race et al (2000) established the relationship between hydration level and loading rate for bovine IVDs, finding that it was necessary to control the loading history, hydration, and loading rate in order to get reproducible results.

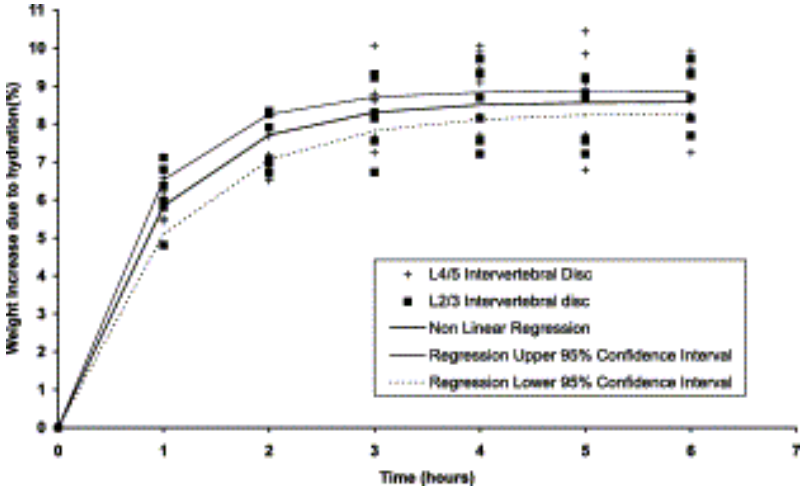

Figure 2-14, IVD Hydration vs time, (Costi et al., 2002)

Costi et al (2002) found that "The fluid content of the IVD is not constant but varies with external load and load history. When a load is applied to an IVD and the stress exceeds the osmotic swelling pressure developed by the hydrated proteoglycans contained in the nucleus, fluid is expelled." The material properties and the biphasic response of an IVD is dependent upon the hydration level of the tissue, which needs to be controlled for in-vitro studies. It is important that tissue hydration matches physiological norms, and that the hydration response of the tissue studied is relevant to the questions being asked. For example, studies conducted on highly degraded tissue are unlikely to have great relevance to healthy tissue. Similarly, it is important that a selected animal model exhibits a hydration response that is sufficiently relevant to provide insights into human tissue behaviour.

Costi et al., (2002) conducted a study examining the hydration behaviour of ovine IVDs and FSUs. It was found that specimens tested in air showed a significant increase in stiffness compared to the specimens that had been hydrated in saline baths prior to testing (Costi et al., 2002, p453). It was also shown that the time required to hydrate IVDs in a bath was similar in ovine and human cadaver discs when normalised for disc volume. For IVDs70% of total weight increase occurred in the first hour of hydration, followed by plateauing of the hydration rate and 96% of fluid absorption having occurred after 3 hrs (Costi et al., 2002). This strongly

suggests that ovine discs should be very close to steady-state if left to hydrate for a minimum of 3 hrs, as can be seen in Figure 2-14.

Chapter 3 Project Aims

The aim of this project was to build an affordable device capable of injecting IVDs at sufficient pressure to induce circumferential tears and delaminations. Such a device would facilitate studies on the biomechanical properties of discs with this specific injury. Studies of interest have investigated needlestick injuries of various gauge needles, and 60-second injections using pressures between 200 kPa (Peek, 2016) and 760 kPa (Fazzalari et al., 2001). Hence the project aim is to develop an injection device capable of operating at high pressures, and that could be useful in a variety of future studies that may require investigation of annular delaminations.

3.1 Project Scope

This project involved two processes:

1. The design and development of a high-pressure injection device
2. Testing to the device to establish the optimal parameters required to induce annular delaminations.

A difficulty with the validation phase of this project is that there were no benchmark targets for the device to be measured against. It was not known if a particular success-rate (% injections resulting a delamination) or length of tear should be expected for a given pressure or time parameter. For this reason, the validation phase was formulated as an experimental in-vitro study on ovine IVDs. Successful demonstration of the device was to be correlated the demonstration of the significance of parameters such as variations in injection pressure or injection duration. Variations to pressure and injection duration are the primary factors investigated in this study on delaminations, but the effects of variations of preload and hydration were similarly unknown. To that end an experiment was carried out investigating two hypotheses:

1. That increasing the pressure of an injection would result in more delaminations and longer delaminations
2. That decreasing the time duration of an injection would not result in a reduced number of delaminations or shorter delaminations.

The experiment is detailed in Chapter 5 Device Testing.

Chapter 4 Device Development

The first part of the project was to design and build an injection device. The demonstrated technique was to insert a needle tangentially between the inner lamellae of the anterior AF. This technique was demonstrated in the into the anterior region of the AF (Fazzalari et al., 2001). By this method the needle was thought to lay between annular lamellae, facilitating separation of the layers as the fluid was injected. This had been demonstrated by Fazzalari et al. at pressures up to 700 kPa (110 psi). In the Fazzalari study, tears were demonstrated and verified in 6 fresh ovine spines. Lumbar discs were injected with saline at 717 ±23 kPa (104 – 110 psi) for 60 seconds. The saline was coloured with india ink, giving the injection fluid a strong contrast colour and facilitating visual inspection. Following injection, the discs were sectioned and inspected, finding consistent tears of 9.1 ± 3.8 mm in length. However, no variation of pressure magnitude or injection duration was considered.

4.1 Device Requirements and Specifications

The desired device was required to be able to create delaminations of indeterminate size in IVD annular tissue in a laboratory setting. The success of the device was to be measured by its reliability, ie the number of delaminations it could create. However, there were a number of criteria that contribute to this goal, and that would make a device suitable for laboratory use. Note that this device was specified exclusively for use on cadaverous tissue. As such measures to provide for the safety and ethical treatment of the patient are not included in the design requirements.

A suitable injector must be:

- Low cost
- Rated to operate at high pressure
- Able to maintain a consistent set pressure during use
- Able to control the time duration of the injection
- Compatible with use of phosphate buffer saline

- Rated for pressures of up to 100 psi (690 kPa)
- User-friendly for a variety of lab users
- Benchtop compatible
- Adaptable to a variety of experimental requirements

Based on the aforementioned requirements the specifications for the device were:

- Cost < $600
- Pressure rating >= 100 psi (690 kPa)
- Constructed with saline compatible materials
- Weigh < 10 kg
- Hand tool weight < 1 kg
- Able to record pressure

4.2 Subsystems

Any design concept for this device must necessarily include some of the same subsystems, as is shown by item 1 in Figure 4-1. A design must include a driving ram, a piston in order to pressurise the fluid or an alternative source of driving pressure. A fluid reservoir or a syringe barrel will be required to hold the saline, as is shown in item 4, Figure 4-1.

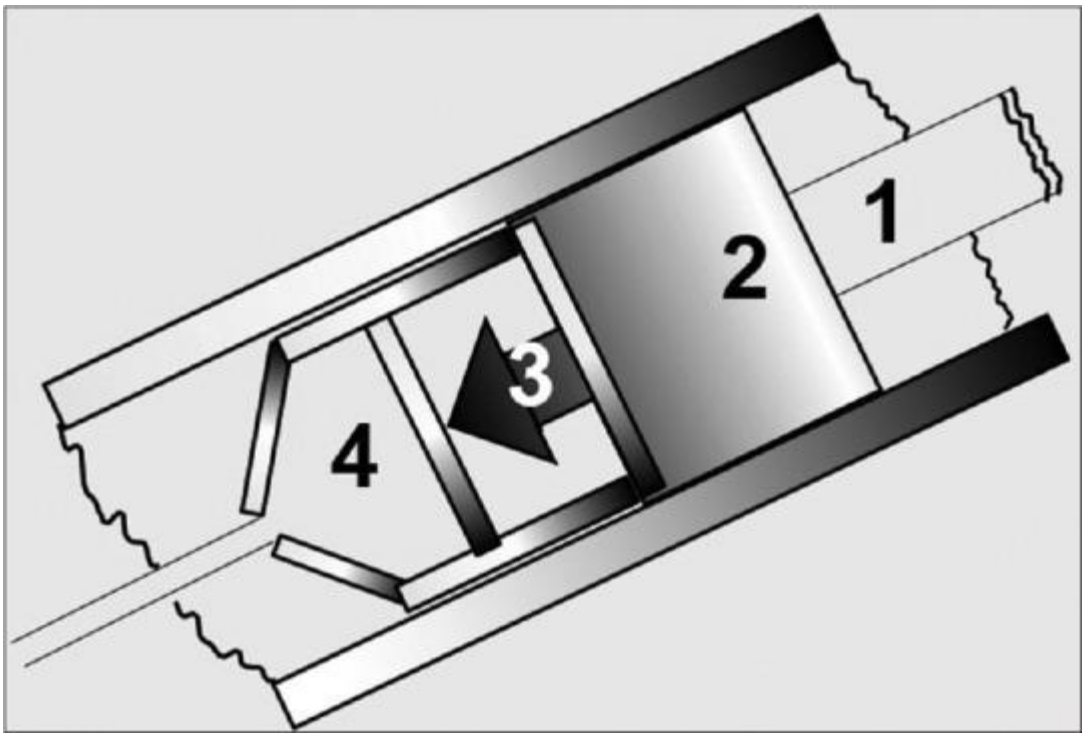

Figure 4-1, Line diagram of piston plunger in pressure injector system: Piston plungers are made of (1) plunger drive ram, (2) drive motor for moving the drive ram, (3) elastic head and a stretcher rod and (4) syringe.(Indrajit et al., 2015)

A design solution may also require a method for recording or monitoring pressure to validate that correct pressure was used across the course of a test. A needle for injection will be required, and may be directly attached to the syringe, or may be remote to the syringe and connected via flexible tubing. It would be preferable to be able to detect the volumetric flow of the fluid as this may provide some insight into the failure mechanisms within the annular tissue.

4.2.1 Pressure source/Drive

A pressure head, as shown in Figure 4-1, is an integral part of the injector design. A source of pressure or a piston drive is an integral component for this device. Potential options are included in Table 4-1.

Table 4-1, Pressure Supply Options

Pressure Source	Pros	Cons

High-Powered Syringe Pump	• Easy to implement volumetric sensing • Relatively simple mechanism	• Existing syringe pumps are either low pressure or excessive cost • Difficult to implement a control system for precise pressure control • Results highly dependent on sensor precision
Off the shelf Microfluidic Dispenser	• High precision volumetric control	• Existing devices significantly exceed the project budget (“Microfluidic Pressure Sensors,” n.d.) • Not recommended for application manufacturer technical staff (ELVEFLOW)
Custom Pneumatic Storage Reservoir	• Simple control mechanisms • Compatible with simple, low-cost construction methods	• Bulky. Unlikely to be compatible with bench top use • Must validate that pressure remains constant throughout tests
Manual Syringe	• Very simple construction • Very low cost	• Requires sensors to validate applied pressure • System variability is dependent on user error

		• Low repeatability
Off-The-Shelf Pneumatic Fluid Dispenser	• Medium Cost ~ $500 (“Digital Fluid Dispenser - TS250,” n.d.) • Available among existing electronics equipment used on campus • Trivial to implement • Use of gas in the system will result in very stable pressure magnitudes, and does not require a complex control mechanism	• The use of gas in the system will likely buffer fluid pressure signals, preventing signal events as tissue failure occurs

During the process of comparing devices, it was discovered that the Flinders University Engineering Services team had a Techcon TS250 pneumatic fluid dispenser, used for dispensing solder paste and rated to 100 psi (690 psi). As there was equipment on campus that could simply be loaned, this substantially lowered the cost barrier, and this became the default, cost-effective option.

4.2.2 Fluid Reservoir

The fluid reservoir is the function performed by the syringe barrel. In the case of pneumatic pressure sources, it may be possible to use an alternative configuration, but to a large degree, the form of the fluid is dependent on the selection of the pressure source. It was possible to purchase pressure rated syringes to suit syringe pumps and fluid dispensers for a trivial cost. Even if a custom pump was to be designed it would be more effective and affordable to supply pressure rated syringes to suit, rather than to manufacture a custom reservoir. It should also be

pointed out that high-pressure devices with an internal diameter less than two metres and a pressure greater than 50 kPa (7.2 psi) the vessel and construction must comply to Australian Standards AS1210 for Pressure vessels with regards to materials, design, and testing ("AS 1210-2010 | Pressure vessels | SAI Global," n.d.).

Fluid reservoir	Pros	Cons
Custom Machined Reservoir Or Syringe Bore In Stainless Steel	• Corrosion-resistant	• Must comply to AS120 • Fluid not visible to check for bubbles
Pressure Rated Syringe	• Low cost • Easily replaced • Standard Fittings • Trivial to implement • Easily adapted to future changes • Transparent syringes allow checking for air bubbles and verifying fluid content	

4.2.3 Pressure/displacement Sensors

The device required a pressure sensor to monitor and log the injection pressures. Options included:

- direct measurement of the saline fluid
- Indirect measurement of fluid pressure via monitoring of air pressure
- inferring fluid pressure from drive pressure or motor torque

Select of a measurement system was dependant on the other design components. Of these, direct measurement of the saline was far preferable. In particular, methods inferring pressure

would have required calibration and verification, a process that may have required direct pressure measurement anyway. It was also hoped that perturbations in the pressure signal may correlate to discrete tissue failure events and provide some additional insight. Of the many potential sensors, the Honeywell PX3 series heavy-duty series was most suitable, being a small form factor, wetted sensor with a small error range of 0.25% of FSS.

Another potential measurand was to detect volumetric fluid flow as this would allow the device to detect and validate the occurrence of a delamination event during the test. The ideal sensor for this type would be a Linear Variable Differential Transformer (LVDT) attached to a piston or plunger mechanism, as LVDTs can have near-infinite resolution, dependent on the signal to noise ratio. This is important as injections into ovine IVDs are measured in microlitres, and likely to be spread over time periods as long as 60 seconds. Again, implementation of volumetric measures was dependant on other design decisions.

4.2.4 Design Options

Three initial options for an injector design were considered:

- A manual syringe with pressure and/or volumetric flow sensor connected
- A syringe pump design
- A liquid fluid dispenser
- A pneumatic pressure reservoir

The strengths and weakness of each option are discussed below.

<u>Manual syringe</u>

The first design concept was a manual syringe with attached pressure sensors and data logging for later validation.

Pros	Cons
• Low cost	• Inconstant pressure

• Minimum parts to manufacture • Possible to mount LVDT to syringe piston. • Not prone to sensor/control errors	• Requires a small diameter syringe (< 3 ml) to achieve high pressure • Requires adaptor for pressure sensor • 3 ml syringe may not be sufficient to prime system, remove bubbles, and complete test

Syringe Pump

The second design concept was to construct a syringe pump with attached sensors and control system, The syringe pump design had the advantage of directly driving the injection via a piston. Existing designs such as CT contrast injectors were available, but these were orders of magnitude in excess of the project budget. Other more affordable products appeared to be optimised for volumetric flow control and would be suitable for a pressure control mode. A custom-made low-end version would have required a stepper motor or linear actuator, rated pressure fittings, and a high precision pressure sensor for control feedback. This concept presented a suite of challenges such as control systems to maintain constant pressure without overshoot spikes and high variability.

Pros	Cons
• Minimum parts to manufacture • Possible to mount LVDT to the plunger for volumetric change detection	• Significant cost • Control system for constant pressure challenging to implement • Requires adaptor for pressure sensor

Pneumatic Dispenser

The third design concept was to attach a syringe to a pneumatic fluid dispenser. This design requires an adaptor for a pressure sensor. This design is not compatible with the use of LVDT to measure volume change or displacement as it provides no access to the syringe piston.

Pros	Cons
• Very lost cost • Minimum parts to manufacture • Excellent pressure control • Minimal development time	• Provide no methods to measure volume change

Pneumatic Reservoir

The pneumatic pressure reservoir concept consisted of a pressurized air tank provide a driving force to a reservoir of liquid saline. This had the advantage of being simple in construction. However, it would require precise valve control, would be very difficult to measure or control the volume being injected. The entire system would be required to meet the requirements of AS1210 standards for pressure vessels. Further, this option involved maintaining the entire system at high pressure. A system of control valves would be required to control the test execution, as well as a system of safety releases valves.

Similarly, liquid fluid dispensers were available in a range of high precision off the shelf devices. These devices had the benefit of being able to dispense liquid in precise quantities. However, in discussion with ELVEFLOW staff, the function of these devices was described as ‘a hammer’ forcing the fluid to be dispensed in discrete controlled volumetric quantities. As such, these devices are likely to confound a pressure-controlled experiment and were not recommended. Further, these devices are significantly outside the project budget.

4.2.5 Design Evaluation

The proposed design concepts were compared in a House of Quality shown in Table 4-2. This showed that the pneumatic dispenser concept was clearly a better option for the requirements of this project. This concept allowed the use of off-the-shelf, pressure rated components, removed the need to develop a custom control system, substantially reduced development time, and what one of the lowest cost options available. Further, this concept, being simple to implement was likely to be easily adopted by other researchers.

Table 4-2, Design House of Quality Comparison

			Functional Requirements											
		Direction of Improvement	▼	▲	▲	□	□	□	▼	▼	▼	▲		
Relative Weight	Customer Importance	Customer Requirements	Cost < $600	Pressure rating >= 690 kPa	Maximise pressure stability	Use standardised or interchangable fittings	Record pressure data	Detect Volumetric displacemnet	Requires minimum parts to be manufactured	Hand tool weight < 0.5 kg	Uses Corrosion resistant materials			
17%	9	Low Cost	●			▽			○				**Relationships**	**Weight**
15%	8	High Pressure Compatible		●		○							Strong ●	9
13%	7	Maintain constant set pressure		○	●	▽	○		○				Medium ○	3
15%	8	Minimise Size							○	●			Weak ▽	1
8%	4	Adaptable for future experiments	▽	○	▽	●	○	○	▽	▽	▽			
9%	5	Minimimum development time	○			●			●				**Direction of Improvement**	
11%	6	Able to record pressure signal					●						Maximize ▲	
6%	3	Able to sense/record volumetric displacement						●						
4%	2	User friendly for lab work							▽	●			Target □	
2%	1	PBS Saline Compatible				●					●		Minimize ▼	
		Importance Rating Sum (Importance x Relationship)	188.68	198	126	245	164	73.6	232	177	24.5	0		
		Relative Weight	13%	14%	9%	17%	11%	5%	16%	12%	2%	0%	Score	
		Manual Syringe With sensors	3	1	0	2	2	2	3	3	2		2.1029	
		Syringe Pump	1	2	1	2	2	3	1	2	2		1.66887	
		Pneumatic Dispensor Control	3	3	3	2	2	1	3	3	2		2.59367	

4.3 Device Construction

The final design for the injector utilised a Techcon TS250 pneumatic fluid dispenser similar to the one shown in Figure 4-2. Incorporating a pressure regulator and time control with millisecond resolution, the dispenser was well suited to simple experiments. The dispenser was designed to connect to a pressure rated syringe and apply pressure for a precise time intervals with millisecond resolution. Compatible 10cc Luer Lock syringe barrels and pistons were ordered from MetCal.

Figure 4-2, Techcon TS250 Pneumatic Paste dispenser ("Digital Fluid Dispenser - TS250," n.d.)

4.3.1 Sensors

Due to the syringe forming a sealed air-driven system, it was unfeasible to attach an LVDT to the syringe piston to measure volumetric displacement. As such the system had to rely on optical measures. A clear syringe was used, with speckling applied to both the syringe barrel and the piston. For each test, a camera was set up to record displacement of the syringe piston.

Smaller syringes such as 3CC and 5CC were assumed to give better resolution of displacement measurement. However, the 10CC syringes were available with Luer lock fittings. Considering that the device included a hypodermic needle under high pressure, the lock feature significantly improved safety, by reducing the risk of the needle becoming an inadvertent projectile. Due to the use of a 10 CC syringe barrel, an expectation of very small flow rates, and possible expansion of the syringe barrel under pressure, reliable volumetric measures were not expected.

To measure pressure, a Honeywell PX3 100 psi (690 kPa) heavy-duty ratiometric pressure transducer was selected. This sensor was saline and liquid tolerant, with a rated accuracy of 0.25% of FSS (Best fit straight line). The laboratory airlines were limited to a supply of 100 psi, and the specified maximum for the TS250 was also 100 psi. As such, 100 psi PX3 sensor was selected, as it provided the smallest scale, thus reducing sensor error.

Data logging was achieved with a National Instruments NI USB-6211 Data Acquisition unit (DAQ) connected to a PC in the lab with National Instruments Signal Express software. The PX3 was connected in a Reference Single Ended Configuration, as is shown in Figure 4-3.

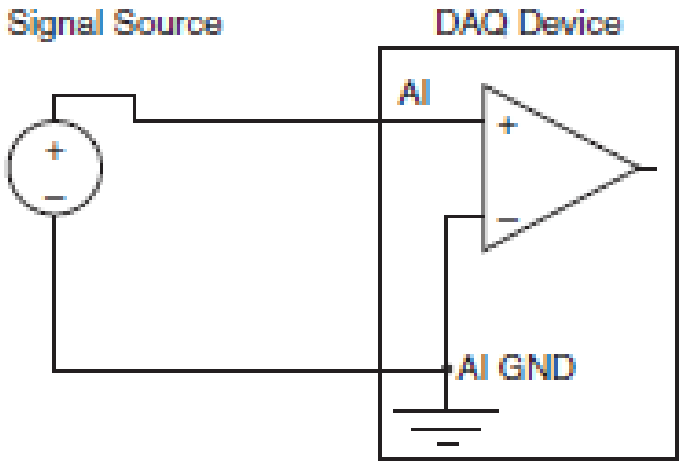

Figure 4-3, Sensor connection to DAQ data logger

To maximise sensor accuracy the PX3 was positioned as close the needle as possible. A stainless-steel adaptor fitting was machined to accept both Luer syringe adaptors with UNC 10-32 thread, and the PX3 pressure sensor with a 1/8 -27 NPT thread. This part was designed in a small form factor of a 20 x 20 bar, as is shown in the following the technical drawing. However, the available material from Engineering services was 50 mm diameter 316 stainless round bar, and this was used to minimise cost and lead time. The sensor block was designed to facilitate the purging of air bubbles prior to use. To purge bubbles, it would be required that the device is held at a 60-30 degree incline with the sensor orientated to the lowest face. This was covered in detail in Appendix A Injector Set-up SOP.

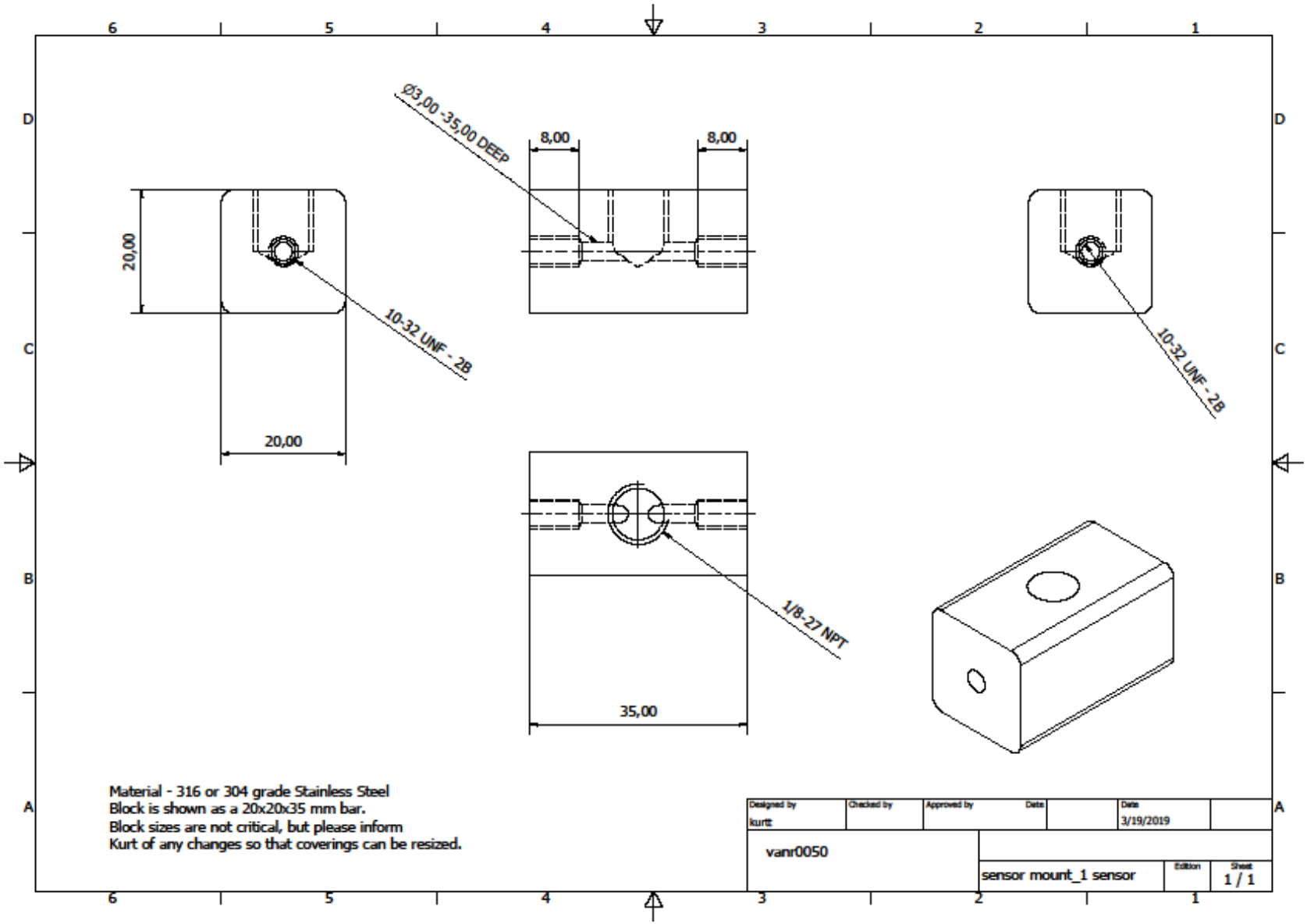

Figure 4-4, Pressor Sensor Adaptor Drawing

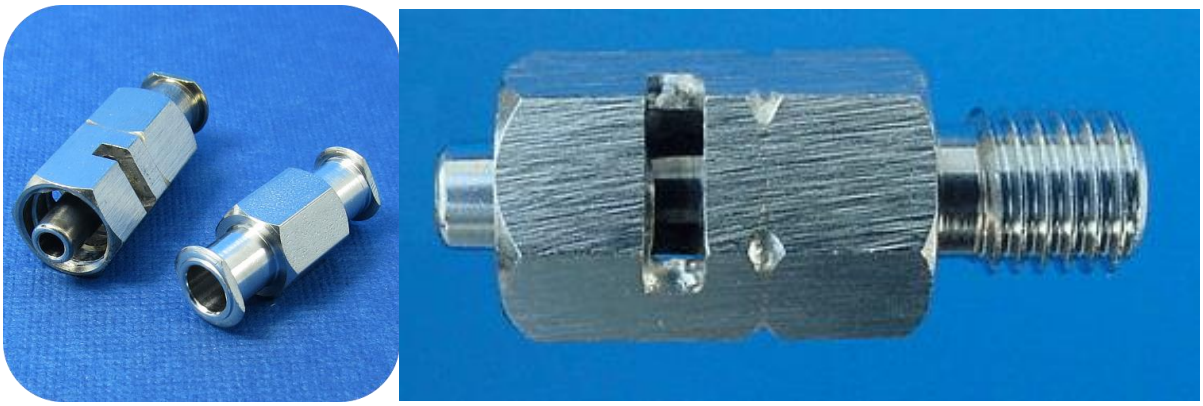

Figure 4-5, Luer Lock Adaptor Fittings ("Stainless Steel Luer Fittings and Connectors | Component Supply," n.d.)

The sensor block attached to the syringe and the hypodermic needle via standard Leur Lock adaptors such as are shown Figure 4-5. The sensor adaptor block was modular and could easily be exchanged with a similar replacement part should it be desired to employ different fittings or a sensor with a different thread connection.

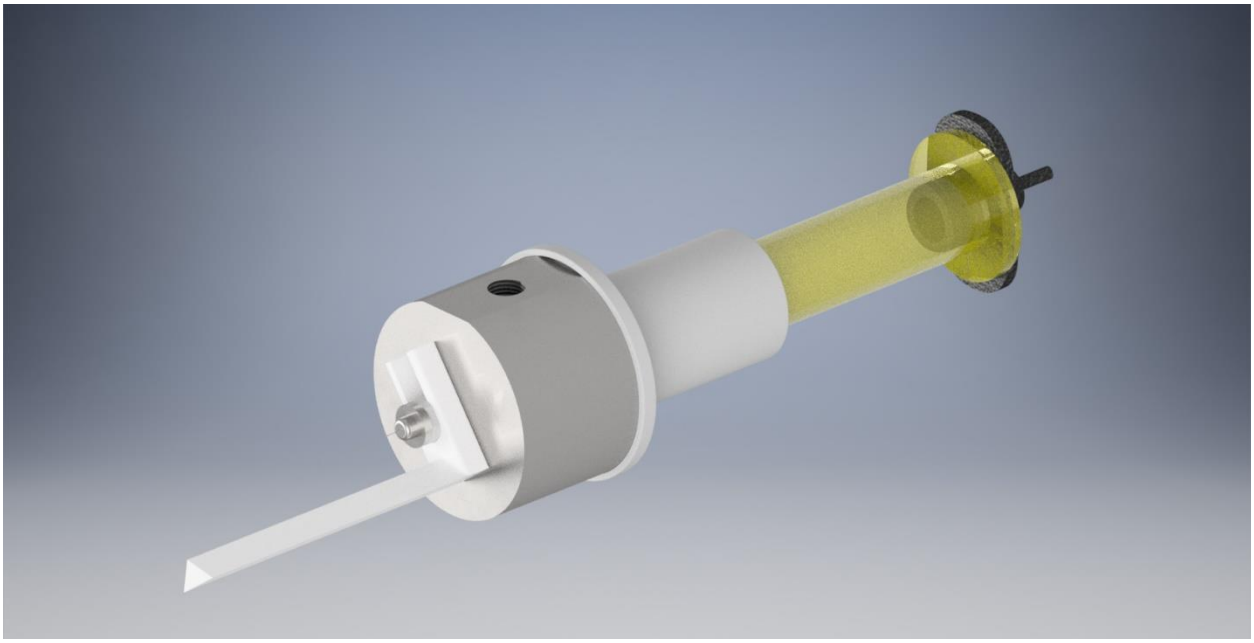

Figure 4-6, Syringe design with pressure sensor mounting block and injection guide

A syringe barrel support was 3d printed to support the barrel of the syringe and prevent damage to the Luer adapter connection between the stainless block and the syringe, as can be

seen in Figure 4-6. Finally, a series of clip-on needle insertion depth gauges were designed to assist in achieving correct needle placement. These gauges were designed to sit alongside the needle with an offset of 6, 7, 8, 9, or 10mm. For each injection, the operator could select the appropriate target depth, and clip the gauge onto the Luer adaptor. These clip-on adaptors were expected to provide guidance, not accurate control. A mark on the guide would indicate the position of the needle tip, helping to prevent over or under insertion of the needle. The depth guides also provide a guard against needle stick injuries, improving the safety of the system. This can be seen in Figure 4-7.

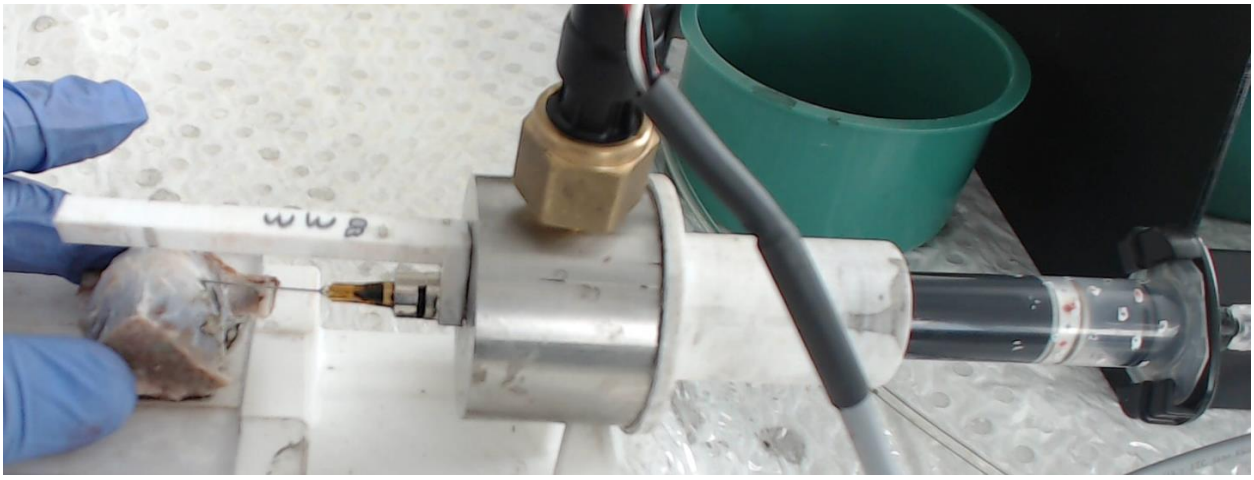

Figure 4-7, Needle depth guide in use

Chapter 5 Device Testing

There was no benchmark to test the effectiveness of the injector against. Instead an experiment was performed to investigate if adjusting the parameters of injection pressure or injection duration would have a positive effect on delamination results. While injections have been used to delaminate ovine disc in prior trials, no studies have performed comparisons of the effect of varying pressure or injection duration. Therefore, this study tested two hypotheses, as was described in Chapter 3;

1. That increasing the pressure of an injection would result in more delaminations and longer delaminations
2. That decreasing the time duration of an injection would not result in a reduced number of delaminations or shorter delaminations.

5.1 Experimental Design

The primary region of interest for annular tear is the innermost annulus in the posterolateral region, being the region where most tears and pre-herniations are thought to originate. However, the anterior region was far more accessible, presenting a greater disc height and a significantly wider cross-section of the annulus. It was also noted that other relevant studies had been conducted on the anterior region. Hence tests conducted on the anterior region would make this study consistent with the prior art and make results easier to interpret.

Having two hypotheses related to the effect of injection duration and of injection pressure, the study was designed to examine the effects of these parameters via a two way Analysis of Variance (ANOVA) statistical comparison. ANOVA tests require several assumptions including:

1. That the error or random portion of the dependent variable is normally distributed
2. That each test group is independent, with no specimens existing in multiple groups
3. That the variance is homogenous between groups

To be able to assess these questions via an ANOVA, the study needed to produce data that would conform to the appropriate assumptions including: homogeneity of variance, and normally distributed data. ANOVAs are more tolerant to violations of these assumptions with study sizes of n>25 or with equally sized groups.

There were nine potential treatment groups in this study, as is shown in Table 5-1.

Table 5-1, Experimental Treatment Groups

		Injection Pressure Groups		
		60 psi	80 psi	98 psi
Injection Duration Groups	15 seconds	Group 1	Group 2	Group 3
	30 seconds	Group 4	Group 5	Group 6
	60 seconds	Group 7	Group 8	Group 9

It was recognised that an experiment with multiple groups was likely to either require a large number of samples, or to suffer from being underpowered. The "G-Power" software (Faul et al., 2009) was used to analyse the a-priori statistical power of the study. Given a desirable study power of 0.8, the power analysis predicted the number of samples required to achieve significance at a given effect size, calculated from η_p^2 (the ratio of variance to effect plus variance). As values for η_p^2 for this type of experiment were not available from the literature, the values given by Cohen (1969, p. 416) were arbitrarily chosen, where large, medium, and small effect sizes were given as η_p^2=0.4, η_p^2=0.25, η_p^2=0.1 respectively. It should be noted that these values were established as a convention for behavioural sciences, and that in discussion, descriptions of a 'large' effect size ranged from η_p^2=0.75 to η_p^2=0.15.

Using Cohen's effect size conventions and assuming;

$\alpha = 0.05$

power $(1-\beta) = 0.8$

the sample size required was calculated for different numbers of treatment groups. These comparisons are summarised in Table 5-2

Table 5-2, A-priori Power Analysis Required Sample Size

		Required number of sample to detect given effect size:		
Number of Treatment Groups	Df (numerator)	η_p^2 = 0.4 (large effect size)	η_p^2 = 0.25 (medium effect)	η_p^2 = 0.1 (small effect size)
9	2	20	33	91
6	2	19	33	84
4	1	15	26	73

It was not feasible to conduct more than 50 trials. The power analysis showed that this study would not be able to show significance for small effect sizes, and if the assumptions for expected Eta values were inaccurate may fail to confirm medium to large effects with 9 treatment groups. As such it was desirable to increase the study power by decreasing the number of groups. It was expected that changes to the injection pressure would have the most significant influence on test results, while it was uncertain that injection duration would have an effect at all. As such the experiment was organised into two series, and all treatment groups with 30 second injection durations were removed.

Series 1 included 4 groups included injections durations of 15 seconds and 60 seconds, and injections pressures 60 psi and 98 psi. These values were selected to give the greatest odds of showing if injection duration had a significant effect by only considering the shortest duration to the longest duration, with only 4 groups.

		Injection Pressure Groups	
		60 psi	98 psi
Injection Duration Groups	15 seconds	Group 1	Group 3
	60 seconds	Group 7	Group 9

Series 2 was designed gather data on the influence of injection pressure on annulus delaminations. Tests were performed at 60 psi, 80 psi and 98psi, with injections durations of both 15 seconds and 60 seconds. If injection duration was shown not to have an effect, the combined series could be pooled into one group for a One-Way ANOVA with 3 groups. Otherwise a Two-Way ANOVA with 6 groups would be required.

5.2 Testing Specifications

This project made use of surplus sheep spines that were available in the Flinders Biomechanics Lab and not useful for other projects. These sheep spines had been sourced from local abattoirs from and included upper lumbar region IVDs, small size IVDs, and IVDs from spines that included some damaged discs.

For this project, the only measure of interest was related to the resistance to delamination between or within lamellae. It was not anticipated that this would change significantly between IVDs of differing thickness, cross-sectional area, or vertebral level, so no exclusions of this type were applied.

IVD inclusion criteria were:

- Ovine lumbar spines from animals slaughtered between the ages of 6 to 18 months.
- Lumbar IVDs between the Thoracolumbar joint and the L5/L6 joint.

IVD's exclusion criteria were:

- cut damage to the annulus
- noticeable pathology in the IVD
- tissue damage or freezer burn due to poor storage
- noticeable degradation of the AF, the NP or surrounding tissue
- costovertebral joints, indicating a thoracic joint

Additionally, tests were rejected if

- the needle struck the vertebral endplate during injection

- the injection missed the target region and penetrated to the NP
- the injection was too shallow and penetrated to less than 1/3 the annular thickness

During early pilot testing a number of IVD's were only subjected to low estimated preloads of 0.01 MPa. However, for the experimental study, all IVDs were specified to be hydrated under a preload NP pressure of 0.1 MPa based on estimations of each discs cross-sectional area. This is explained in more detail in section 5.4.2 Hydration. All tests were performed with a 25g needle, tangentially into the annulus. The 25g needle was considered to be a good balance between the need to have as thin a needle as possible, and the difficulty in avoiding needle flex, and potentially missing the targeted region of interest.

5.3 Success Criteria

The purpose of these tests was to induce delaminations in the IVD anterior annulus. An injection was defined to be a successful demonstration of the injector if it resulted in an ink trail observable to the naked eye, and longer than an arbitrary 3 mm tear length threshold.

It should be noted that these tests did not specify needle placement into either the ILM or the lamella. Both Tavakoli et al (2016) and Gregory et al. (2012) showed the ILM may have an important mechanical role in annular delamination, but Veres et al. (2008) showed that delaminations can also occur within lamella. As such it was considered beyond the scope of this test insolate and investigate discrete tissue regions, and any injection delivered to the inner anterior AF was to be included in the test data.

5.4 Methodology

The hypothesis proposed two primary questions?

1. What is the effect of variations in injection pressure?
2. What is the effect of variations in injection duration?

Initial pilot tests were conducted including variations in pressure (60psi, 80psi, 98psi), variations is injection duration (15s, 30s, 60s), and also in variations estimated hydration preload

(0.01MPa – 0.5MPa). These pilot tests allowed the injection technique to be tested, and discrepancies to be accounted for before the main experiment was conducted.

It was decided to give pressures in psi rather than kPa during the experiment as the outer scale on the TS250 dial was in psi, which was more convenient to read. The target pressure for the upper threshold tests was 100 psi, but the laboratory pressurised air supply did not reliably provide 100 psi, so a slightly reduced pressure had to be used.

5.4.1 Preparation

The first step in preparing an IVD for delamination was to select suitable specimens. Suitable sheep spines had been wrapped in saline-soaked absorbent material, sealed in plastic, and stored at -25C. Spines that had not been wrapped or sealed in plastic tended to exhibit dehydrated tissue and freezer burn, and were excluded from the study.

Spines were defrosted and cleaned of excess flesh. The transverse processes were cut off, and discs were separated from one another by sectioning the vertebrae. Posterior elements were removed by cutting along the frontal plane of the spinal canal. Hence each specimen was reduced to a unit consisting of an intact IVD, sandwiched between the vertebral endplates and remaining vertebral bone. Any joint having less than 10mm of vertebral body attached to the IVD was arbitrarily excluded from the study out of concern that reductions in structural stiffness of the vertebral body would affect results.

Figure 5-1, Lumbar spine cleaning

5.4.2 Hydration

Hydration of IVD tissue is an important factor for in-vitro testing. The aim is to achieve an in vitro model with similar response and behaviour to in vivo tissue. Tissue hydration is the primary modulator of the viscoelastic properties of IVDs, so it is important to hydrate the IVD to clinically relevant parameters. Standard practice is to submerge a disc in 0.15 Mol Phosphate Buffer Saline solution (PBS) while it is mechanically loaded with sufficient weight to achieve a physiological relevant pressure in the NP.

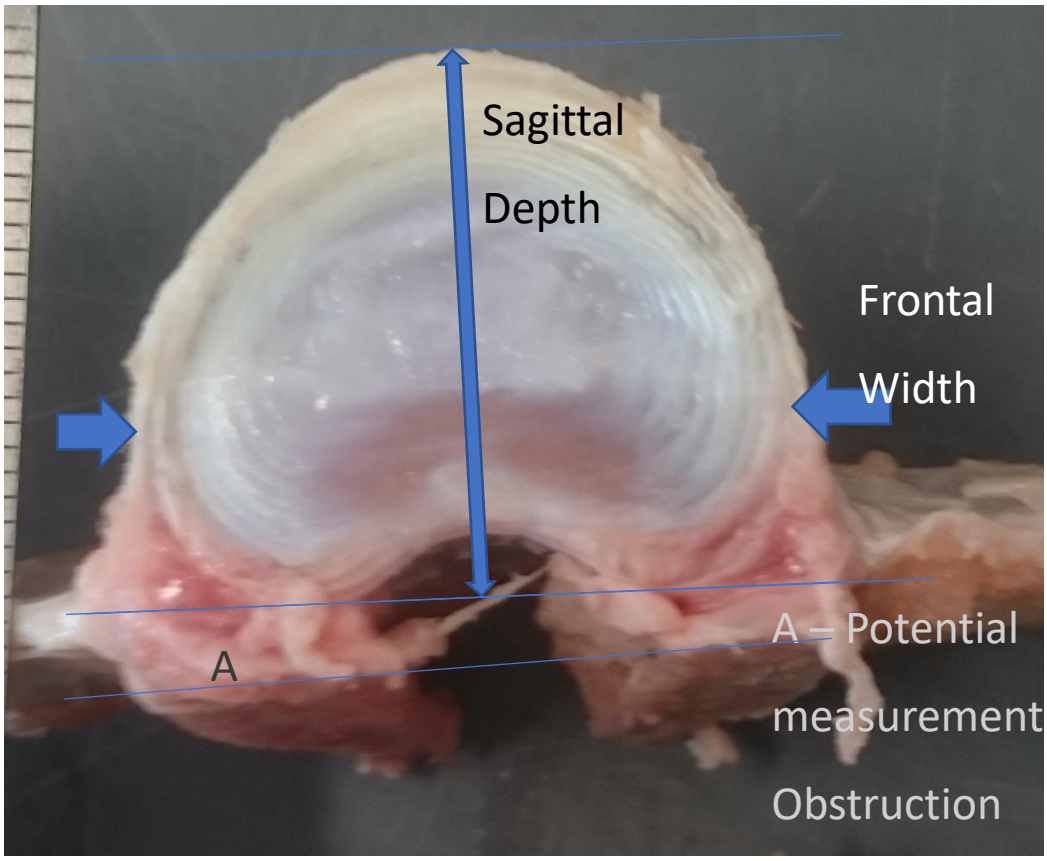

Figure 5-2, Disc measurement and obstructions

Finding an estimate of the discs cross-sectional area and calculating the load to apply to achieve the specified nucleus pressure. An internal pressure of 0.1 MPa was considered to be a normal disc pressure correlated to rest and laying down. A nucleus pressure of 0.5 MPa is correlated to activities like sitting upright for a long period of time (Wilke et al., 1999). To find the estimate of disc area, the disc area is assumed to be 84% of its bounding box (Nachemson and Morris, 1964). The intact IVDs frontal and sagittal dimensions were measured with a Vernier gauge. This often involved a degree of estimation if the posterior of the specimen was partially obstructed, as is highlighted in Figure 5-2. The disc area was then calculated with the formula

$$A = w * d * 0.84$$

Where

A = estimated disc area in mm^2

w = disc width (frontal plane) in mm

d = disc depth (sagittal plane) in mm

Nucleus pressure is given by

$$NP\ Pressure\ = 1.5 * P\ (MPa)\ \text{(Nachemson and Morris, 1964)}$$

Where P is the pressure in MPa applied to the IVD given by

$$P\ (MPa) = \frac{L\ (N)}{A\ (mm^2)}$$

Where

L = load (N)

Hence to the required load to achieve the desired nucleus pressure is given by

$$NP = 1.5 * \frac{L}{A}$$

$$L = \frac{NP * A}{1.5}$$

For each IVD a target nucleus pressure was selected, and the IVD was submerged in PBS under load in a hydration rig for a minimum of three hours. After three hours, it was considered that any disc would have reached a hydration equilibrium, and further hydration time would have no further effect (Costi et al., 2002). It was possible to verify hydration equilibrium state had been reached by monitoring the displacement of the weight with an LVDT. However, this would have complicated the experimental setup and limited the number of discs that could be hydrated at one time, drastically increasing the time required to perform the injection trials. As a large number of IVDs had to be processed, it was considered efficient to simply ensure that all IVD were hydrated for a minimum of three hours.

Figure 5-3, Specimens hydrating in PBS under load

5.4.3 Injections

For each test the specimen would be removed from the PBS hydration bath, excess moisture removed with a paper towel and immediately placed on a stand beside the injector. Injections were performed free of any weight, load, or clamping force.

For each test, the specimen would be inspected by eye, and the experimenter selected a clip-on needle guide to set the needle depth relative to the estimated anterior annulus thickness. Based on experience from the pilot trials, it was necessary to leave a 2mm gap between the disc and the needle guide to allow for guidance corrections. Table 5-3 was developed to select needle guides

Table 5-3, Needle Depth Guide Selection Table

Disc Sagittal Depth	Estimated Anterior Annulus Thickness	Use needle guide offset
< 20 mm	< 7mm	6 mm
20 – 25 mm	7 -8.5 mm	7 mm
25 – 30 mm	8.5 – 10mm	8 mm
> 30 mm	> 10 mm	9 mm

The guides did not enforce needle position but were merely an aid to depth estimation. In later tests, it was found that despite the use of depth guide, the needle tended to flex, and could easily be inserted on too shallow a tangent, or too deep and penetrate the nucleus. After this effect was noticed, the technique was improved by carefully aligning the needle bevel to the frontal plane of the disc, as shown in Figure 5-4. This greatly reduced the number of tests excluded due to poor needle placement.

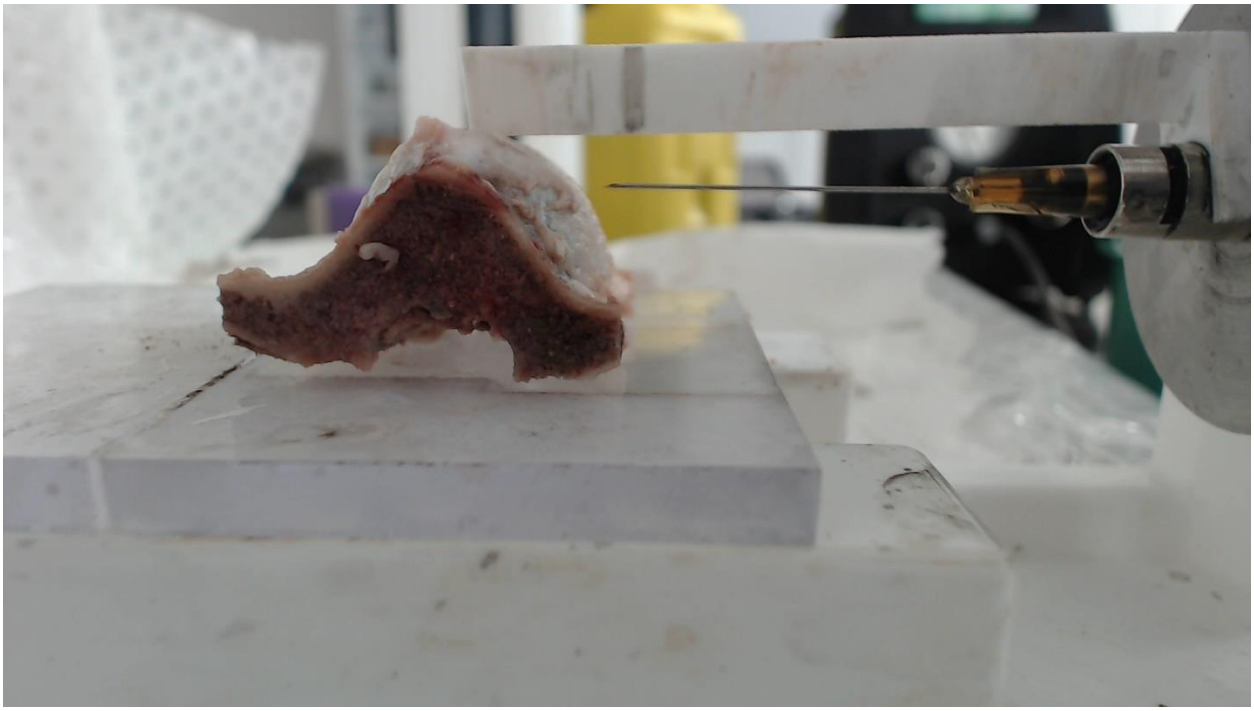

Figure 5-4, Use of a needle guide with needle bevel orientated to the frontal plane

5.4.4 Test Series 1 – Injection Duration

The test was arranged into 4 groups spanning the parameters with the greatest difference, as is shown in Table 5-4. Each group was assigned 8 specimens, totalling 32 specimens for the study. If it could be shown that injection duration between 15 and 60 seconds did not show a significant effect, it would be reasonable to pool durations for a later comparison of selected pressures.

Table 5-4, Injection Duration Study Groups

Preload = 0.1 MPa	15 s	60 s
98 psi	8 specimens	8 specimens
60 psi	8 specimens	8 specimens

All series 1 tests were done at a standard preload of 0.1 Mpa, estimated from the size and geometry of the IVD disc. Once 8 discs had been injected for each group, the IVDs were sectioned and imaged for analysis.

Injections were conducted in the following manner;

1. Fill the syringe barrel with saline, mixed with a small amount of india ink to provide an obvious contrast in the case of any delamination.
2. Following saline injection SOP as detailed in Apendix A, ensure that the system has no air bubbles.
3. Insert the needle tangentially to the anterior disc surface. The target location shall be the specified location, with needle parallel to the annular lamellae. The target depth shall be 2/3 of estimated total annular thickness, ±30%.

5.4.5 Test Series 2 – pressure differences

The aim of this test series is to address the hypothesis that injections occurring at an increased pressure will result in increased delamination incidence and increased tear length for the delaminating.

To test this hypothesis comparison tests were conducted at differing pressures for the same time of application.

If the null hypothesis was returned for test series 1, the time lengths could be statistically pooled, for a more powerful study with less degrees of freedom as is shown in Table 5-5. The null hypothesis is not returned, the study design shown in Table 5-6 must be followed.

Table 5-5, Series 2 study design neglecting time factor

N required	All tests
60 psi	8 specimens
80 psi	8 specimens
98 psi	8 specimens

Table 5-6, Series 2 study design including time factor

	15 s	60 s
60 psi	8 specimens	8 specimens
80 psi	8 specimens	8 specimens
98 psi	8 specimens	8 specimens

5.4.6 Other Comparisons

Where several discs were available from a single spine, same spine controls were used to perform tests with other variations for the sake of comparisons in the discussion section. These included varying the preload weight during hydration and performing tests in the posterolateral region. In some tests, needle placement errors result in rejection of the disc for the main study

without an injection having been performed. In such cases, secondary posterolateral tests were performed so as to avoid wasting the IVD.

5.4.7 Collecting Results

After each injection, the specimen IVD was sectioned using a thin blade. Care was taken to cut along the mid-plane of the IVD. This location was generally aligned with the same plane into which the injection was performed, and it was assumed that the defect length at this location would be reasonably representative of the magnitude of the tissue delamination/defect.

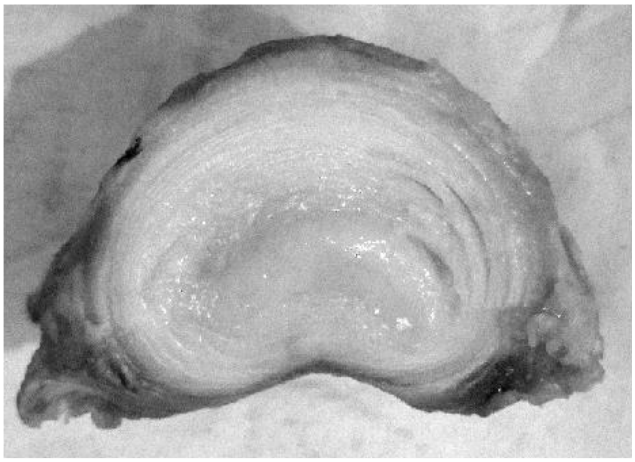

Figure 5-5, IVD with pre-existing annular tears

The butterflied disc was then placed beside a scale measure such as a steel rule and photographed. Disc images were uploaded to MatLab, and points on the image defined to identify the perimeter of the disc periphery, the NP periphery, and the geometry of any inked delamination. A MatLab script was used to find the disc centroid. A polar coordinate system was established with the disc centroid at the origin, and zero degrees extending from the centroid down through the posterior of the disc. To create a smooth plot, points between the defined points were interpolated using Piecewise Cubic Hermite Interpolating Polynomial or 'pchip' function. This function was less likely to create excess oscillation and discontinuities than a traditional spline interpolation.

Once the coordinate system had been established, disc area, geometry, tear length, tear depth, and the tear arc width were trivial to calculate. The tear depth was calculated as a ratio of the thickness of the AF. For every point in the tear, the annular thickness was found as the difference of the disc periphery radial distance from the centroid compared the NP periphery radial distance from the centroid. This code used in included in Apendix C (MAtLab Script for IVD Geometry Digitisation).

Chapter 6 Results

The process of injecting, imaging and digitising each IVD generated graphically results which are recorded in Apendix B (Anterior Results Imaging). The numerical results are discussed and analysed in this chapter but are tabulated in Apendix E (Results and Geometry for All IVDs).

6.1 IVD Usage and Study Group Changes

In the course of this study 97 IVDs were progressively harvested from 46 frozen ovine spines. The usage of these IVDs is summarized in **Error! Reference source not found.**. Of the 46 spines, several were excluded from the study when tissue degradation, freezer burn, and brittle vertebral bone was noted during cleaning and preparation. Another 18 IVDs were rejected due to cuts and injuries inflicted by the butchering at the abattoir or due to vertebral damage within 10 mm of the IVD.

73 IVDs were successfully hydrated and used for delamination tests over the course of this study. Nine discs were used in a pilot trial with injections into super swollen discs hydrated under a small pre-load of only 0.015 -0.039 MPa (9.8 N). Another seven discs were used in a pilot exploration of injections into the posterolateral region. The remaining 56 IVDs were assigned to treatment groups according to the experimental design described in 5.1 Experimental Design.

Some early tests included injection durations of 30 seconds for comparison with the 15-second and 60-second injections. After several IVDs had been rejected due to various errors and damage, it was found that only 3 specimens remained in

Total IVDs Harvested	97
Rejected spine IVDs	6
Damaged IVDs	18
PL Pilot Trial	8
Super Swell Pilot Trial	9

Anterior injection trials	56
Injections Depth Errors	5
Needle Struck Vertebral Endplate	3
Test processing errors	2
Excluded 30-sec injections	3
Included in study	43

Table 6-1, IVD Allocations and Use

the 30-second groups. Considering that power analysis showed that the number of groups needed to be reduced, it was decided to discontinue and exclude the 30-second trial groups.

In addition to presenting the results delaminations, the results confirmed the cross-sectional area of the IVDs. It was noticed that many of the discs were significantly larger than the recorded area estimates. Consequently, the pre-load pressure during hydration was less than specified and was more varied than anticipated. The difference between the 0.1 MPa preload groups and the 0.015 MPa preload pilot data was much smaller than anticipated, and less discretely distributed. Therefore, this error presented an opportunity to increase the number of samples by pooling data from the pilot trial with the data from the 0.1 MPa groups.

6.2 Mean Results

The results for the study are summarized in Table 6-2, including 98, 80, and 60 psi groups, 60 second and 15-second injection duration groups, and no exclusions based on hydration preload. Table 6-3 summarises the mean result for the same variable groups, with all hydration pre-loads < 0.04 MPa excluded. Mean results are graphically presented in Figure 6-1 through Figure 6-4.

Table 6-2, Result for all specimen groups and loading cases

Test Groups		IVDs Tested	IVDs (tear > 3 mm)	Success Rate	Delamination Length (mm)		Injection Depth (% of AF)		Hydration Preload (Mpa)	
Inject Pressure (psi)	Inject Duration (s)	(n)	Total	% delamination > 3 mm	Mean (mm)	SD	Mean	SD	Mean	SD
98	60	10	8	80%	16.8	15.05	64%	15%	0.057	0.018
98	15	11	7	64%	9.6	11.77	66%	10%	0.058	0.019
80	60	9	5	56%	19.2	22.85	66%	14%	0.059	0.020
80	15	5	2	40%	8.8	12.22	62%	8%	0.075	0.003
60	60	8	5	63%	13.8	17.40	62%	8%	0.068	0.009
60	15	7	1	14%	5.2	12.21	57%	7%	0.067	0.011

Table 6-3, Delamination Results for Hydration Preload 0.04 - 0.10 MPa

Test Groups		IVDs Tested	IVDs (tear > 3 mm)	Success Rate	Delamination Length (mm)		Injection Depth (% of AF)		Hydration Preload (Mpa)	
Inject Pressure (psi)	Inject Duration (s)	(n)	Total	% delamination > 3 mm	Mean (mm)	SD	Mean	SD	Mean	SD
98	60	7	6	86%	14.7	10.98	67%	15%	0.067	0.008
98	15	9	5	56%	6.5	6.28	67%	10%	0.066	0.009
80	60	7	4	57%	19.8	24.44	69%	15%	0.068	0.010
80	15	5	2	40%	8.8	12.22	62%	8%	0.075	0.003
60	60	8	5	63%	13.8	17.40	62%	8%	0.068	0.009
60	15	7	1	14%	5.2	13.31	57%	6%	0.067	0.012

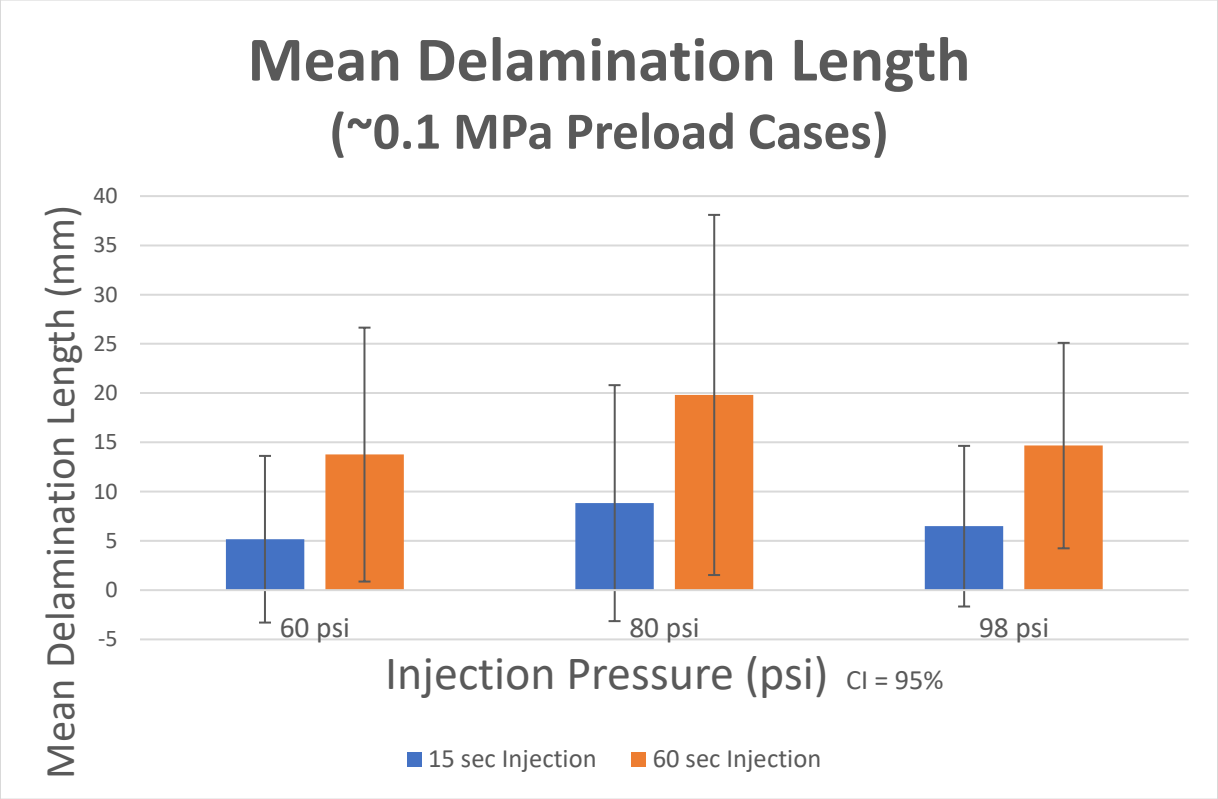

Figure 6-1, Mean delamination lengths, 0.1 MPa pre-loads

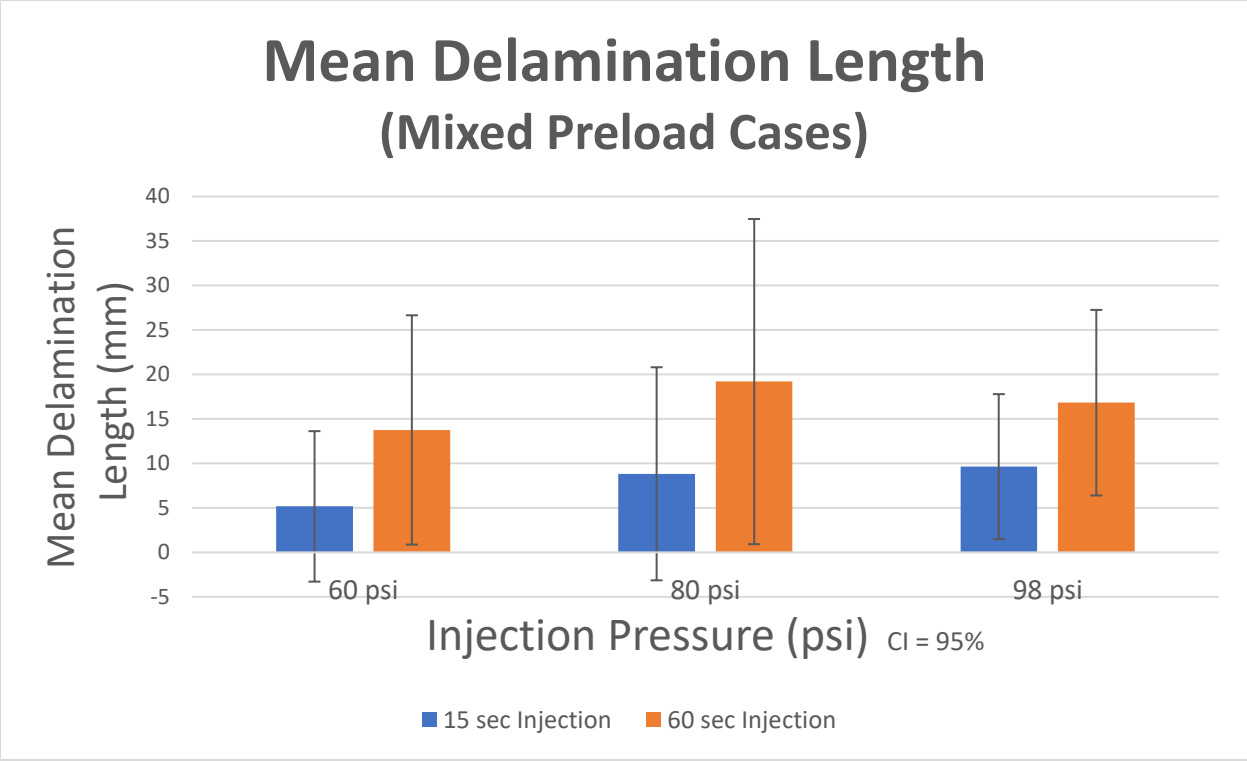

Figure 6-2, Mean delamination lengths, mixed pre-loads

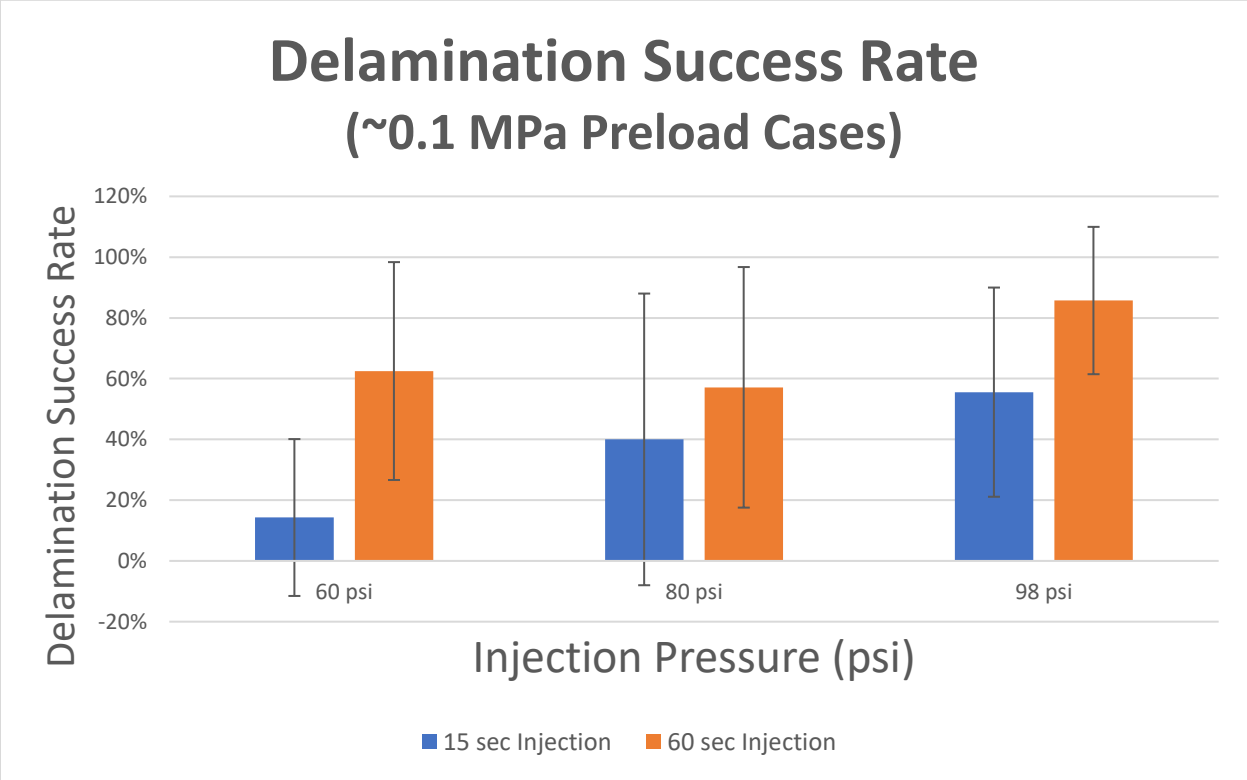

Figure 6-3, Delamination success rates, 0.1 MPa pre-loads

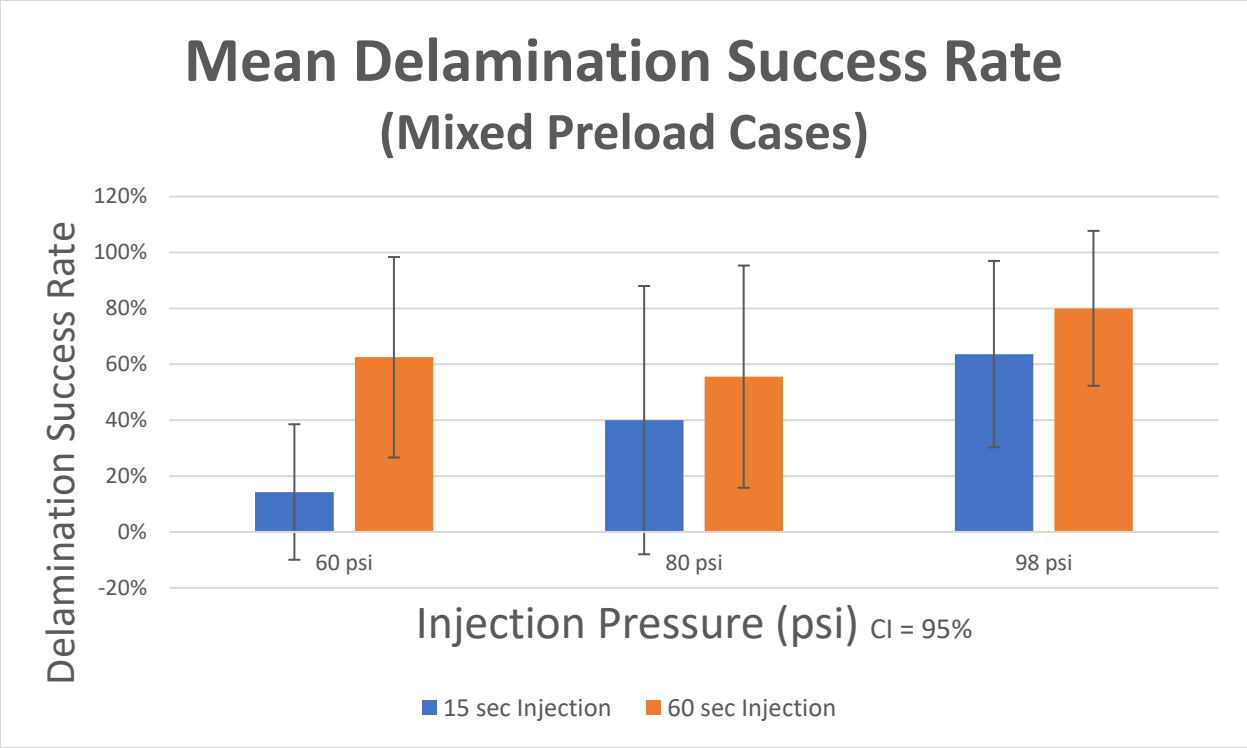

Figure 6-4, Delamination success rates, Mixed pre-loads

Figure 6-1 and Figure 6-2 show that the largest delaminations occurred in the 80 psi groups for 60-second injections. The pattern was similar in the 15-second injection groups, with Figure 6-2 showing that the full dataset had a similar mean for the 80 psi and 98 psi 15-second groups. On the other hand Figure 6-3 and Figure 6-4 showed that the 98 psi groups created the most delaminations (delamination > 3mm) with success rates better than 80% regardless of preload. However, the confidence interval (CI) error bars in Figure 6-1 - Figure 6-4 show that the results are unlikely to be significant. The large range of the CI combined with very small success rates in some groups and very large success rates in other groups, showing that the error bars could extend below zero, and above 100%. This indicates that the data is likely skewed and not normally distributed.

Similarly Table 6-2 and Table 6-3 also show that the 80 psi 60-second groups had the largest deviations for delaminations, indicating that this group probably contained outliers skewing the mean result.

6.3 Statistical Results

Chapter 7 With one dependent variable (DV) and two independent variables (IVs), a two-way ANOVA was the appropriate statistical test to test the hypotheses from 5.1 Experimental Design:

> Hypothesis 1) An increase in injection pressure will result in more delaminations and longer delaminations
>
> Hypothesis 2) An increase in the time duration of an injection will result in more delaminations and longer delaminations

This also implies

> Hypothesis 3) There is an interaction between injection pressure and duration affecting the number of delaminations and length of delaminations.

With only two groups in the injection duration variable, most post hoc tests were not available in the SPSS package. Similarly, no non-parametric alternative was found for a two way ANOVA with small numbers of groups. To meet the ANOVA test assumptions, including normal distribution of data, and no significant outliers, the data had to be transformed using the formula:

$$\text{Transformed Variable} = \ln(\text{DV}+1)$$

where DV is the dependent variable.

Tests were conducted with the untransformed data, to establish the need for transformation, and with the transformed data. An Analysis of Covariance (ANCOVA) was also conducted to verify the decision to pool data without control for hydration or disc area. The statistical tests and assumptions are described in more detail in Apendix D SPSS Statistics Outputs.

Table 6-4, Statistical Results, All groups and preload conditions

Statistical Test	Two Way ANOVA	Two Way ANOVA	Two way ANCOVA
Pressure Groups (psi)	60, 80, 98	60, 80, 98	60, 80, 98
Injection Duration groups (s)	15, 60	15, 60	15, 60
Independent Variables	Pressure, Duration	Pressure, Duration	Pressure, Duration
Dependent Variable	Length (L)	ln(L+1)	ln(L+1)
Levene's Test	0.199	0.072	0.48
Kolmogorov-Smirnov	0.000*	0.200	0.200
Shapiro-Wilkes	0.000*	0.160	0.160
Pressure	0.710	0.287	0.416
Time	0.069	0.071	0.099
Pressure * Time	0.961	0.834	0.822
Preload			0.552
Area			0.928

Table 6-4 summarises the statistical test performed on the complete data set, showing that the raw data severely violated the normality assumptions, failing to support the null hypothesis in Kolmogorov-Smirnov and Shapiro-Wilkes tests (p = 0). The transformed data did not violate assumptions, showing non-significant results for normality tests (p = 0.2, p = 0.16) and Levene's Equality of Error Test (p = 0.072).

The results did not show a relationship between injection pressure and delamination length (p = 0.287), or for a combination of injection pressure and injection duration (p = 0.834). Results were only marginally significant for a relationship between injection duration and delamination length (P = 0.071). Table 6-4 also showed no significant results in the ANCOVA for co-variants Preload (MPa) (p = 0.552) and IVD Area (mm^2) (p = 0.928).

With small samples (n < 25), the ANOVA is more sensitive to unbalanced study designs. The statistical tests were repeated with selected groups that formed a balanced study. This study included only the 60 and 98 psi data, only the 15 and 60-second data, and excluded the specimens with a preload < 0.04 MPa. These results are summarised in Table 6-5.

Table 6-5, Statistical test results on 98 and 60 psi, and only preloads of 0.04 MPa or greater

Statistical Test	Two Way ANOVA	Two Way ANOVA	Two way ANCOVA
Pressure Groups (psi)	60, 98	60, 98	60, 98
Injection Duration groups (s)	15, 60	15, 60	15, 60
Independent Variables	Pressure, Duration	Pressure, Duration	Pressure, Duration
Dependent Variable	Length (L)	ln(L+1)	ln(L+1)
Levene's Test	0.093	0.787	0.592
Kolmogorov-Smirnov	0.002	0.200	0.200
Shapiro-Wilkes	0.001	0.506	0.506
Pressure	0.802	0.166	0.145
Time	0.069	0.041*	0.042*
Pressure * Time	0.963	0.713	0.854
Preload			0.734
Area			0.341

Table 6-5 showed a very similar set of results to Table 6-4. The raw data severely failed normality assumptions ($p = 0.001$) and only marginally passed the equality of variance assumption ($p = 0.93$), while the transformed data did not violate ANOVA assumptions. Again, results only showed significance for the injection duration compared to delamination length. The ANCOVA did not show that hydration preload or disc area had any effect on the results ($p > 0.1$).

6.4 Binary Logistic Regression

As an alternative to using log transformed data, the data was transformed to a binary representation. All tested with a resultant delamination > 3mm were defined as a 1, with all non delaminated specimens defined as a 0. Logistic regression was carried out in order to test hypothesises;

Hypothesis 1) An increase in injection pressure will result in more delaminations

Hypothesis 2) An increase in the time duration of an injection will result in more delaminations

This test also test for interactions with variances to the preload hydration. This covariant was not included in the experimental design, but was tested due to the variance in preload magnitudes that occurred.

The results of the regression test are presented in Table 6-6, which showed marginal significance for both injection pressure (p = 0.066) and injection duration (0.083). Again, no significance was found for hydration preload as a covariant (p = 0.761)

Table 6-6, Binary Logistic Regression results, all data, delamination occurrence vs pressure, duration and preload

Variables in the Equation

		B	S.E.	Wald	df	Sig.	Exp(B)	95% C.I.for EXP(B) Lower	Upper
Step 1[a]	Injection Pressure (psi)	.038	.021	3.391	1	.066	1.039	.998	1.081
	Injection Duration (s)	.024	.014	3.008	1	.083	1.025	.997	1.053
	Hydration Preload (MPa)	-5.885	19.341	.093	1	.761	.003	.000	8081E+13
	Constant	-3.407	2.512	1.839	1	.175	.033		

a. Variable(s) entered on step 1: Injection Pressure (psi), Injection Duration (s), Hydration Preload (MPa).

Chapter 7 Discussion

This study aimed two hypotheses:

1) An increase in injection pressure will result in more delaminations and longer delaminations

2) An increase in the time duration of an injection will result in more delaminations and longer delaminations

This study was not able to show that these factors had a significant effect on the size or success rate of the resultant delaminations. However, it should be noted that despite varied sample quality and an number of unexpected technical challenges, the injector device was able to create delaminations in a number of IVDs, and there were no other factors present that delaminations could be causally correlated to. With further testing, there is still a lot to learn with similar experiments, and it may possible to establish the optimal parameters with which to delaminate IVDs.

7.1 Confounding factors

The results were defined in terms of the length of delaminations resulting from injections. There were a number of factors that had the potential to confound the results.

7.1.1 Spinal Factors

The primary concern was that the spines used for the study may have included specimens with tissue degradation due to long term storage. Each spine was examined and any spine showing signs of tissue damage was rejected. Any spine that had not been stored properly with PBS soaked wrappings or was not properly sealed was similarly rejected, as were spines that exhibited brittle or weak bone during specimen preparation, or IVDs that were found to have excessive pre-existing tears circumferential annular tears. However, it must be assumed that some low-quality specimens were included.

Such specimens had the potential to confound results by inflating the success rate or by resulting larger magnitude tears, obscuring the true effect and significance of parameters like injection pressure and duration. Despite this, it was not considered worthwhile to grade disc

quality via medical imaging for this initial study. It was hoped that the large number of specimens would counter the effect of any outliers.

Another potential confounding factor was the varied size of the IVDs. No IVDs were specified or excluded on the basis of disc area. It was not anticipated that disc size would be a relevant factor, as a pressurised fluid injection should have a local effect on the tissue and that this effect would be independent of the larger disc geometry. While not expected, it was possible that discs of differing sizes would have different magnitudes of delamination strength. Thus disc size would have the potential to bias the study results. This issue was addressed by performing ANCOVAs in order to control for effects from disc size. In addition, during injection trials, it was possible to arbitrarily assign an IVD to any of the pressure or duration groups. Generally, IVDs were simply randomly assigned, or assigned to groups that had the lowest number of specimens. However, a running tally was kept of the estimated average disc area for each group. This allowed IVDs to be assigned with a bias to balancing the mean disc size for each group. In this way, the mean disc size for each group was made as homogenous as possible.

7.1.2 Measurement Errors

The methods of this study required an estimate of IVD area. A major problem in this study was the failure of disc size estimates. For each IVD, the disc depth and width were measured with a vernier gauge, aiming to measure as close as possible to the marks shown in Figure 7-1. However, as is indicated by (A) in Figure 7-1, measurements to the disc limits were sometimes obstructed by residual posterior element surfaces or by additional ligamentous tissue. In such cases, the depth of the obstruction was estimated and subtracted from the measured size. This estimate increased the magnitude of any measurement errors.

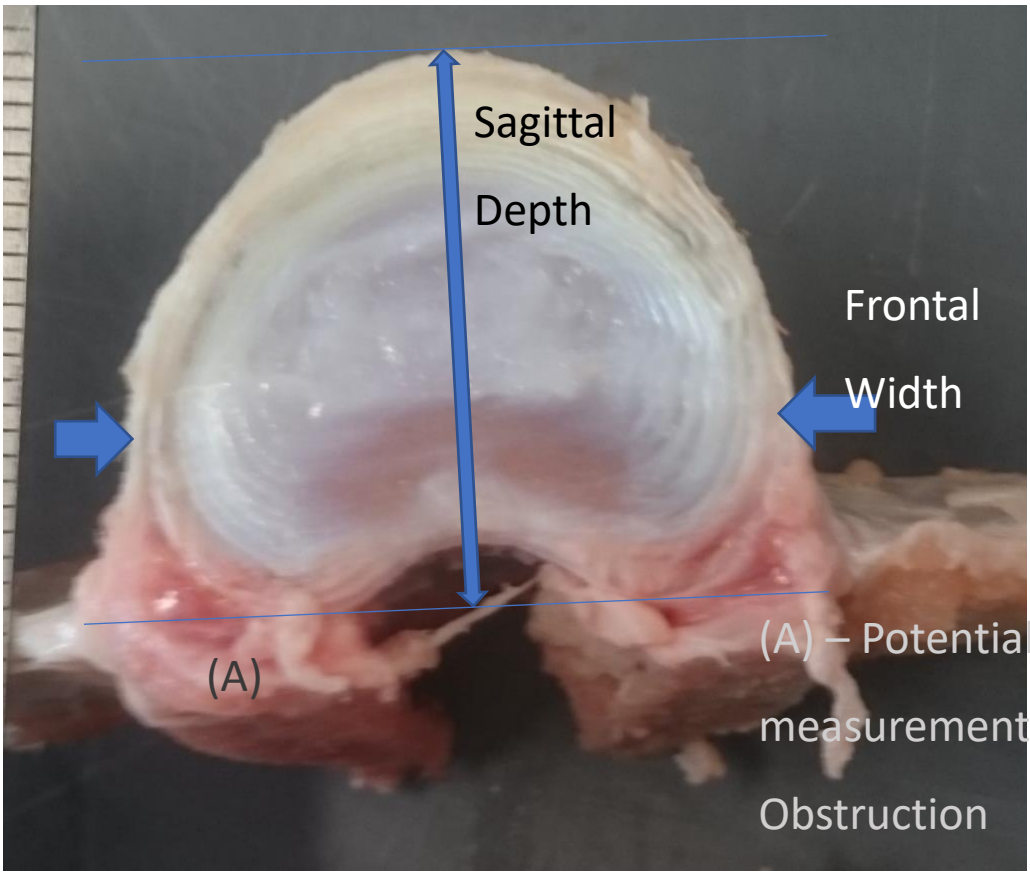

Figure 7-1, Positions for disc measurement

Similarly, measuring the frontal width involved estimating the correct point to place the vernier gauge without clamping additional ligamentous tissue. For both width and depth measurement, there was a considerable perception that it would be easy to create errors by overestimating the correct measurements. As a result, the investigator probably carried a significant bias to underestimate and under-report the estimated disc sizes. It was also found that a page of lab notes had been incorrectly transposed, leading to further error in the estimated disc areas.

The estimated hydration preload weights were calculated from the disc area preloads. The load applied to each IVD necessarily had to be composed from the discrete masses that were available in the lab, as can be seen in Figure 5-3. This meant that it was often impossible to load IVD to exactly the specified preload. Each IVD was loaded to with 3 Newtons or ±10% of the expected load, but this variation added another layer of potential error to the hydration loads.

After the injections were carried out, disc sizes were verified by measuring sectioned IVDs against a scale rule. Once the results had been processed, the actual hydration load experienced by the IVD was calculated from the measured disc area and the recorded preload. As can be seen in Figure 7-2 all the main study IVDs experienced a lower hydration preload than the specified 0.1 Mpa. This was probably due to the aforementioned disc area estimation errors.

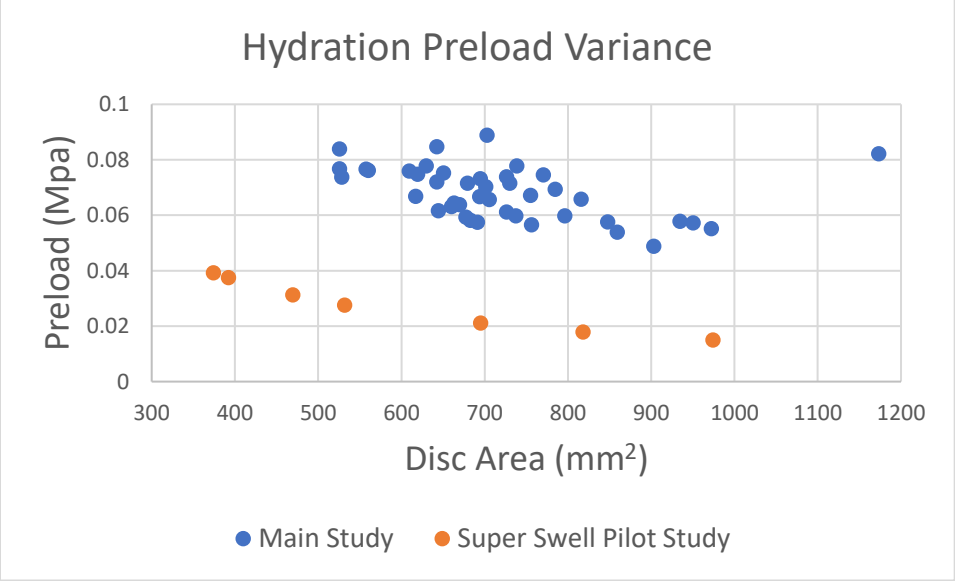

Figure 7-2, Actual preload magnitudes vs disc area

7.1.3 Needle Placement Challenges

Over the course of this study, 18 IVDs had to be rejected due to needle placement errors. Early pilots tests on low-quality IVDs did not indicate any difficulties in achieving correct needle placement, tangentially inserted into the inner anterior annulus, and the needle bevel was not aligned to any particular orientation. During the main study, an inordinate number of IVDs were found to have missed the target zone of the inner annulus. In some examples, it even appeared that the needle had flexed and followed the curve of lamella rather than penetrate further into the annulus, resulting in injections of ink very close to the outer surface of the annulus. It was difficult to verify that the needle was indeed following the lamellae, as very few IVDs in this study showed a visible needle track. It was noted that if a spine segment was not restrained

after the needle was inserted, some specimens would jump sideways, indicating that the needle was under flexion towards the outer annulus. An attempt to correct this was made by orientating the needle bevel to the transverse plane. In these cases, the needle had a marked tendency to flex towards either sagittal direction and impact the vertebral endplate. Any test in which the needle impacted the endplates was also immediately excluded from the study. In this way, it was noted that the needle was showing a tendency to dive towards the bevel, similar to behaviour one would observe with a bevelled chisel.

The solution to these challenges was to align the needle to the sagittal plane with the bevel face to the IVD anterior. This tended to bias the needle toward deeper penetration. Thus needle placement required the operator to both to estimate the thickness of the annulus from the shape of the disc and to estimate the depth of the correction required. However, once this needle alignment was adopted there were very few needle placement rejects.

7.2 Study Results

Table 7-1, Delamination success rate for injection groups (all data)

	Injection Duration (s)	
	15	60
98 psi	64%	80%
80 psi	40%	57%
60 psi	56%	86%

Of the 50 IVDs included in the results, 28 met the success criteria of inner annular delamination with a length > 3 mm. This translated to a success rate of 56% with a mean tear length of 23 mm. This clearly indicates that the device was successful in a majority of cases. Table 7-1 shows that with a success rate as high as 86% was achieved for 60 psi injections with a duration of 60 seconds. However statistical analysis did not show conclusive results. ANOVAs were conducted on the full data set of data, on a data restricted to preloads > 0.04 MPa (limit chosen as a boundary to remove the low preload pilot study specimens), and on data including only 98 psi and 60 psi groups with preload > 0.04 MPa (chosen to create a study with equal-sized groups). In each ANOVA or ANCOVA the results were similar, showing a significant or marginally significant effect for injection duration, but no significance for the injection pressure, the combined duration and pressure, and no significance for the covariants of disc area or preload. This can be seen in Table 6-4, and Table 6-5 in the

results section. Table 6-6 summarises logistic regression results, which only showed a marginal significance for a relationship between either injection pressure and injection duration having an effect on delamination occurrence.

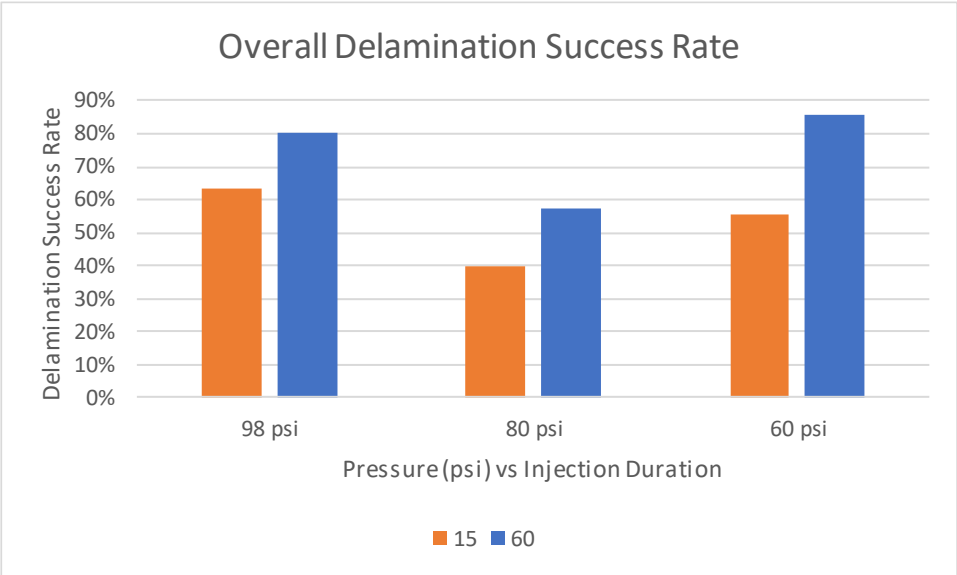

Figure 7-3, Success rates for injections to cause delamination

Figure 7-3 shows the breakdown of the success rate for each test group. This figure also provides an insight into the difficulty of finding significant trends in the data. In terms of the rate of successful delaminations, no clear correlation can be seen for pressure, but the success rate is clearly correlated to the duration of the injection. For comparison the mean results for each group are shown in Figure 7-4, demonstrating that looking at mean tear length shows a different pattern than looking at tear occurrence. The mean shows the expected trend, with resultant mean delamination length positively correlated both to injection duration and to injection pressure. However, the expected correlation for pressure is partly confounded by larger tear mean correlating to the 80 psi group than the 98 psi group. Figure 7-4 also demonstrates that the confidence intervals decrease both as pressure increases and as injection duration increases.

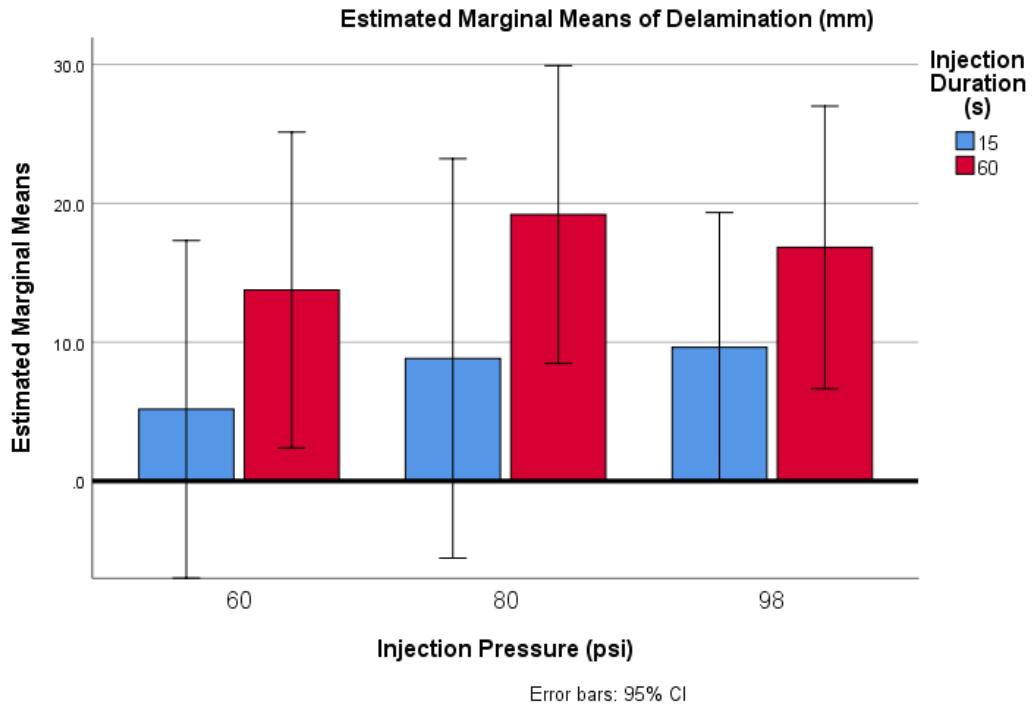

Figure 7-4, Mean delaminations vs Pressure and Duration

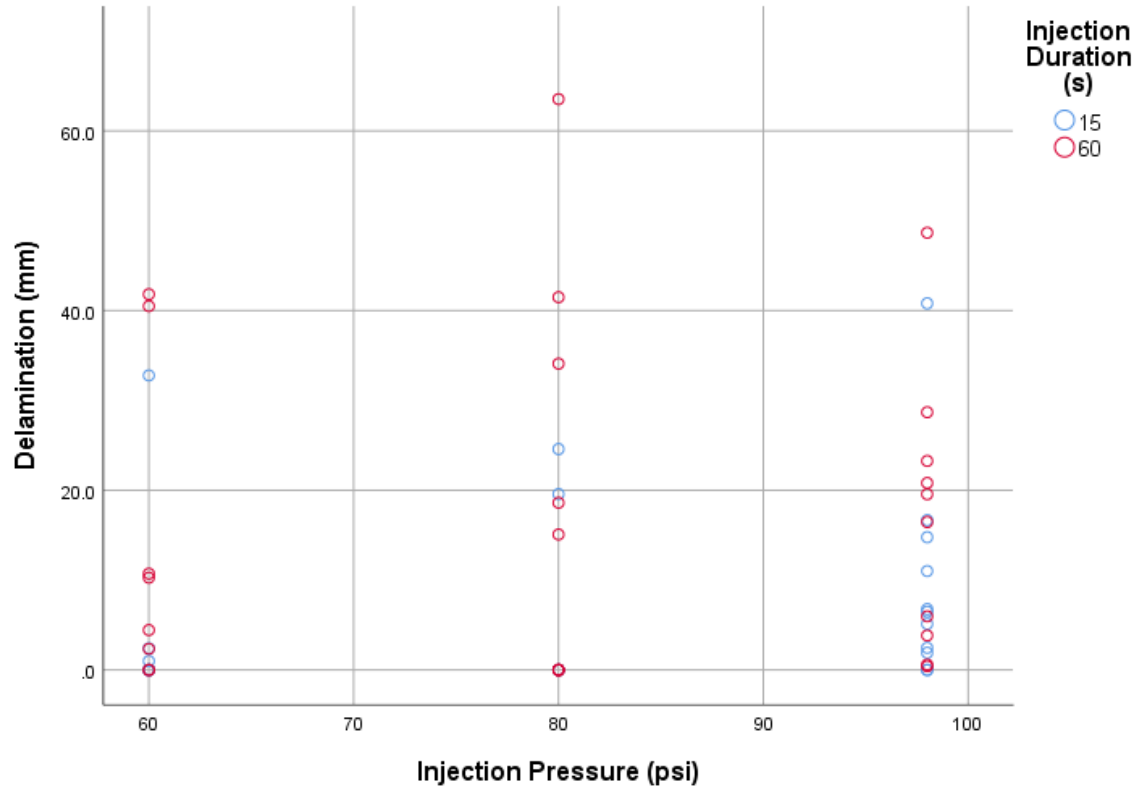

Figure 7-5, Scatterplot of all results

Figure 7-5 shows the scatterplot of the results and demonstrates the difficulty in attempting to find significant trends in the data. The sample size for each group is small while the variance of the outliers is quite large, obscuring the pattern. The trend is particularly obscured by the clustering of values at or near zero in each group.

A box chart was used to identify outliers, and a data set sans outliers was processed in SPSS. The result of this analysis is recorded in Apendix D. The mean results are shown in Figure 7-6, and a much clearer pattern is apparent. Without outliers, it appears that increases in both injection duration and injection duration contribute to longer resultant delaminations. Again, the confidence intervals decrease with increases in either of the independent variables, indicating that the effect becomes more reliable. However, as is discussed in Apendix D, the data distributions for this data set exhibited major violations of the ANOVA assumptions, so no P values could be confidently reported.

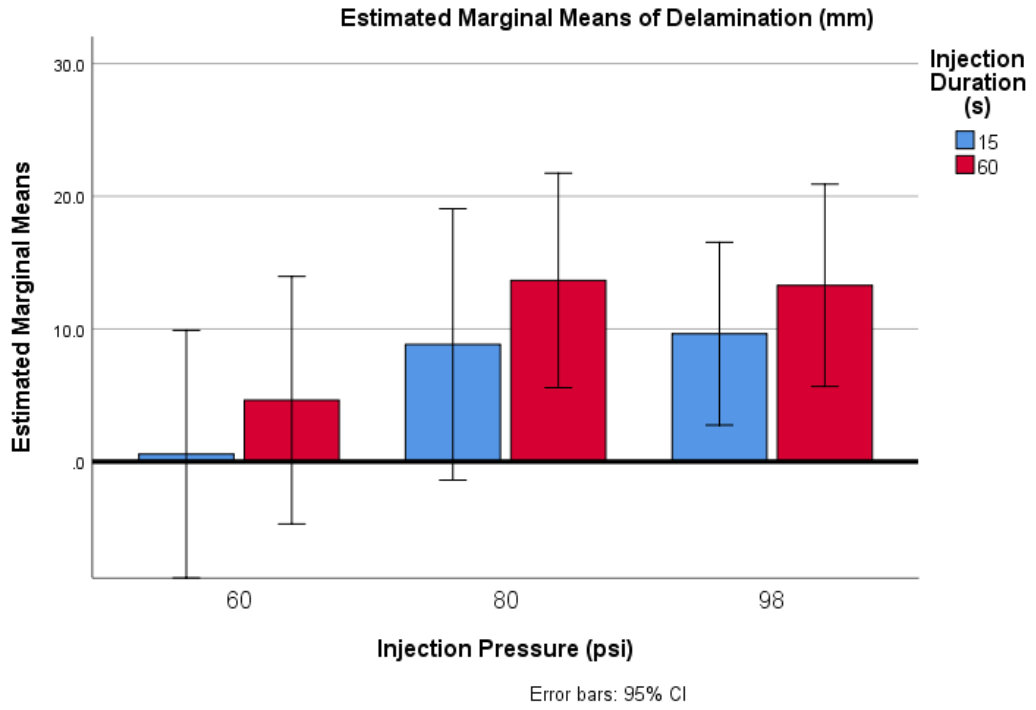

Figure 7-6, Mean delaminations with outliers removed

Figure 7-6 also shows that the mean delamination size was similar for both 80 psi and 98 psi groups. This may be an indication that of a potential threshold pressure above which

delamination results begin to plateau. But considering the confidence intervals, this interpretation is far from certain.

A possible explanation of the data, in general, is that at low-pressure magnitudes the ability to create delaminations is marginal, and the duration of injection has a more significant effect, giving the tissue time to delaminate. At higher pressure injections, the annulus may delaminate more reliably in a shorter time, making duration a less important concept. This would explain the apparent trends in the mean data that do not show as significant in the statistical analysis.

This study exhibited a high degree of uncertainty as was shown in the statistical tests. As an exploratory study, it was appropriate to make use of the large number of surplus spines that were available, including spines that had damaged lower lumbar discs, and spines that did not meet the size requirement for other studies. For this reason, this study had a bias towards using small-sized IVDs, and upper lumbar spinal segments. However, it is highly likely that variations in the quality and condition of the specimen contributed to the uncertainty of the results. This is highlighted by the fact that 36 of the IVDs had to be rejected. A post hoc power analysis using the GPower software (Faul et al., 2009), showed the power that was achieved given the detected effect sizes. The power analysis results are summarised in Table 7-2, which shows that for the observed effect sizes, a sample size of 166 would have been require in order to achieve significance (P = 0.05).

Table 7-2, Post Hoc Power Analysis

	Pressure	Time	Pressure*time
samples (n)	50	50	50
Groups	3	2	6
dfn	2	1	2
dfd	44	44	44
Eta^2	0.055	0.072	0.08
Effect size (f-value)	0.2412	0.2785	0.2949
critical F value	3.209	1.527	3.209
Study power	0.2945	0.5944	0.4210
min samples required to achieve significance at this effect size	166	104	114

Hence a much larger study would have been required to confidently define the effects due to pressure or time. However, the device did in fact delaminate a large number of IVDs. The study was not able to provide insight into the optimal parameters for delaminating IVDs with pressurised injections. On the other hand, the statistical results appear to show that there is no interaction between injection duration and injection pressure in predicting successful delaminations or the size of resultant delaminations. This can inform the design of future experiments, by empowering future investigators to focus on defining the effect of variations in injection pressure.

Chapter 8 Conclusion

This project was to develop a low-cost device capable of producing circumferential delaminations in the inner annulus. This was achieved with a simple pneumatic injector device and a lost cost off the shelf fluid dispenser. 56% of IVSs tested were delaminated with a mean delamination length of 22.3mm (SD ±15.2mm), indicating that the device was successful in meeting the project aim of creating delaminations. However, with a success rate of just 56%, the reliability of this device was not satisfactory.

The statistical analysis showed some significance for injection duration correlated to delamination length. It did not show a clear relationship between the pressure of the injections, or for the interaction of injection duration with pressure. In fact, the 80 psi group exhibited a success rate of 86% which was greater than that of the 98 psi group with a delamination success rate of 80%. When outliers were removed from the data a clear correlation was shown between injection pressure and delamination results, but this reduced data set was not compatible with statistical analysis. Attempting to control for co-variants of disc size and hydration preload did not improve the significance of the results, indicating that neither covariant had a significant effect on the outcomes.

Assessment for the results showed promise that resultant delamination size may be correlated to both injection duration and injection pressure. The results of the also support the idea that a delamination threshold may exist at some level in the vicinity of 80 psi (550 kPa).

This study was likely highly confounded by variation in specimen quality. It is recommended that these results be duplicated with a similar study using carefully fresh specimens that have been graded or otherwise controlled for IVD quality.

This injector could be used to delaminate IVDs for biomechanical studies. However, there is a high degree of uncertainty related to the success rate of this device until further validation is carried out. Should this injector technique be used for biomechanical studies prior to further validation, it would be necessary to validate the delamination result for each IVD, such as with medical imaging. It is suggested that a future study should examine the effects of varied injection pressures, while keeping the injection durations constant for all tests.

Chapter 9 References

Alini, M., Eisenstein, S.M., Ito, K., Little, C., Kettler, A.A., Masuda, K., Melrose, J., Ralphs, J., Stokes, I., Wilke, H.J., 2008. Are animal models useful for studying human disc disorders/degeneration? Eur. Spine J. 17, 2–19. https://doi.org/10.1007/s00586-007-0414-y

AS 1210-2010 | Pressure vessels | SAI Global [WWW Document], n.d. URL https://infostore.saiglobal.com/en-au/Standards/AS-1210-2010-127108_SAIG_AS_AS_268450/ (accessed 6.27.19).

Ashman, R.B., Bechtold, J.E., Edwards, W.T., Johnston, C.E.I., McAfee, P.C., Tencer, A.F., 1989. In Vitro Spinal Arthrodesis Implant Mechanical Testing Protocols. J. Spinal Disord. 2, 274–281.

Bogduk, N., 1997. Clinical Anatomy of the Lumbar Spine and Sacrum, 3rd ed. Churchill Livingstone.

Botwin, K.P., Gruber, R.D., Savarese, R., 2005. Lumbar discography. Tech. Reg. Anesth. Pain Manag. 9, 3–12. https://doi.org/10.1053/j.trap.2005.01.001

Buenaventura, R.M., Shah, R.V., Patel, V., Benyamin, R., Singh, V., 2007. Systematic Review of Discography as a Diagnostic Test for Spinal Pain: An Update. Pain Physician 19.

Carragee, E., Don, A., Hurwitz, E., Cuellar, J., Carrino, J., Herzog, R., 2009. 2009 ISSLS Prize Winner: Does Discography Cause Accelerated Progression of Degeneration Changes in the Lumbar Disc. Spine 34, 2338–2345. https://doi.org/10.1097/BRS.0b013e3181ab5432

Cohen, J.P., 1969. Statistical Power Analysis for the Behavioral Sciences. xvi + 416 pp. Acad. Press N. Y. 169, 167–168. https://doi.org/10.1126/science.169.3941.167

Costi, J.J., Hearn, T.C., Fazzalari, N.L., 2002. The effect of hydration on the stiffness of intervertebral discs in an ovine model. Clin. Biomech. 17, 446–455. https://doi.org/10.1016/S0268-0033(02)00035-9

Cuellar, J.M., Stauff, M.P., Herzog, R.J., Carrino, J.A., Baker, G.A., Carragee, E.J., 2016. Does provocative discography cause clinically important injury to the lumbar intervertebral disc? A 10-year matched cohort study. Spine J. 16, 273–280. https://doi.org/10.1016/j.spinee.2015.06.051

Dario, A.B., Ferreira, M.L., Refshauge, K.M., Lima, T.S., Ordoñana, J.R., Ferreira, P.H., 2015. The relationship between obesity, low back pain, and lumbar disc degeneration when genetics and the environment are considered: a systematic review of twin studies. Spine J. 15, 1106–1117. https://doi.org/10.1016/j.spinee.2015.02.001

Digital Fluid Dispenser - TS250 [WWW Document], n.d. URL http://www.techconsystems.com/en/fluid-dispensers/digital-fluid-dispensers/basic-digital-dispensers/ts250-digital-fluid-dispenser/?sef_rewrite=1 (accessed 6.27.19).

Elliott, D.M., Yerramalli, C.S., Beckstein, J.C., Boxberger, J.I., Johannessen, W., Vresilovic, E.J., 2008. The Effect of Relative Needle Diameter in Puncture and Sham Injection Animal Models of Degeneration. Spine 33, 588–596. https://doi.org/10.1097/BRS.0b013e318166e0a2

Faul, F., Erdfelder, E., Buchner, A., Lang, A.-G., 2009. Statistical power analyses using G*Power 3.1: Tests for correlation and regression analyses. Behav. Res. Methods 41, 1149–1160. https://doi.org/10.3758/BRM.41.4.1149

Fazzalari, N.L., Costi, J.J., Hearn, T.C., Fraser, R.D., Vernon-Roberts, B., Hutchinson, J., Manthey, B.A., Parkinson, I.H., Sinclair, C., 2001. Mechanical and Pathologic Consequences of Induced Concentric Anular Tears in an Ovine Model. Spine 26, 2575.

Gregory, D.E., Bae, W.C., Sah, R.L., Masuda, K., 2012. Anular delamination strength of human lumbar intervertebral disc. Eur. Spine J. 21, 1716–1723. https://doi.org/10.1007/s00586-012-2308-x

Hansson, T., Roos, B., 1981. The Relation Between Bone Mineral Content, Experimental Compression Fractures, and Disc Degeneration in Lumbar Vertebrae | Ovid [WWW Document]. URL https://oce-ovid-com.ezproxy.flinders.edu.au/article/00007632-198103000-00007/HTML (accessed 6.26.19).

Hoy, D., March, L., Brooks, P., Blyth, F., Woolf, A., Bain, C., Williams, G., Smith, E., Vos, T., Barendregt, J., Murray, C., Burstein, R., Buchbinder, R., 2014. The global burden of low back pain: estimates from the Global Burden of Disease 2010 study. Ann. Rheum. Dis. 73, 968–974. https://doi.org/10.1136/annrheumdis-2013-204428

Hurwitz, E.L., Randhawa, K., Yu, H., Côté, P., Haldeman, S., 2018. The Global Spine Care Initiative: a summary of the global burden of low back and neck pain studies. Eur. Spine J. 27, 796–801. https://doi.org/10.1007/s00586-017-5432-9

Iatridis, J.C., ap Gwynn, I., 2004. Mechanisms for mechanical damage in the intervertebral disc annulus fibrosus. J. Biomech. 37, 1165–1175. https://doi.org/10.1016/j.jbiomech.2003.12.026

Iatridis, J.C., Weidenbaum, M., Setton, L.A., Mow, V.C., 1996. Is the Nucleus Pulposus a Solid or a Fluid? Mechanical Behaviors of the Nucleus Pulposus of the Human Intervertebral Disc. Spine 21, 1174.

Indrajit, I.K., Sivasankar, R., D'Souza, J., Pant, R., Negi, R.S., Sahu, S., Hashim, P., 2015. Pressure injectors for radiologists: A review and what is new. Indian J. Radiol. Imaging 25, 2–10. https://doi.org/10.4103/0971-3026.150105

Korecki, C.L., Costi, J.J., Iatridis, J.C., 2008. Needle Puncture Injury Affects Intervertebral Disc Mechanics and Biology in an Organ Culture Model. Spine 33, 235–241. https://doi.org/10.1097/BRS.0b013e3181624504

Martin, J.T., Gorth, D.J., Beattie, E.E., Harfe, B.D., Smith, L.J., Elliott, D.M., 2013. Needle puncture injury causes acute and long-term mechanical deficiency in a mouse model of intervertebral disc degeneration. J. Orthop. Res. Off. Publ. Orthop. Res. Soc. 31, 1276–1282. https://doi.org/10.1002/jor.22355

Moore, R.J., Latham, J.M., Vernon-Roberts, B., Fraser, R.D., 1994. Does plate fixation prevent disc degeneration after a lateral anulus tear? Spine 19, 2787–2790.

Nachemson, A., Morris, J.M., 1964. IN VIVO MEASUREMENTS OF INTRADISCAL PRESSURE. DISCOMETRY, A METHOD FOR THE DETERMINATION OF PRESSURE IN THE LOWER LUMBAR DISCS. J. Bone Joint Surg. Am. 46, 1077–1092.

Osti, O.L., Vernon-Roberts, B., Fraser, R.D., 1990. 1990 Volvo Award in experimental studies. Anulus tears and intervertebral disc degeneration. An experimental study using an animal model. Spine 15, 762–767.

Race, A., Broom, N.D., Robertson, P., 2000. Effect of Loading Rate and Hydration on the Mechanical Properties of the Disc. Spine 25, 662.

Schollum, M., Robertson, P., Broom, N., 2008. ISSLS Prize Winner: Microstructure and Mechanical Disruption of the Lumbar Disc Annulus: Part I: A Microscopic Investigation of the Translamellar Bridging Network | Ovid [WWW Document]. URL https://oce-ovid-com.ezproxy.flinders.edu.au/article/00007632-200812010-00004/HTML (accessed 5.29.19).

Tavakoli, J., Amin, D.B., Freeman, B.J.C., Costi, J.J., 2018. The Biomechanics of the Inter-Lamellar Matrix and the Lamellae During Progression to Lumbar Disc Herniation: Which is the Weakest Structure? Ann. Biomed. Eng. https://doi.org/10.1007/s10439-018-2056-0

Tavakoli, J., Elliott, D.M., Costi, J.J., 2016. Structure and mechanical function of the inter-lamellar matrix of the annulus fibrosus in the disc: INTER-LAMELLAR MATRIX OF THE INTER-VERTEBRAL DISC. J. Orthop. Res. 34, 1307–1315. https://doi.org/10.1002/jor.23306

Tomecek, F.J., Anthony, C.S., Boxell, C., Warren, J., 2002. Discography interpretation and techniques in the lumbar spine. Neurosurg. Focus 13, 1–8. https://doi.org/10.3171/foc.2002.13.2.14

Tymecka-Woszczerowicz, A., Wrona, W., Kowalski, P.M., Hermanowski, T., 2015. Indirect costs of back pain – Review. Pol. Ann. Med. 22, 143–148. https://doi.org/10.1016/j.poamed.2015.07.003

Urban, J.P., Roberts, S., 2003. Degeneration of the intervertebral disc. Arthritis Res Ther 5, 120. https://doi.org/10.1186/ar629

Urban, J.P.G., Maroudas, A., 1981. Swelling of the Intervertebral Disc in Vitro. Connect. Tissue Res. 9, 1–10. https://doi.org/10.3109/03008208109160234

Urban, J.P.G., Smith, S., Fairbank, J.C.T., 2004. Nutrition of the intervertebral disc. Spine 29, 2700–2709.

Veres, S.P., Robertson, P.A., Broom, N.D., 2010. The influence of torsion on disc herniation when combined with flexion. Eur. Spine J. 19, 1468–1478. https://doi.org/10.1007/s00586-010-1383-0

Veres, S.P., Robertson, P.A., Broom, N.D., 2008. ISSLS Prize Winner: Microstructure and Mechanical Disruption of the Lumbar Disc Annulus: Part II: How the Annulus Fails Under Hydrostatic Pressure | Ovid [WWW Document]. URL https://oce-ovid-com.ezproxy.flinders.edu.au/article/00007632-200812010-00005/HTML (accessed 7.29.19).

Vernon-Roberts, B., Fazzalari, N.L., Manthey, B.A., 1997. Pathogenesis of Tears of the Anulus Investigated by Multiple-Level Transaxial Analysis of the T12-L1 Disc. Spine 22, 2641.

Vernon-Roberts, B., Moore, R., Fraser, R., 2007. The Natural History of Age-related Disc Degeneration: The Pathology and Sequelae of Tears | Ovid [WWW Document]. URL https://oce.ovid.com/article/00007632-200712010-00004/HTML (accessed 3.14.19).

Walker, J., El Abd, O., Isaac, Z., Muzin, S., 2008. Discography in practice: a clinical and historical review. Curr. Rev. Musculoskelet. Med. 1, 69–83. https://doi.org/10.1007/s12178-007-9009-9

Wang, Y., Liu, T., Song, L.-S., Zhang, Z.-X., Li, Y.-Q., Lu, L.-J., 2015. Anatomical Characteristics of Deer and Sheep Lumbar Spines: Comparison to the Human Lumbar Spine. Int. J. Morphol. 33, 105–112. https://doi.org/10.4067/S0717-95022015000100018

Wilke, H.J., Kettler, A., Wenger, K.H., Claes, L.E., 1997. Anatomy of the sheep spine and its comparison to the human spine. Anat. Rec. 247, 542–555. https://doi.org/10.1002/(SICI)1097-0185(199704)247:4<542::AID-AR13>3.0.CO;2-P

Wilke, H.J., Neef, P., Caimi, M., Hoogland, T., 1999. New In Vivo Measurements of Pressures in the Intervertebral Disc in Daily Life | Ovid [WWW Document]. URL https://oce.ovid.com/article/00007632-199904150-00005/HTML (accessed 4.17.19).

Apendix A Injector Set-up SOP

1. Ensure that the work area is clean, neat, organised, and ready for safe use.
2. Ensure that a sharps container is available for needle disposal
3. Slide support block onto the pressure syringe barrel
4. Attach syringe barrel to the sensor block Luer fitting
5. Press support block to attach to sensor block via friction fitting

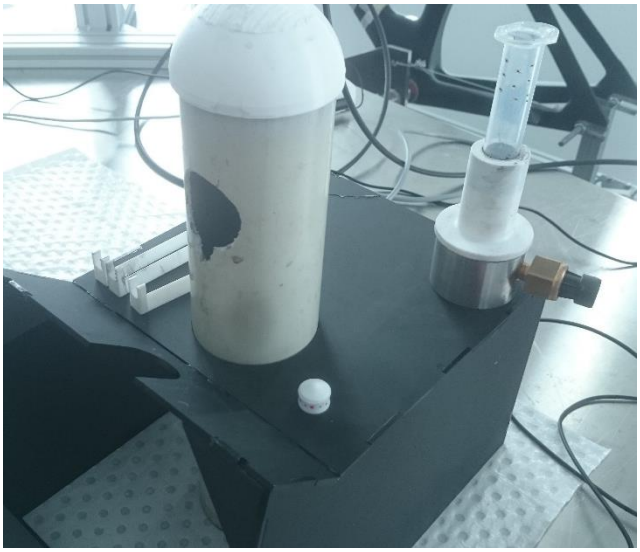

Figure A-1,Needle assembly in safety stand, prior to filling

6. Attach the hypodermic syringe to the sensor block
7. Carefully remove the needle cover.
8. Place needle assembly, needle down, into safety stand, such that needle protrudes down into the shielded section of the stand as in Figure A-1, preventing potential needle-stick injuries.
9. Place catcher bowl under the syringe.
10. The barrel is now pointing vertically upwards.
11. Fill syringe barrel with PBS buffer solution, coloured with india ink as shown in Figure A-2
12. Tap the sensor block sharply with a screwdriver or other hard implement to dislodge bubbles

Figure A-2, Filling injector syringe barrel

13. When the syringe barrel is full, and fluid has filled the adaptor block, there should be a slow drip from the hypodermic needle. Place the pneumatic piston fitting into the syringe barrel, preventing further fluid loss.
14. Remove syringe assembly and invert it, being careful of the exposed needle. Place syringe assembly into inclined syringe stand with needle safely in the catcher tube, as shown in Figure A-3
15. Rotate the sensor body until the pressure fitting is at it lowest achievable position.
16. Tap sensor block sharply with a hard implement to dislodge any bubbles.
17. Connect the pneumatic line at the desired pressure. Ensure that the needle is still safely pointed into the collector tube. The collector tube will contain the needle in the event of a failure under pressure.

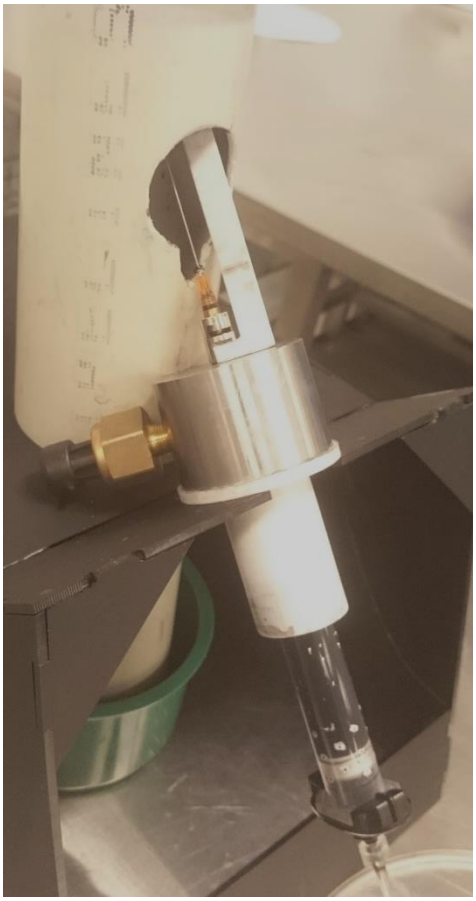

Figure A-3, Filled syringe in safety stand, ready for priming

18. Set timer control to 0.1-0.3 seconds.
19. Observing the needle, perform a brief spray into the collector tube. Observe stream to ensure that the needle is not blocked. The fluid will be collected in the drip tray.
20. Observing the pneumatic piston, perform a brief spray into the collector tube. If the application of pressure spray is observed to force air past the pressure piston into the saline mixture, replace the piston and/or syringe barrel and restart the procedure.
21. Regularly tapping the sensor block to dislodge bubble and air pockets, continue performing small sprays into collector tube until piston does not rebound significantly following a pressure spray. This indicates that the system is now free of bubbles and air-pockets.

22. Connect Sensor cable, and perform one more spray, observing to see if senor readings are as expected.
23. Ensure that syringe is more than half full before performing an injection.
24. The injector is now ready for general use. Set time and pressure parameters on the fluid dispenser as required.
25. This procedure must be followed each time the syringe barrel is disconnected or refilled.

Apendix B Anterior Results Imaging

Ovine Intervertebral Disc Cross Section - S1L1
AN injection :30s at 60 psi (414 kPa)

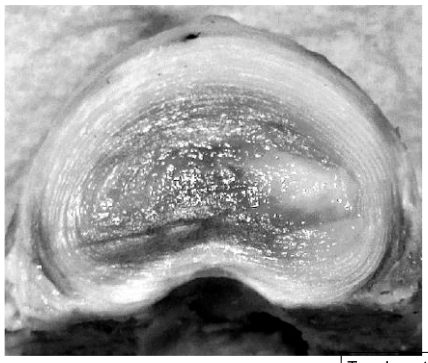

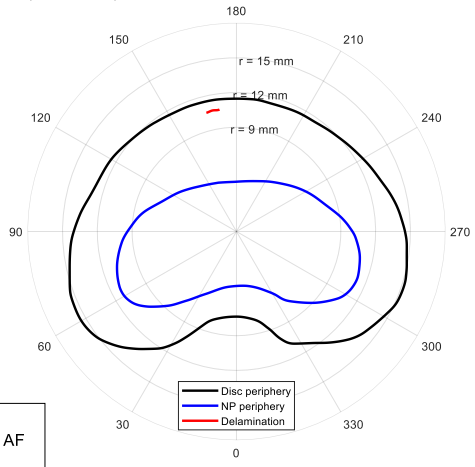

Tear Length :1.2 mm
Needle depth :12.6% of AF
Tear Arc :6.3 degrees
Disc Area :489.6 mm^2

Ovine Intervertebral Disc Cross Section - S4L2
AN injection :60s at 98 psi (676 kPa)

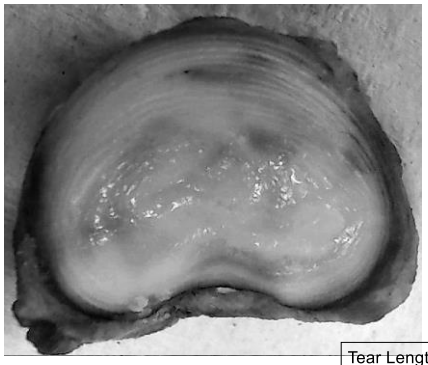

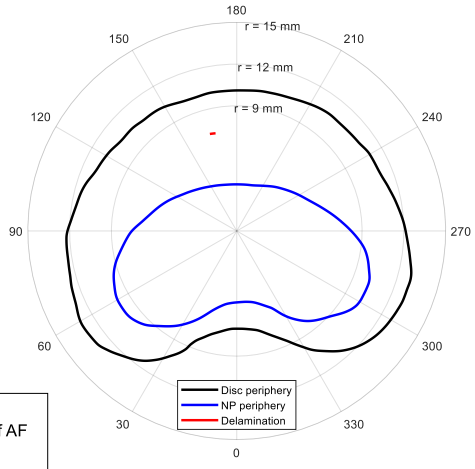

Tear Length :0.4 mm
Needle depth :43.1% of AF
Tear Arc :3.2 degrees
Disc Area :374.1 mm^2

Ovine Intervertebral Disc Cross Section - S5L1
AN injection :60s at 98 psi (676 kPa)

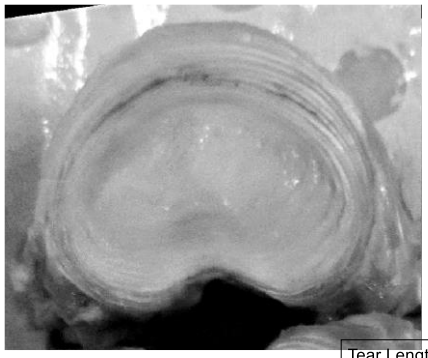

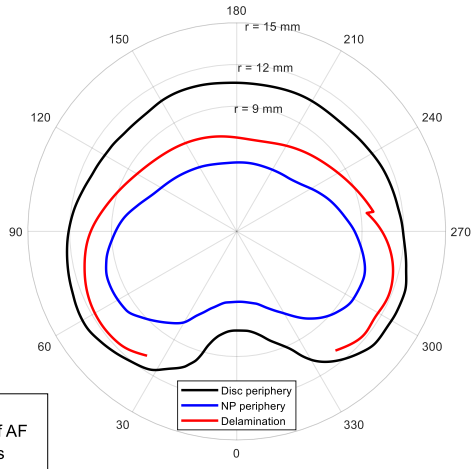

Tear Length :48.7 mm
Needle depth :67.4% of AF
Tear Arc :284.7 degrees
Disc Area :392.1 mm^2

Ovine Intervertebral Disc Cross Section - S5L2
AN injection :15s at 98 psi (676 kPa)

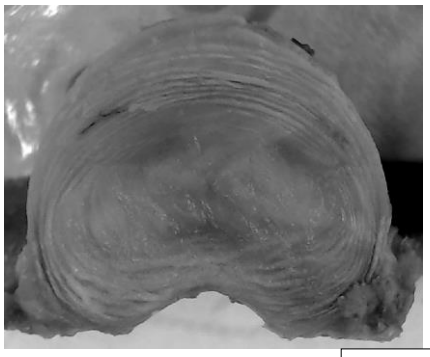

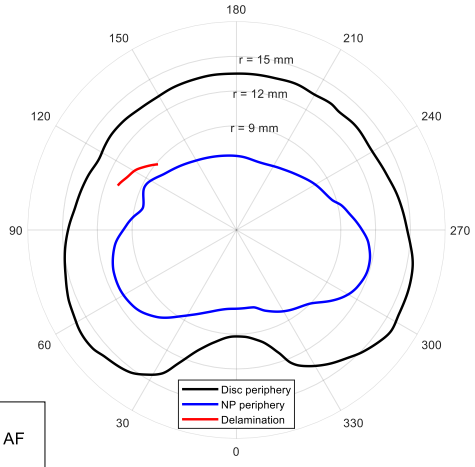

Tear Length :4.1 mm
Needle depth :50.0% of AF
Tear Arc :19.4 degrees
Disc Area :603.6 mm^2

Ovine Intervertebral Disc Cross Section - S6L1
AN injection :15s at 98 psi (676 kPa)

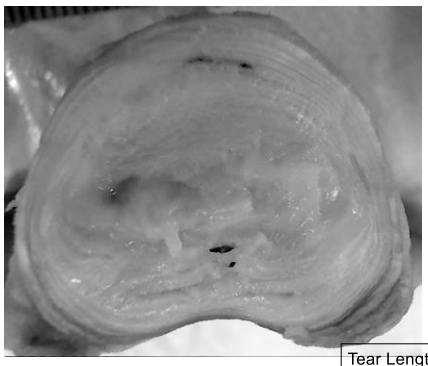

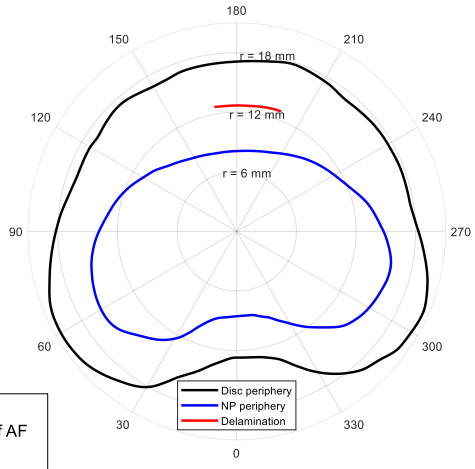

Tear Length :6.8 mm
Needle depth :50.1% of AF
Tear Arc :30.4 degrees
Disc Area :974.3 mm^2

Ovine Intervertebral Disc Cross Section - S6L2
AN injection :60s at 98 psi (676 kPa)

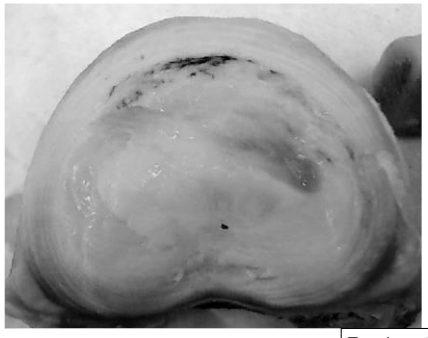

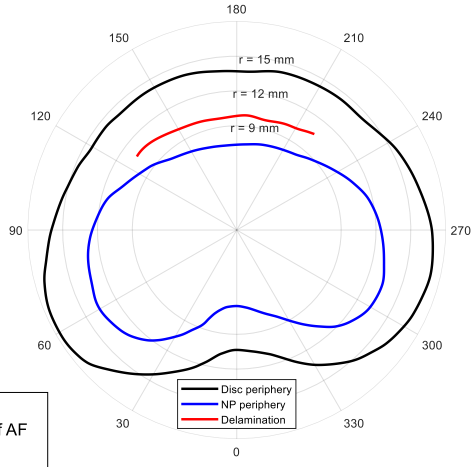

Tear Length :16.5 mm
Needle depth :64.1% of AF
Tear Arc :92.5 degrees
Disc Area :695.1 mm^2

Ovine Intervertebral Disc Cross Section - S9L1
AN injection :30s at 80 psi (552 kPa)

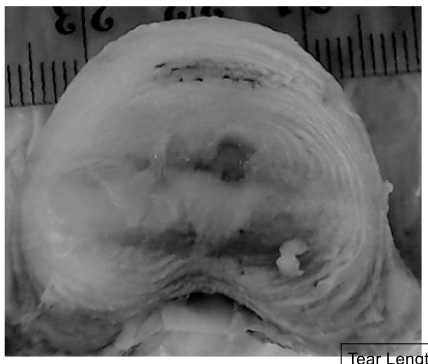

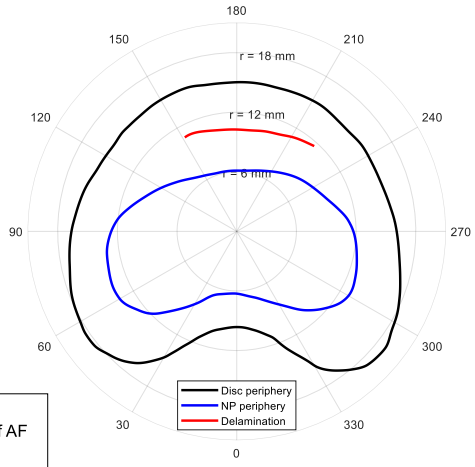

Tear Length :13.4 mm
Needle depth :52.4% of AF
Tear Arc :71.1 degrees
Disc Area :757.9 mm^2

Ovine Intervertebral Disc Cross Section - S10L1
AN injection :30s at 80 psi (552 kPa)

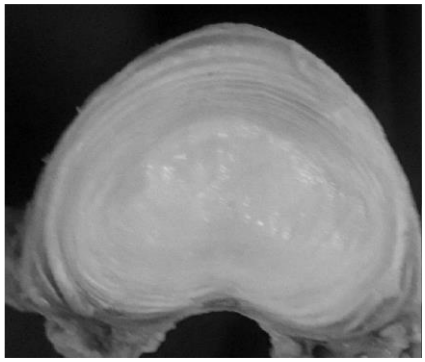

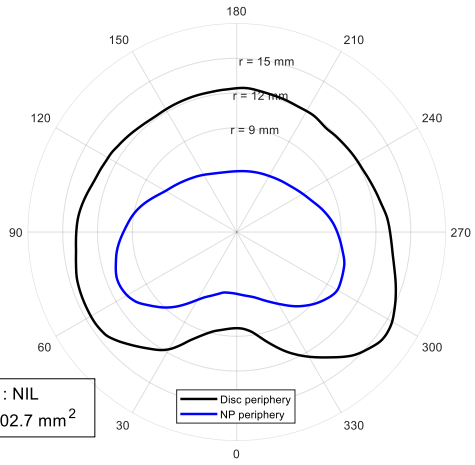

Tear Length : NIL
Disc Area :502.7 mm^2

Ovine Intervertebral Disc Cross Section - S11L1
AN injection :60s at 80 psi (552 kPa)

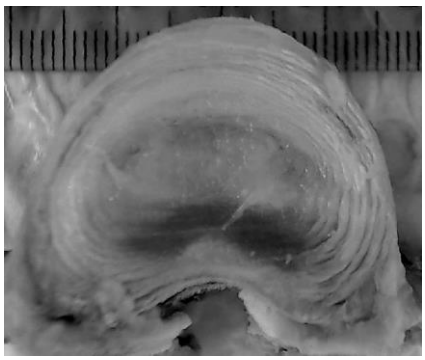

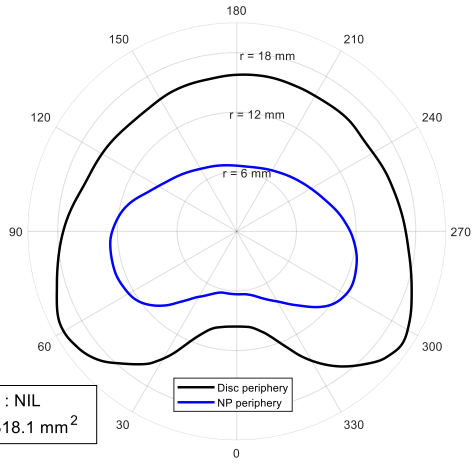

Tear Length : NIL
Disc Area :818.1 mm^2

Ovine Intervertebral Disc Cross Section - S12L1
AN injection :60s at 80 psi (552 kPa)

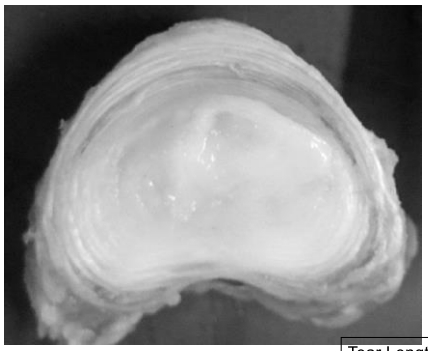

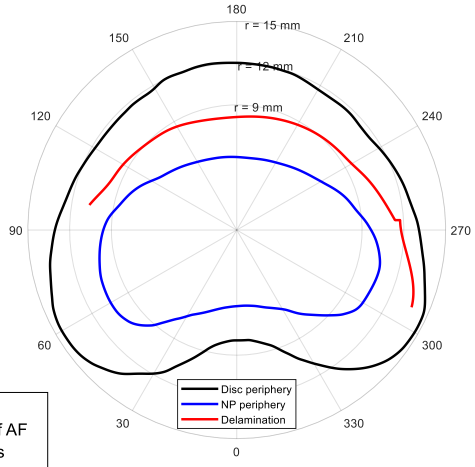

Tear Length :34.1 mm
Needle depth :55.2% of AF
Tear Arc :194.2 degrees
Disc Area :469.5 mm^2

Ovine Intervertebral Disc Cross Section - S15
AN injection :15s at 98 psi (676 kPa)

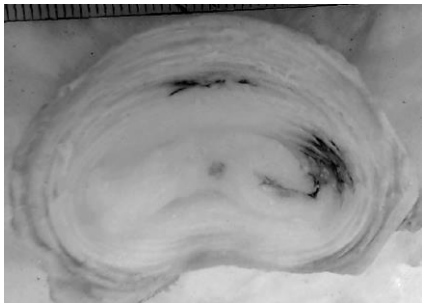

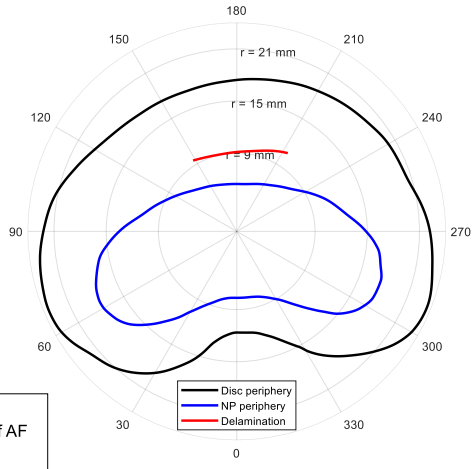

Tear Length :11.0 mm
Needle depth :68.6% of AF
Tear Arc :64.7 degrees
Disc Area :1173.2 mm^2

Ovine Intervertebral Disc Cross Section - S16L1
AN injection :30s at 98 psi (676 kPa)

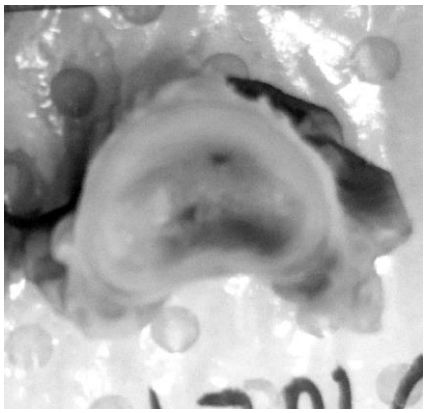

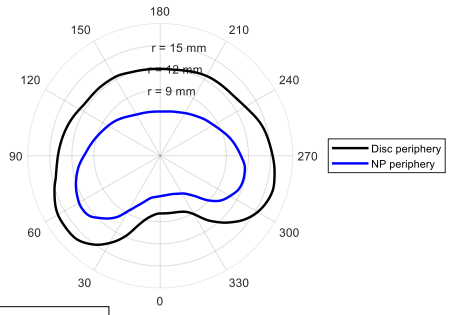

Tear Length : NIL
Disc Area :534.1 mm^2

Ovine Intervertebral Disc Cross Section - S16L2
AN injection :15s at 98 psi (676 kPa)

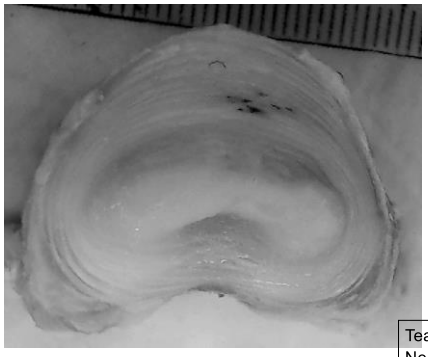

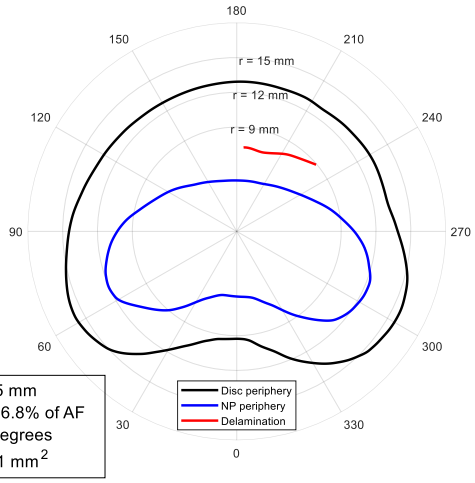

Tear Length :6.5 mm
Needle depth :66.8% of AF
Tear Arc :45.3 degrees
Disc Area :560.1 mm^2

Ovine Intervertebral Disc Cross Section - S17L1
AN injection :60s at 98 psi (676 kPa)

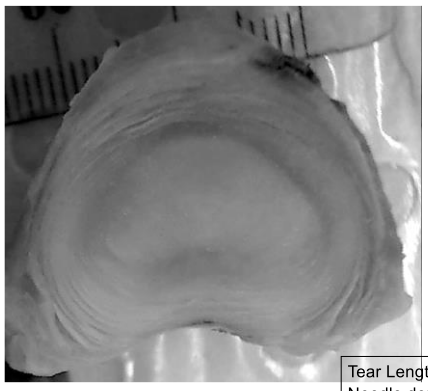

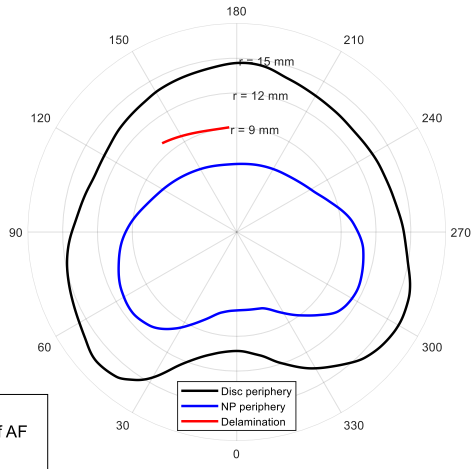

Tear Length :6.0 mm
Needle depth :61.2% of AF
Tear Arc :35.9 degrees
Disc Area :617.0 mm^2

Ovine Intervertebral Disc Cross Section - S21LX
AN injection :60s at 80 psi (552 kPa)

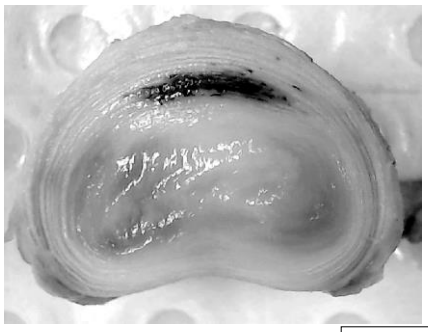

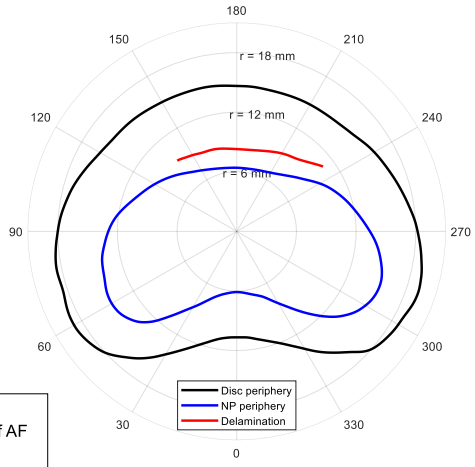

Tear Length :15.1 mm
Needle depth :76.0% of AF
Tear Arc :93.1 degrees
Disc Area :796.1 mm^2

Ovine Intervertebral Disc Cross Section - S22L1
AN injection :60s at 80 psi (552 kPa)

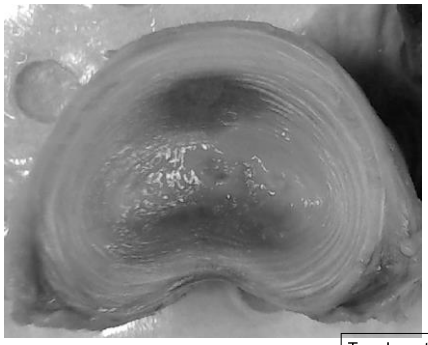

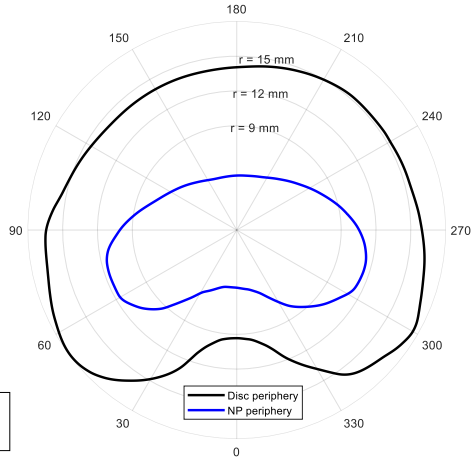

Tear Length : NIL
Disc Area :702.8 mm^2

Ovine Intervertebral Disc Cross Section - S23L1
AN injection :15s at 80 psi (552 kPa)

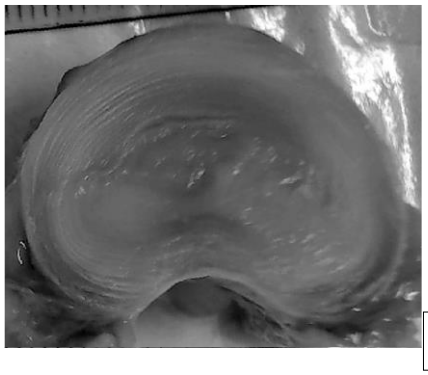

Tear Length : NIL
Disc Area :525.5 mm^2

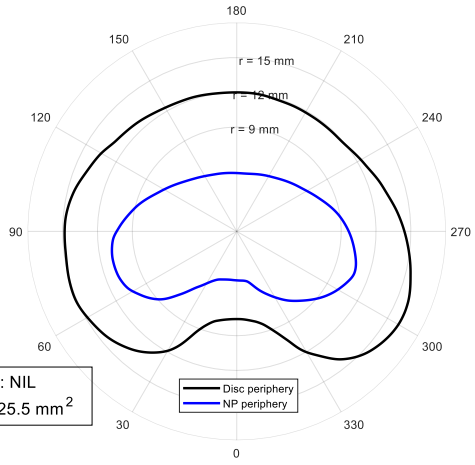

Ovine Intervertebral Disc Cross Section - S29LX
AN injection :15s at 80 psi (552 kPa)

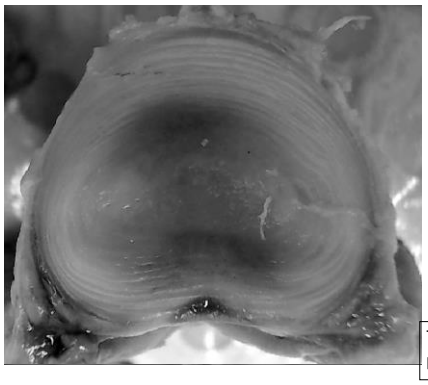

Tear Length : NIL
Disc Area :730.0 mm^2

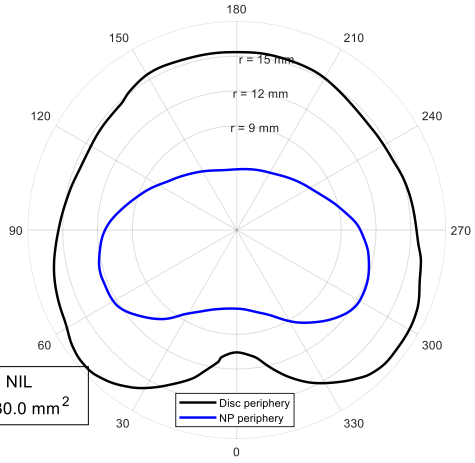

Ovine Intervertebral Disc Cross Section - S30LX
AN injection :60s at 80 psi (552 kPa)

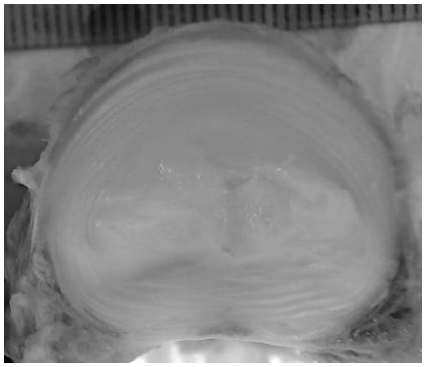

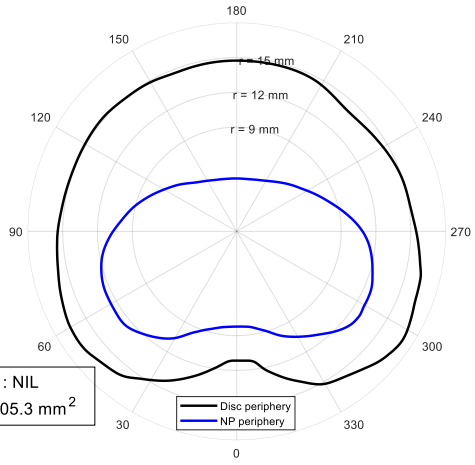

Tear Length : NIL
Disc Area :705.3 mm^2

Ovine Intervertebral Disc Cross Section - S31TL
AN injection :15s at 98 psi (676 kPa)

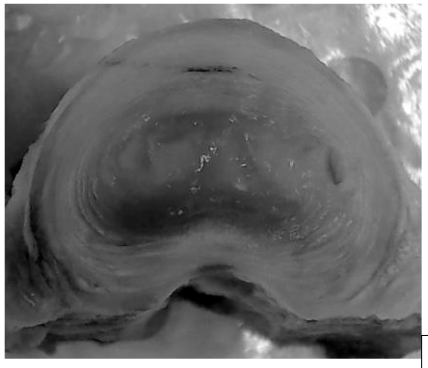

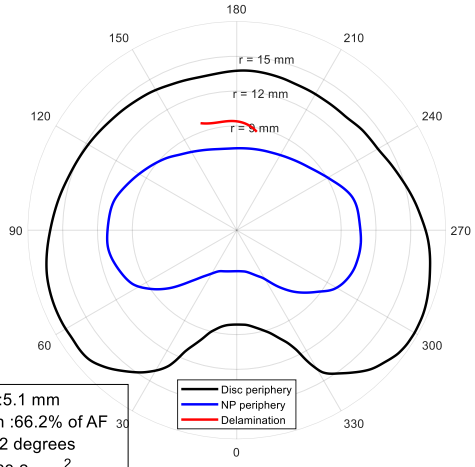

Tear Length :5.1 mm
Needle depth :66.2% of AF
Tear Arc :30.2 degrees
Disc Area :663.2 mm^2

Ovine Intervertebral Disc Cross Section - S31L1
AN injection :15s at 80 psi (552 kPa)

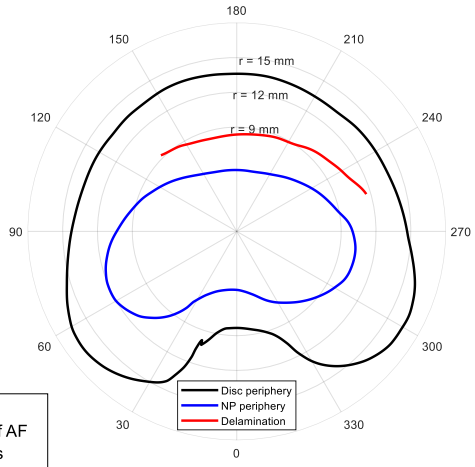

Tear Length :19.6 mm
Needle depth :62.5% of AF
Tear Arc :118.8 degrees
Disc Area :609.4 mm^2

Ovine Intervertebral Disc Cross Section - S31L2
AN injection :60s at 98 psi (676 kPa)

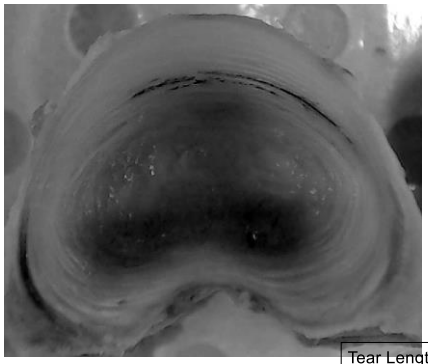

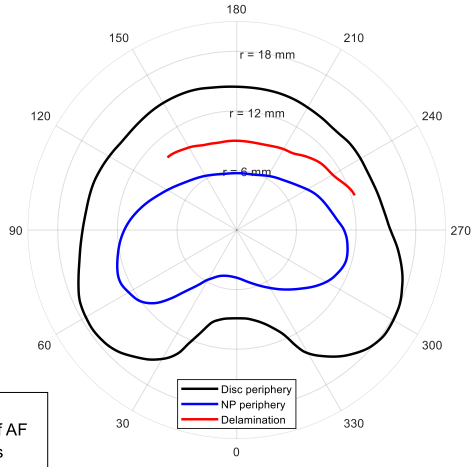

Tear Length :20.8 mm
Needle depth :62.8% of AF
Tear Arc :117.3 degrees
Disc Area :694.1 mm^2

Ovine Intervertebral Disc Cross Section - S31L3
AN injection :60s at 80 psi (552 kPa)

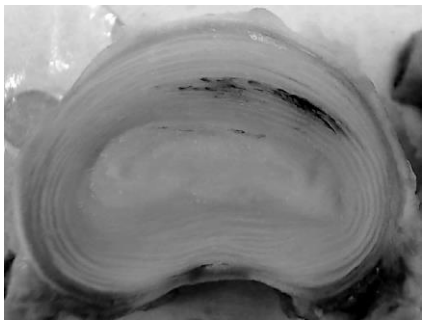

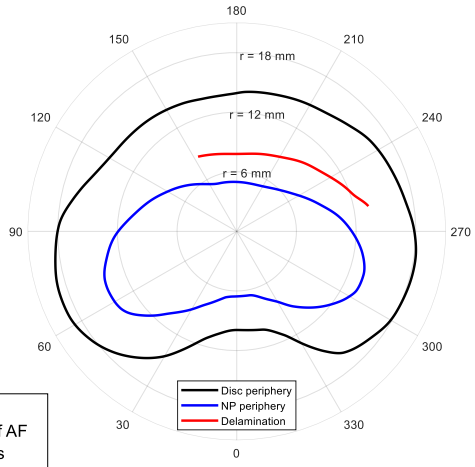

Tear Length :18.6 mm
Needle depth :66.5% of AF
Tear Arc :106.5 degrees
Disc Area :755.0 mm^2

Ovine Intervertebral Disc Cross Section - S31L4
AN injection :60s at 98 psi (676 kPa)

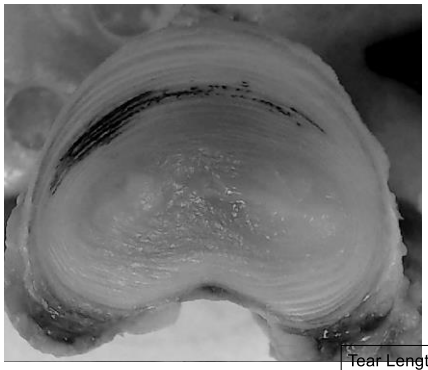

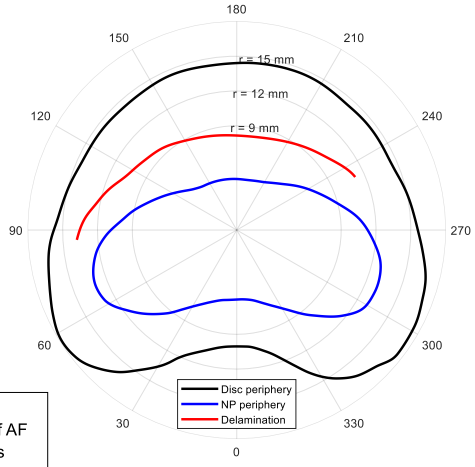

Tear Length :28.7 mm
Needle depth :61.1% of AF
Tear Arc :159.4 degrees
Disc Area :694.6 mm^2

Ovine Intervertebral Disc Cross Section - S31L5
AN injection :15s at 80 psi (552 kPa)

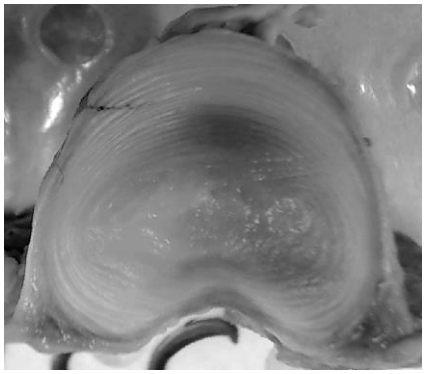

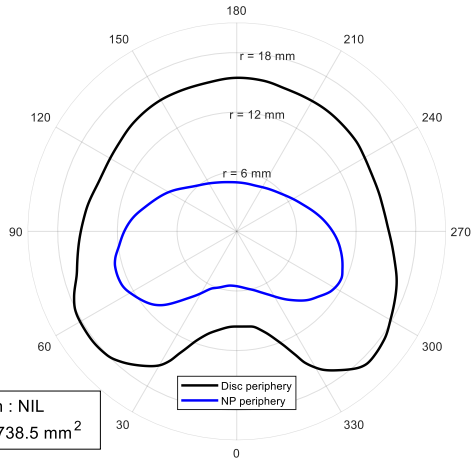

Tear Length : NIL
Disc Area :738.5 mm^2

Ovine Intervertebral Disc Cross Section - S32L2
AN injection :15s at 98 psi (676 kPa)

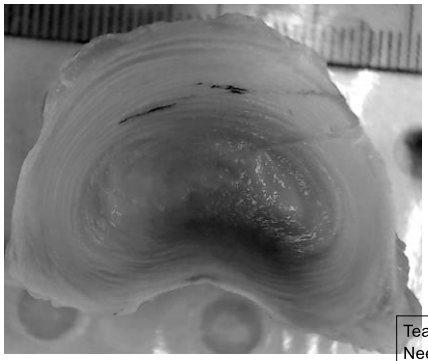

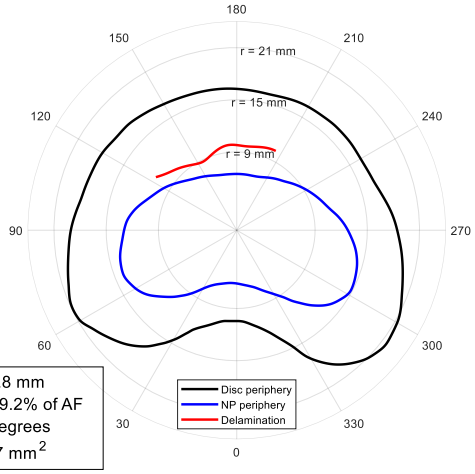

Tear Length :14.8 mm
Needle depth :69.2% of AF
Tear Arc :82.9 degrees
Disc Area :934.7 mm^2

Ovine Intervertebral Disc Cross Section - S33L1
AN injection :60s at 98 psi (676 kPa)

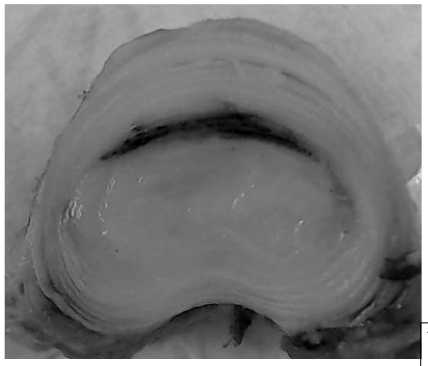

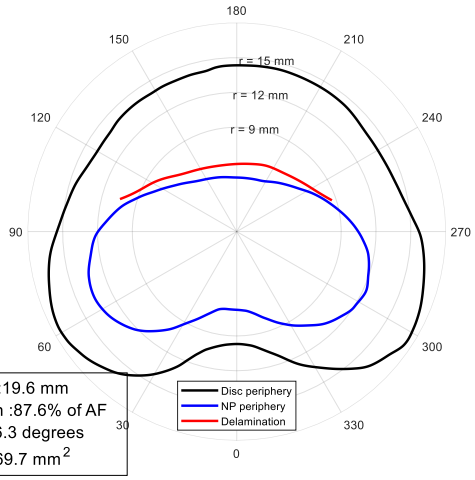

Tear Length :19.6 mm
Needle depth :87.6% of AF
Tear Arc :146.3 degrees
Disc Area :669.7 mm^2

Ovine Intervertebral Disc Cross Section - S33L3
AN injection :15s at 98 psi (676 kPa)

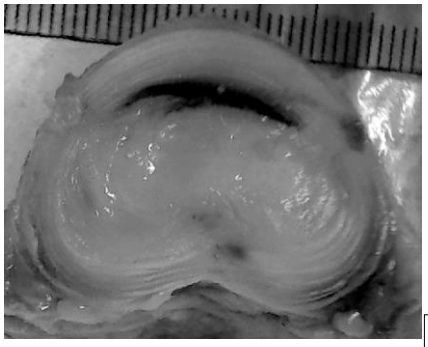

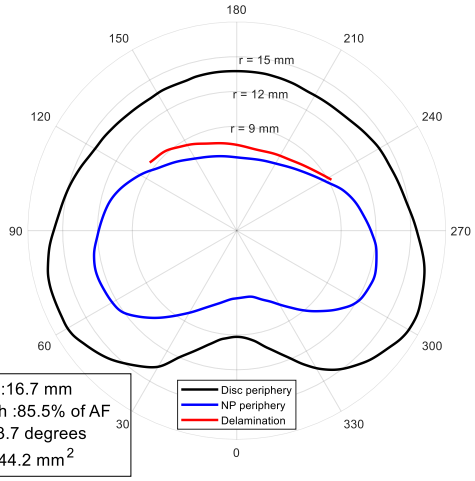

Tear Length :16.7 mm
Needle depth :85.5% of AF
Tear Arc :113.7 degrees
Disc Area :644.2 mm^2

Ovine Intervertebral Disc Cross Section - S33L4
AN injection :15s at 98 psi (676 kPa)

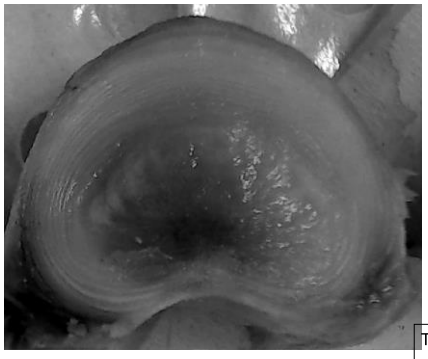

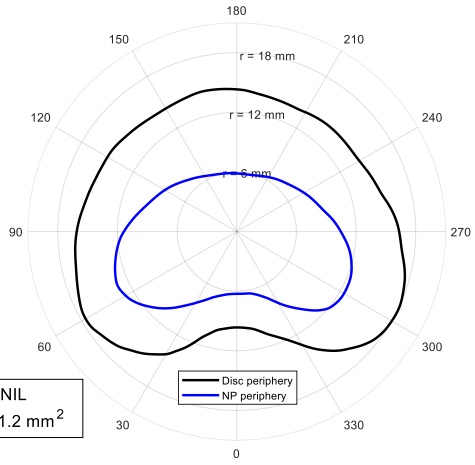

Tear Length : NIL
Disc Area :691.2 mm^2

Ovine Intervertebral Disc Cross Section - S34L1
AN injection :60s at 98 psi (676 kPa)

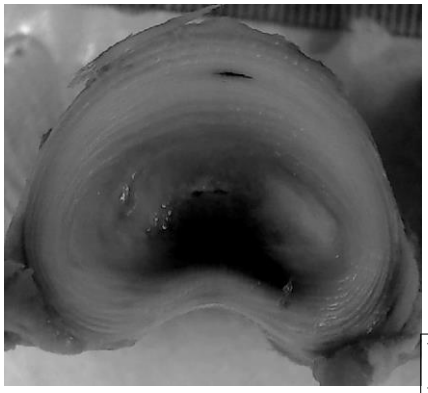

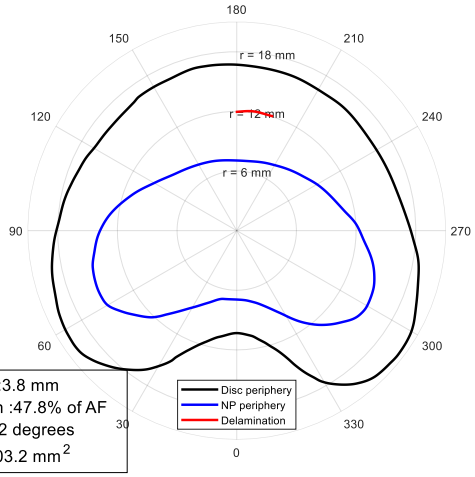

Tear Length :3.8 mm
Needle depth :47.8% of AF
Tear Arc :18.2 degrees
Disc Area :903.2 mm^2

Ovine Intervertebral Disc Cross Section - S34L2
AN injection :15s at 98 psi (676 kPa)

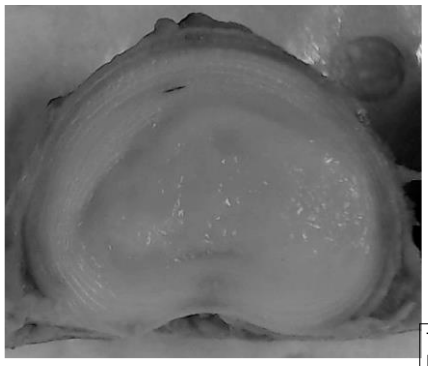

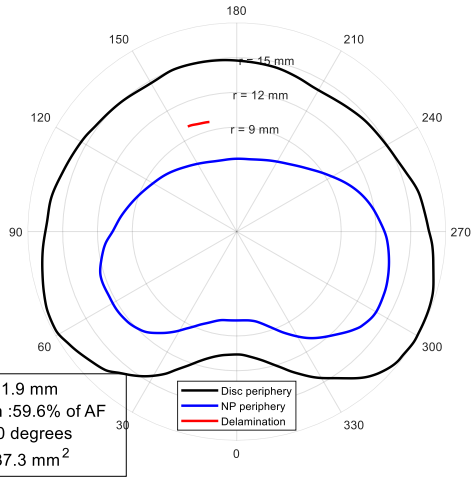

Tear Length :1.9 mm
Needle depth :59.6% of AF
Tear Arc :11.0 degrees
Disc Area :737.3 mm^2

Ovine Intervertebral Disc Cross Section - S35LX
AN injection :15s at 60 psi (414 kPa)

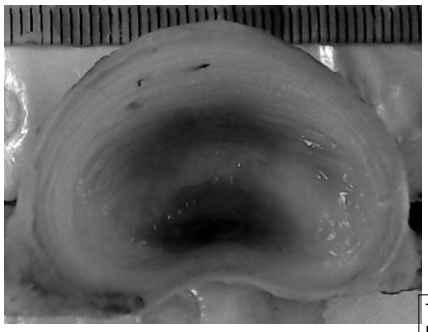

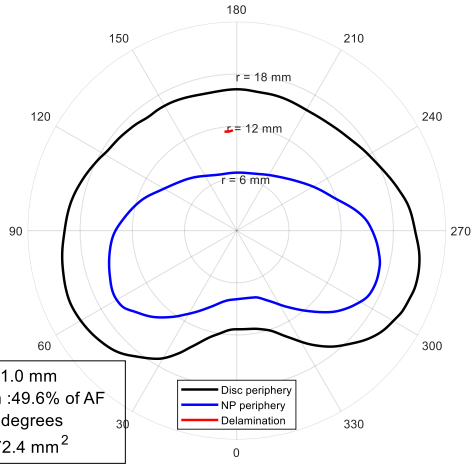

Tear Length :1.0 mm
Needle depth :49.6% of AF
Tear Arc :4.9 degrees
Disc Area :972.4 mm^2

Ovine Intervertebral Disc Cross Section - S36L1
AN injection :15s at 60 psi (414 kPa)

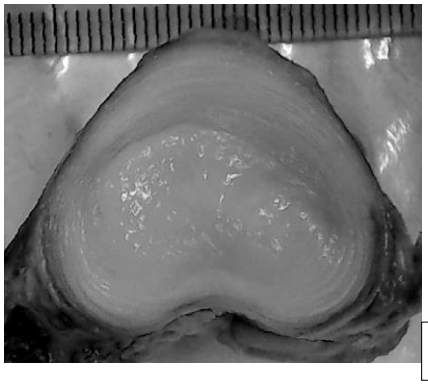

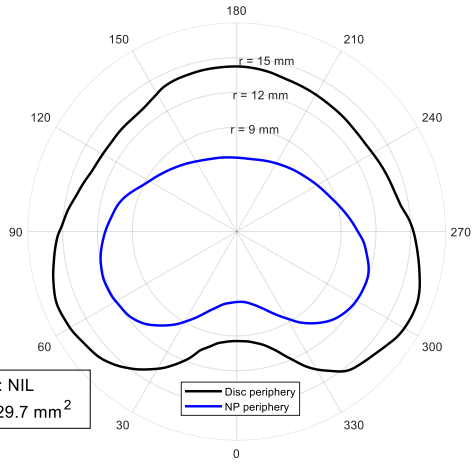

Tear Length : NIL
Disc Area :629.7 mm^2

Ovine Intervertebral Disc Cross Section - 36L2
AN injection :60s at 60 psi (414 kPa)

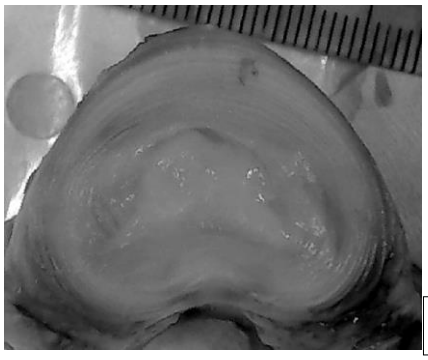

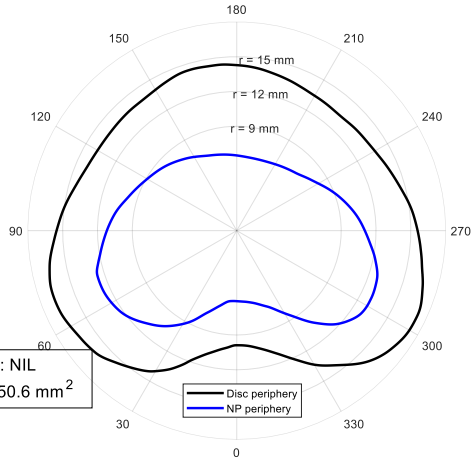

Tear Length : NIL
Disc Area :650.6 mm^2

Ovine Intervertebral Disc Cross Section - S37L1
AN injection :15s at 60 psi (414 kPa)

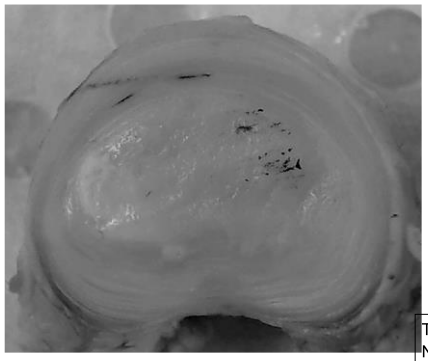

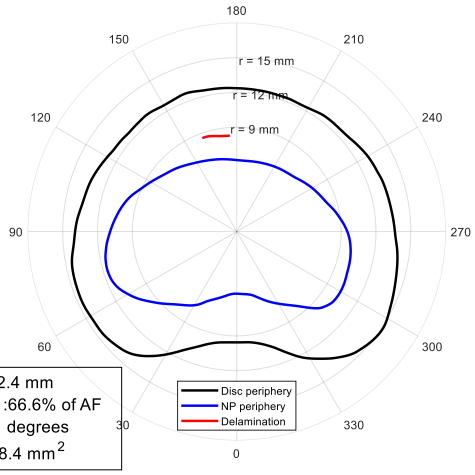

Tear Length :2.4 mm
Needle depth :66.6% of AF
Tear Arc :16.1 degrees
Disc Area :528.4 mm^2

Ovine Intervertebral Disc Cross Section - S37L2
AN injection :15s at 98 psi (676 kPa)

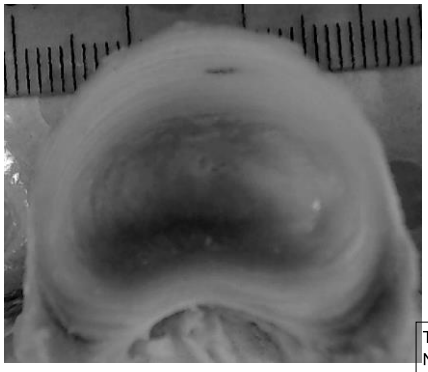

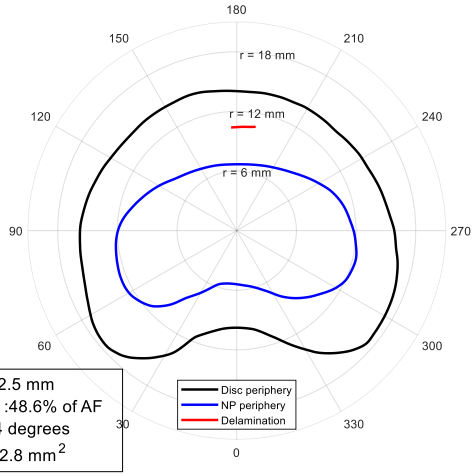

Tear Length :2.5 mm
Needle depth :48.6% of AF
Tear Arc :13.4 degrees
Disc Area :682.8 mm^2

Ovine Intervertebral Disc Cross Section - S37L3
AN injection :15s at 60 psi (414 kPa)

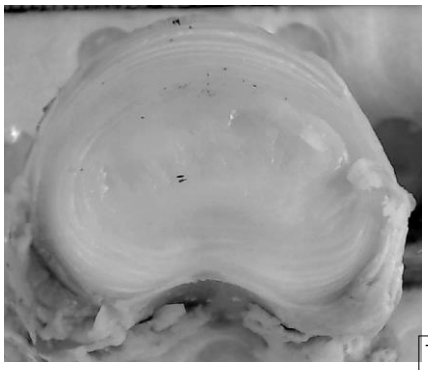

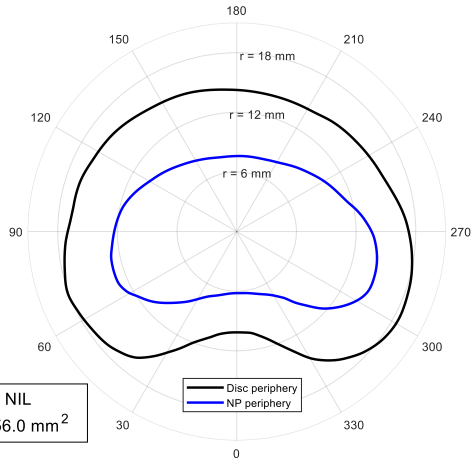

Tear Length : NIL
Disc Area :756.0 mm^2

Ovine Intervertebral Disc Cross Section - S37L4
AN injection :60s at 60 psi (414 kPa)

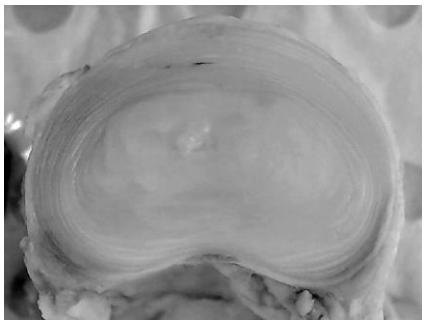

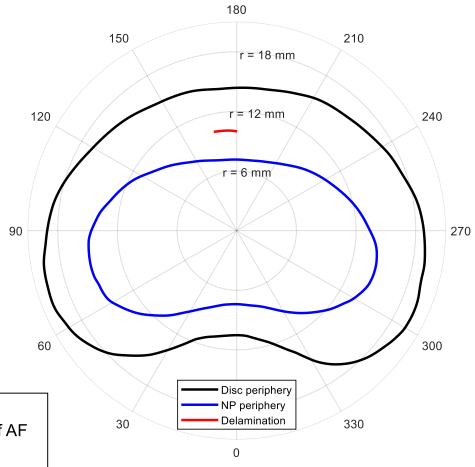

Tear Length :2.3 mm
Needle depth :59.4% of AF
Tear Arc :13.2 degrees
Disc Area :847.7 mm^2

Ovine Intervertebral Disc Cross Section - S37L5
AN injection :60s at 60 psi (414 kPa)

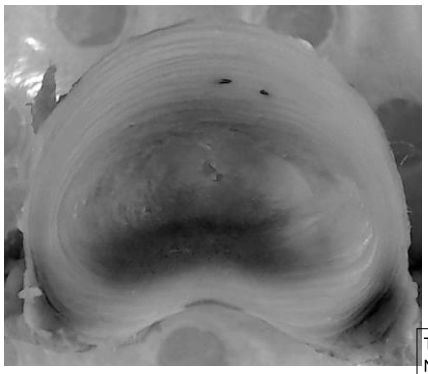

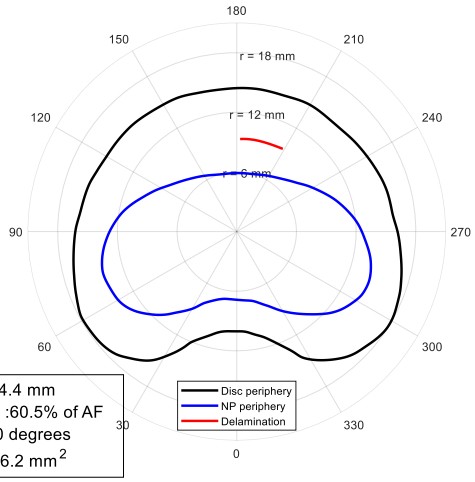

Tear Length :4.4 mm
Needle depth :60.5% of AF
Tear Arc :27.0 degrees
Disc Area :726.2 mm^2

Ovine Intervertebral Disc Cross Section - S38L1
AN injection :60s at 98 psi (676 kPa)

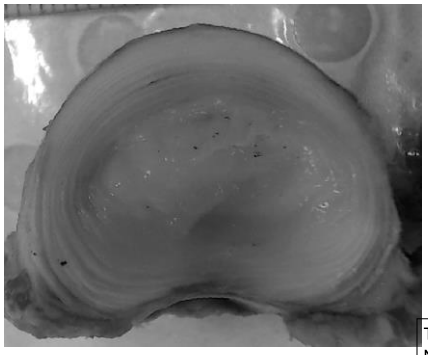

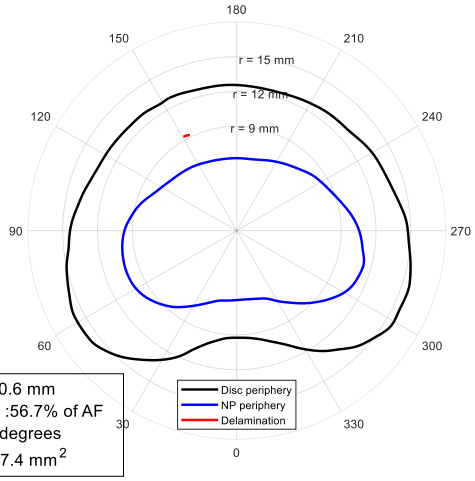

Tear Length :0.6 mm
Needle depth :56.7% of AF
Tear Arc :3.5 degrees
Disc Area :557.4 mm^2

Ovine Intervertebral Disc Cross Section - S38L2
AN injection :15s at 60 psi (414 kPa)

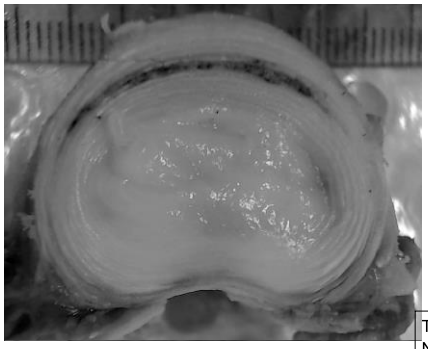

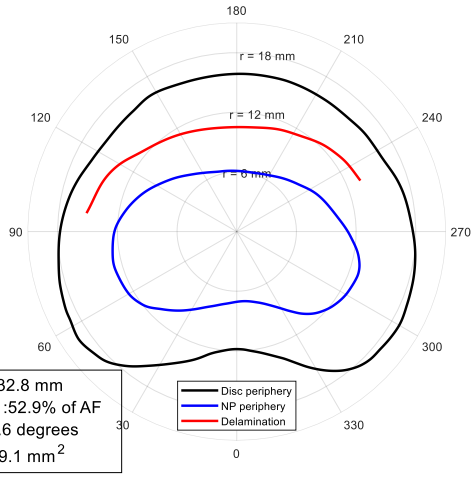

Tear Length :32.8 mm
Needle depth :52.9% of AF
Tear Arc :150.6 degrees
Disc Area :859.1 mm^2

Ovine Intervertebral Disc Cross Section - S38L3
AN injection :60s at 60 psi (414 kPa)

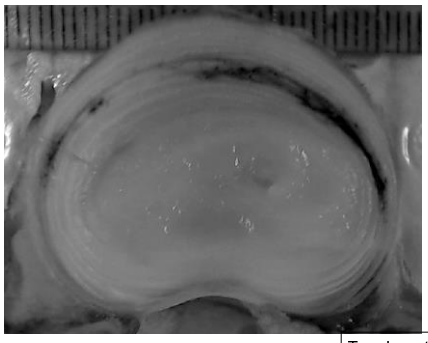

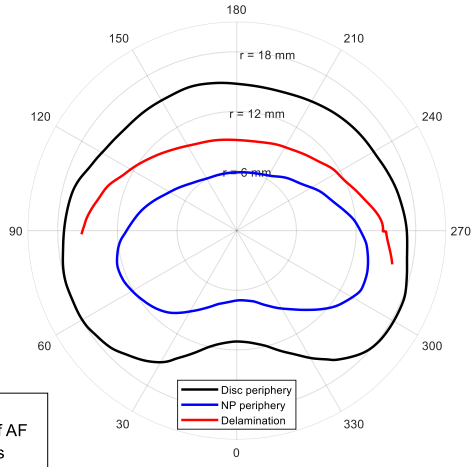

Tear Length :41.8 mm
Needle depth :62.2% of AF
Tear Arc :193.6 degrees
Disc Area :784.7 mm^2

Ovine Intervertebral Disc Cross Section - S39L1
AN injection :15s at 98 psi (676 kPa)

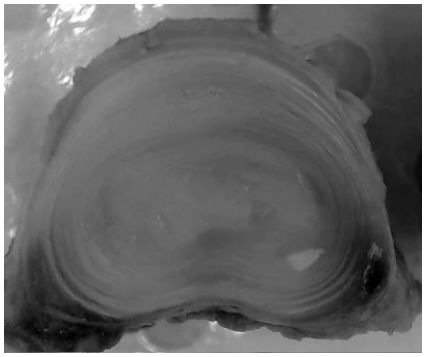

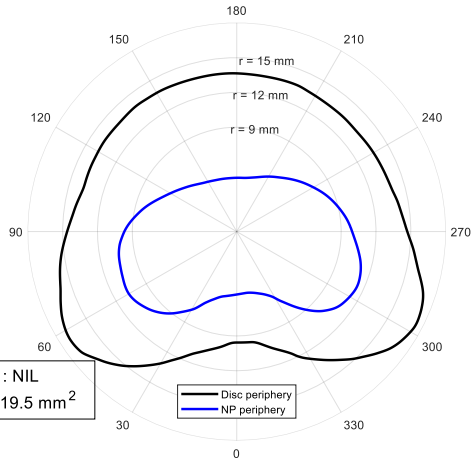

Tear Length : NIL
Disc Area :619.5 mm^2

Ovine Intervertebral Disc Cross Section - S39L2
AN injection :60s at 80 psi (552 kPa)

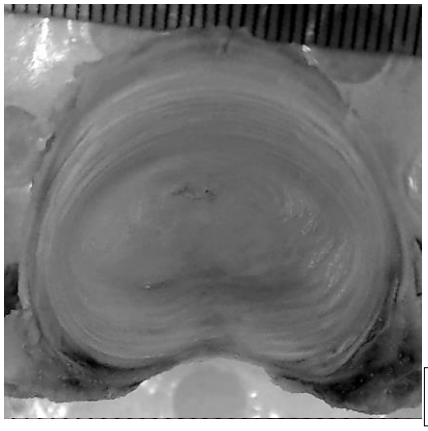

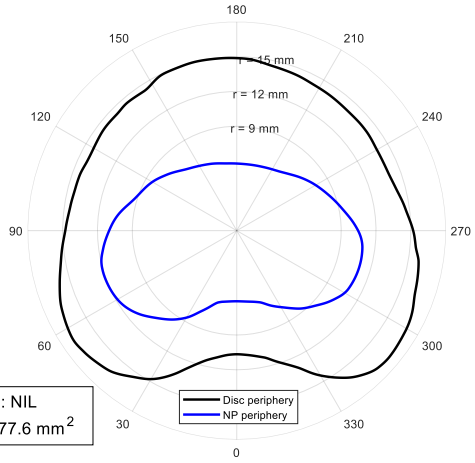

Tear Length : NIL
Disc Area :677.6 mm^2

Ovine Intervertebral Disc Cross Section - S39L3
AN injection :60s at 80 psi (552 kPa)

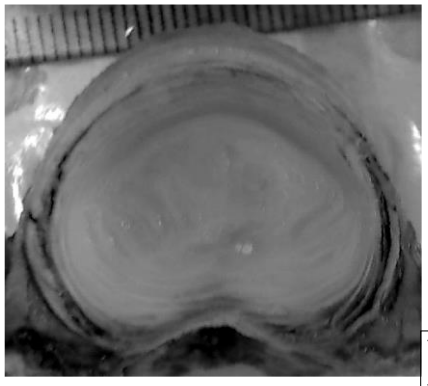

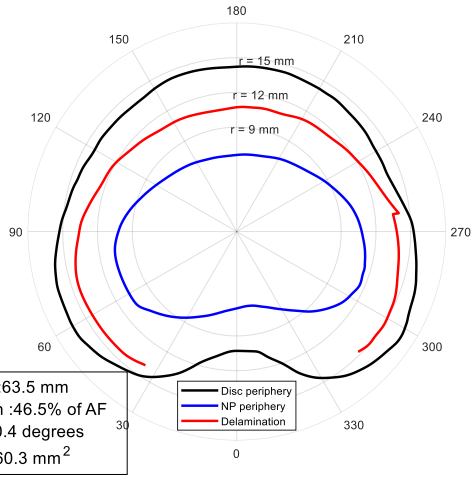

Tear Length :63.5 mm
Needle depth :46.5% of AF
Tear Arc :280.4 degrees
Disc Area :660.3 mm^2

Ovine Intervertebral Disc Cross Section - S42L2
AN injection :60s at 60 psi (414 kPa)

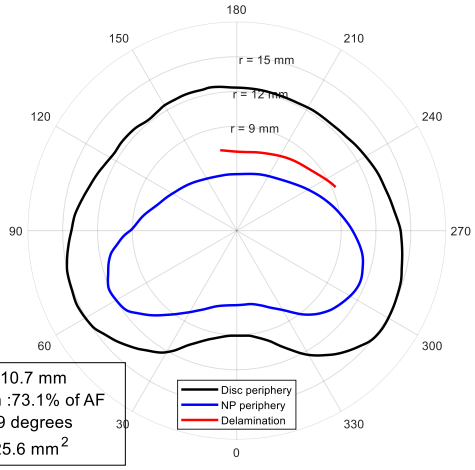

Tear Length :10.7 mm
Needle depth :73.1% of AF
Tear Arc :77.9 degrees
Disc Area :525.6 mm^2

Ovine Intervertebral Disc Cross Section - S43L1
AN injection :60s at 98 psi (676 kPa)

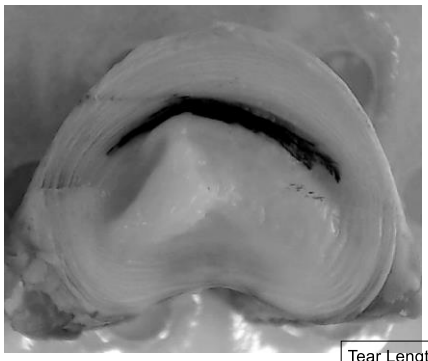

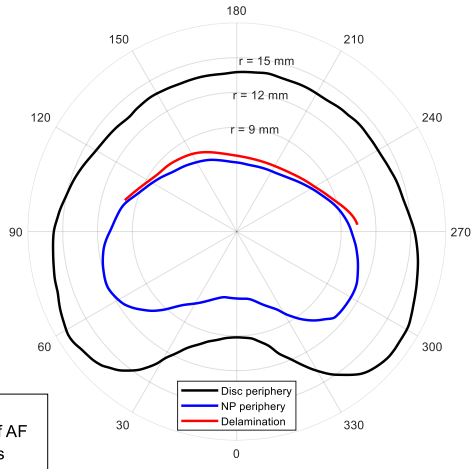

Tear Length :23.3 mm
Needle depth :91.8% of AF
Tear Arc :161.1 degrees
Disc Area :642.5 mm^2

Ovine Intervertebral Disc Cross Section - S43L2
AN injection :60s at 60 psi (414 kPa)

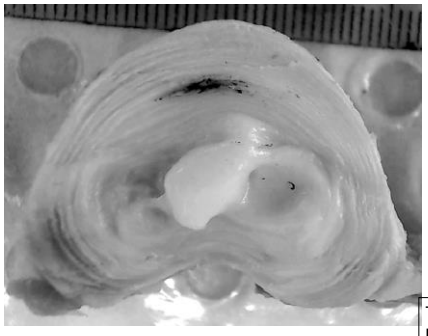

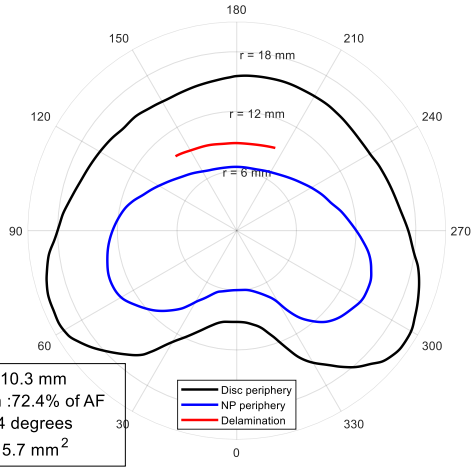

Tear Length :10.3 mm
Needle depth :72.4% of AF
Tear Arc :64.4 degrees
Disc Area :815.7 mm^2

Ovine Intervertebral Disc Cross Section - S44L2
AN injection :60s at 60 psi (414 kPa)

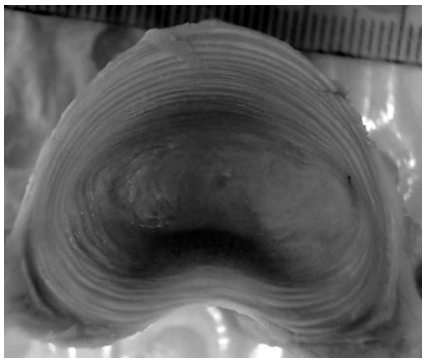

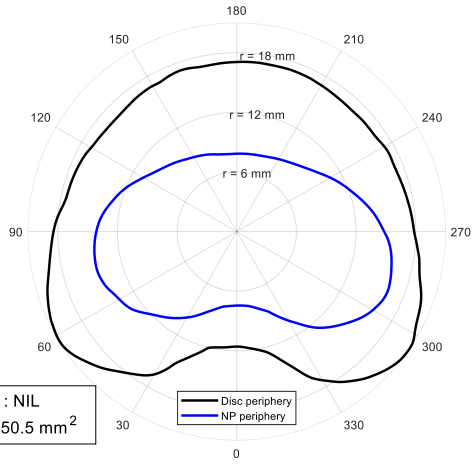

Tear Length : NIL
Disc Area :950.5 mm^2

Ovine Intervertebral Disc Cross Section - S44L3
AN injection :15s at 60 psi (414 kPa)

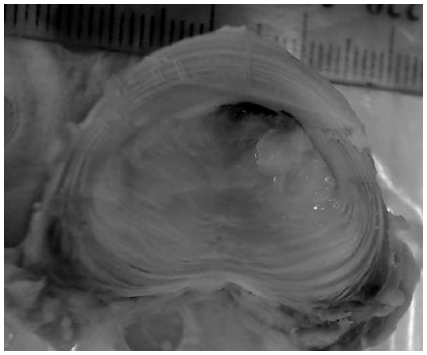

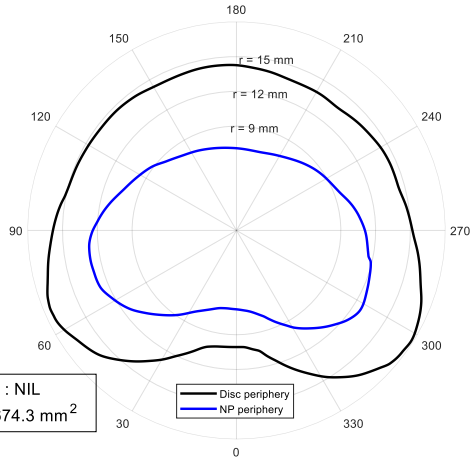

Tear Length : NIL
Disc Area :674.3 mm^2

Ovine Intervertebral Disc Cross Section - S45L1
AN injection :15s at 60 psi (414 kPa)

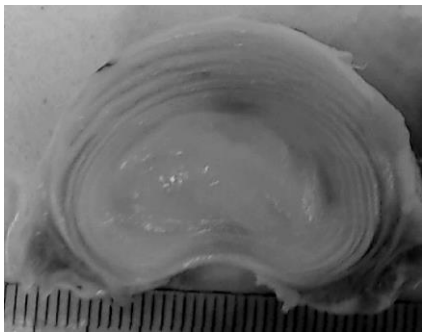

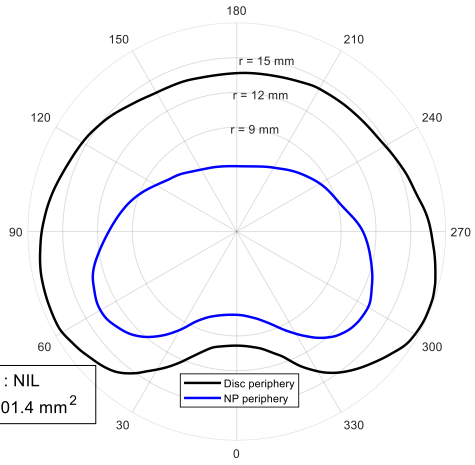

Tear Length : NIL
Disc Area :701.4 mm^2

Ovine Intervertebral Disc Cross Section - S45L2
AN injection :60s at 80 psi (552 kPa)

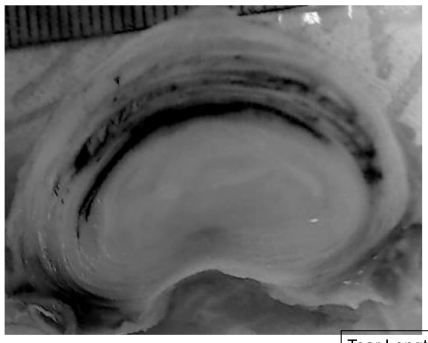

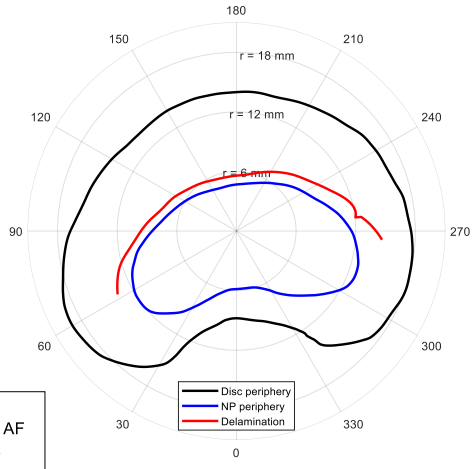

Tear Length :36.0 mm
Needle depth :89.3% of AF
Tear Arc :211.5 degrees
Disc Area :726.4 mm^2

Ovine Intervertebral Disc Cross Section - S45L3
AN injection :15s at 80 psi (552 kPa)

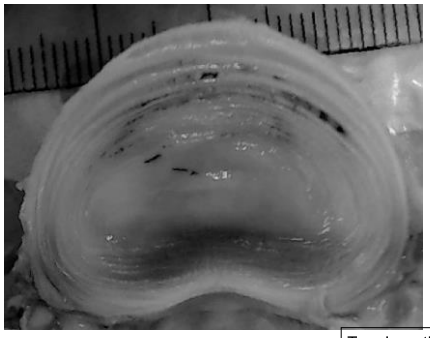

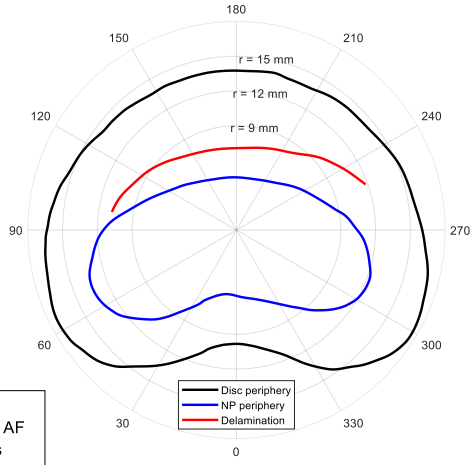

Tear Length :24.6 mm
Needle depth :71.1% of AF
Tear Arc :152.3 degrees
Disc Area :679.4 mm^2

Ovine Intervertebral Disc Cross Section - S46L1
AN injection :15s at 60 psi (414 kPa)

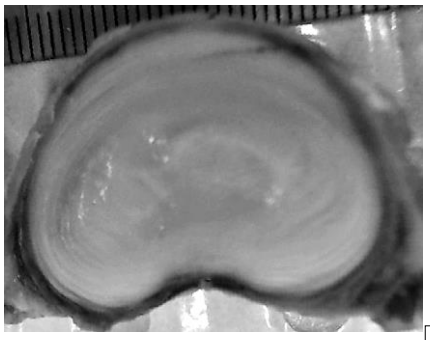

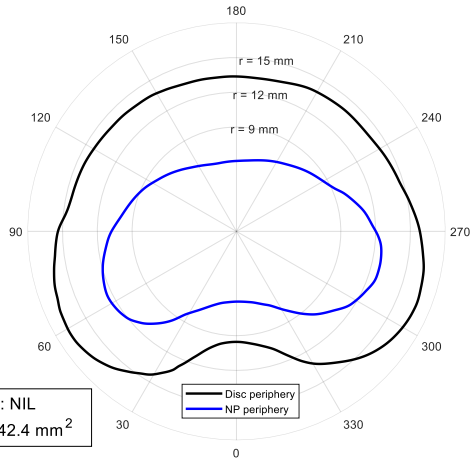

Tear Length : NIL
Disc Area :642.4 mm^2

Ovine Intervertebral Disc Cross Section - S46L2
AN injection :60s at 60 psi (414 kPa)

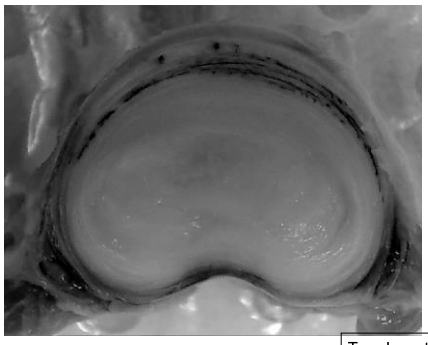

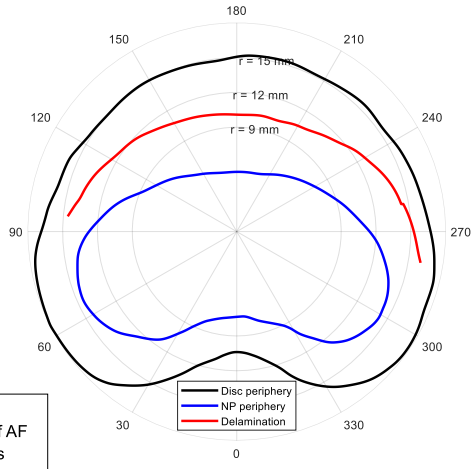

Tear Length :40.5 mm
Needle depth :48.8% of AF
Tear Arc :184.5 degrees
Disc Area :770.5 mm^2

Apendix C MAtLab Script for IVD Geometry Digitisation

```
%June 2019 - Program to allow manual digitisation of Disc Area and tear
%Geometry. Results and Figures presented for easy collation
%By Kurt van Ryswyk, Developed from examples by John Costi

%Result format
%--------
%AAA = [SpecNum, TestRun, DiscWidth, DiscDepth, DiscArea, NP_Area,
%       InjectDepth, IsTear, Injectlocation, TLng, TearDepth, T_Arc_rad,
T_Arc_deg];

%Procedure
%--------
%Load Image file
%Measure image Scale
%Measure Disc periphery 3 times, convert to polar and average
%Measure Disc NP 3 times, convert to polar and average
%Ask if tear is visible
%Measure tear geometry 3 times, convert to polar and average
%find centroid of disc
%translate and rotate image
%translate and rotate all coordinate plots
%Output

%CONVENTION
%--------
%DP - variable related to Disc Perimeter
%NP - variable related to Nuclues Perimeter
%TG - variable related to Tear Geometery%
%cell - as prefix, cell array to store different sized arrays
%xy - original xy points stored in an array
%xys - xy points 'splined', ie interpolated to even, these spacing
%trans or tr - as suffix, coordinates have been translated to re-defined
orgin point
%_s - as suffix, variable has been scaled to mm

close all;
clearvars;

debugy = 0; %debug graphs on=1 and off=0

stp = pi/2000;
rpts = 3;  %number of times to repeat measurement loops

%%  Select specimen image

[fname, fpath] = uigetfile('C:\Users\kurtt\Documents\Thesis\Study\Spines
sets\*.*');
figure; %plot axial xray - to be used for digitising

fpathname = strcat(fpath,fname);

discImg = imread(fpathname);

% a = imsharpen(discImg);
% b = imadjust(a,[.2 .3 0; .7 .7 1],[]);
% c = rgb2gray(discImg);
```

```
% c = imadjust(c);

discImg = rgb2gray(discImg);
discImg = imadjust(discImg);
discImg = imsharpen(discImg);

% montage({discImg, a, b, c}, 'size', [2,2]);
% answer = inputdlg('Enter a number (1-4) to select clearest disc image');
% ans = str2num(answer{1});
% switch ans
%     case 2
%         discImg = a;
%     case 3
%         discImg = b;
%     case 4
%         discImg = c;
% end
% clear a
% clear b
% clear c

close all
figure
imshow(discImg);
title(fname,'fontsize',14,'fontweight','bold');
hold on;

%% Specimen Selection and Finding Preexisting File
%Costi March 28 2016 - allow repeated digitising to occur for comparing
consisency by specifying a prefix that will be added to the start of the
filename



specNum = 0; %set initial specimen number to zero
while specNum == 0
    prompt = {'specimen number', 'Enter Test Run number', 'Pressure (psi)',
'Duration (s)', 'Preload (N)', 'Injection Region (AN or PL)'};
    dlg_title = 'Select specimen and filename prefix';
    num_lines = 1;
    answer = inputdlg(prompt,dlg_title,num_lines);
    specNum = answer{1};
    testRun = str2double(answer{2});
    psi = str2double(answer{3});
    dur =str2double(answer{4});
    preload =str2double(answer{5});
    loc = answer{6};
end

paramfile = [specNum 'disc_DigRun_'  num2str(testRun) '.mat'];

%Costi March 28 2016 - first check to see if the filename exists, if it
does then ask user to enter a prefix (if not already entered) and save as
an alternative filename with prefix
%also ask user if they wish to overwrite the file if it exists
if exist(paramfile,'file')
    pexist = 1;
else
    pexist = 0;
```

```
end

while pexist
    choice = questdlg(['File: ' paramfile ' already exists. Overwrite?']);
    % Handle response
    switch choice
        case 'No'
            prompt = {'Enter filename prefix e.g. J1'};
            dlg_title = 'Enter prefix';
            num_lines = 1;
            answer = inputdlg(prompt,dlg_title,num_lines);
            prefix = answer{1};
            paramfile = [upper(prefix) '-DigRun_' num2str(specNum) '.mat'];

            if exist(paramfile,'file') %check if filename exists again
                pexist = 1;
            else
                pexist = 0;
            end
        case 'Yes'
            pexist = 0; %force overwrite
        case 'Cancel'
            pexist = 1;
    end
end

%% Select Bar Length
%now set xlim and ylim for the figure and redraw axes to zoom in to
calibration block
%first store the full image size xlim and ylim values for zooming back out
later
, = xlim;
ylimfull = ylim;

%% Set Zoom for length scale
rpts = 3;
imshow(discImg);
uiwait(msgbox('Click 2 points to zoom in on length scale, left then right
click','Image Calibration','CreateMode','modal'))
xyZoom = [];
n = 0;
but = 1; %left mouse button
while but == 1 %left mouse button has been clicked
    % zoom on
    [xi,yi,but] = ginput(1);
    n = n+1;
    xyZoom(:,n) = [xi;yi];   %store points
end
xyblock = [xyZoom(:,1),xyZoom(:,end)];
xlimmin = min(xyblock(1,:));
xlimmax = max(xyblock(1,:));
ylimmin = min(xyblock(2,:));
ylimmax = max(xyblock(2,:));

xlim([xlimmin xlimmax]);
ylim([ylimmin ylimmax]);


% user sets size to select
lengthbar = str2double(inputdlg('Enter Scaled Length in mm'));
```

```
imgscale = zeros(1, rpts);
for i=1:rpts %request user to take three sets of calibration block length
measurements and use the average length for scaling
    hl = msgbox(['Scale measure NUMBER ' num2str(i) '. Select two points
that define ' ...
        num2str(lengthbar) ' mm. - right click on end point'],'Image
Calibration','CreateMode','modal');
    uiwait(hl);

    xycal = [];
    n = 0;

    but = 1; %left mouse button
    while but == 1 %left mouse button has been clicked
        % zoom on
        [xi,yi,but] = ginput(1);
        plot(xi,yi,'rx')
        n = n+1;
        xycal(:,n) = [xi;yi];   %store points
    end

    %Calc length in 2D
    X = [xycal(:,1),xycal(:,end)]; %just first and last points
    %     plot(X,'b-');
    pause(0.5);

    calength = pdist(X');   %transpose for variable per row format
    %    calength = sqrt( (X(1,2)-X(1,1))^2 + (X(2,2)-X(2,1))^2 ); %test
result

    imgscale(i) = (lengthbar)/calength; %convert to mm per pixel scale

    clf; %clear figure to remove the text from the calibration block
scaling
    imshow(discImg);
    xlim([xlimmin xlimmax]);
    ylim([ylimmin ylimmax]);
    hold on;
end

%calculate average scale factor
meanimgscale = mean(imgscale);

%now - zoom back out to full image size
xlim([xlimfull(1) xlimfull(2)]);
ylim([ylimfull(1) ylimfull(2)]);


%% Zoom in to Disk
clf; %clear figure to remove the text from the calibration block scaling

hold on;

h1 = msgbox('Next select two DIAGONAL points that define a box around the
disc periphery - use right click to select second point (type d to delete
last point)' ...
    ,'Image Calibration','CreateMode','modal');
uiwait(h1);
```

```
xydisc = [];
n = 0;

but = 1; %left mouse button
while but == 1 %left mouse button has been clicked
    % zoom on
    [xi,yi,but] = ginput(1);
    n = n+1;
    plot(xi,yi,'rx');
    xydisc(:,n) = [xi;yi];
end

%redraw figure using the approximate disc coordinates to 'zoom in' for
better resolution when selecting the disc periphery
sz = size(xydisc);
s2 = sz(2);
if s2>=3 %sometimes more than 2 points could be clicked if user forgets to
right-click for the 2nd final point - remove all other points except for
1st and last points selected
    xydisc(:,2:s2-1)=[];
end

%now set xlim and ylim for the figure and redraw axes to zoom in to
calibration block
%first store the full image size xlim and ylim values for zooming back out
later
xlimfull = xlim;
ylimfull = ylim;

xlimmin = min(xydisc(1,:));
xlimmax = max(xydisc(1,:));
ylimmin = min(xydisc(2,:));
ylimmax = max(xydisc(2,:));

xlim([xlimmin xlimmax]);
ylim([ylimmin ylimmax]);


%% Select Disk Periphery
cellDPclicks = cell(1,rpts);   %cell array to store multiple point sets of
different lengths

for i = 1:rpts
    DPxy = [];
    clf; %clear figure to remove previous markings
    imshow(discImg);
    hold on;
    xlim([xlimmin xlimmax]);
    ylim([ylimmin ylimmax]);

    ttl = strcat('Disc Periphery NUMBER ',  num2str(i), ' of 0',
num2str(rpts));
    cptn = 'Select points that define the disc periphery - use right click
to select final point, and d to delete previous points';
    h1 = msgbox(cptn, ttl,'CreateMode','modal');
    uiwait(h1);

    n = 0;
    but=1;
```

```
    while (but ~= 3)%left mouse button has been clicked, but = 3 = right
mouse click
        [xi,yi,but] = ginput(1);
        n = n+1;
        hh(n) = plot(xi,yi,'rx');
        DPxy(:,n) = [xi;yi];

        %Costi March 28 2016 - allow user to delete a point by pressing D
or d
        if ((but==68||but==100) && n > 1) % 'typed D or d AND there is at
least one point
            delete(hh(n-1:n));
            n = n-2;
            DPxy = DPxy(:,1:n);
        end
    end
    %right mouse button has been clicked

    % Plot Curve
    % Interpolate with a spline curve and finer spacing.
    %add duplicate first point to last point to close the spline

    t = 1:n+1;
    ts = 1: 0.01: n+1;

    DPxys = pchip(t,[DPxy DPxy(:,1)],ts)';  %pchip reduces dicontinuities
errors
%     cellDPclicks{i} = DPxys;    %spline to prevent perimeter
discontinuites
    cellDPclicks{i} = DPxy';

    fp_1 = plot(DPxys(:,1),DPxys(:,2),'b-');

    pause(1);   %given user a moment to see to splined plot

    if debugy == 1
        DPxClick{i} = DPxy(1,:)'
        DPyClick{i} = DPxy(2,:)'
    end

end

%% Select NP Periphery
% Initially, the list of points is empty
cellNPclicks = cell(1,rpts);
for i = 1:rpts

    %         clf; %clear figure to remove previous markings
    %         imshow(discImg);
    %         hold on;
    %         xlim([xlimmin xlimmax]);
    %         ylim([ylimmin ylimmax]);

    try
        delete(fp_1)
        delete(hh)
    catch %take no action but don't crash
    end
```

```
    ttl = strcat('NP Periphery NUMBER ',num2str(i),' of ',num2str(rpts));
    cptn = 'Select points that define NP periphery - right click to select
final point, d to delete previous point';

    h1 = msgbox(cptn, ttl,'CreateMode','modal');
    uiwait(h1);

    but=1;
    NPxy = [];
    n = 0;

    while (but ~= 3)%left mouse button has been clicked, but = 3 = right
mouse click
        [xi,yi,but] = ginput(1);

        n = n+1;
        hh(n) = plot(xi,yi,'rx');
        NPxy(:,n) = [xi;yi];

        %Costi March 28 2016 - allow user to delete a point by pressing D
or d
        if ((but==68||but==100) && n > 1) % 'typed D or d AND there is at
least one point
            delete(hh(n-1:n));
            n = n-2;
            NPxy = NPxy(:,1:n);
        end
    end
    %right mouse button has been clicked

    % Interpolate with a spline curve and finer spacing.
    t = 1:n+1;
    ts = 1: 0.01: n+1;
    %add duplicate first point to last point to close the spline
    NPxys = pchip(t,[NPxy NPxy(:,1)],ts)';
%     cellNPclicks{i} = NPxys; %Save list of points. Splined prevents
discontinuities.
    cellNPclicks{i} = NPxy';

    % Plot the interpolated curve.
    fp_1 = plot(NPxys(:,1),NPxys(:,2),'b-');
    pause(1)    %give user a moment to see

    if debugy == 1
        NPxClick{i} = NPxy(1,:)
        NPyClick{i} = NPxy(2,:)
    end

end

%% Select Tear Periphery
% Initially, the list of points is empty

dlgTitle    = 'Tear Exists';
dlgQuestion = 'Is there a visible circumferential tear?';
IsTear = questdlg(dlgQuestion,dlgTitle,'Yes','No', 'Yes');
dlgTitle    = 'Other Tears';
dlgQuestion = 'Are other delaminations present?';
OtherTears = questdlg(dlgQuestion,dlgTitle,'Yes','No', 'Yes');
```

```
cellTGclicks = cell(1,rpts);
switch IsTear
    case 'Yes'
        for i = 1:rpts
            TGxy = [];

            clf; %clear figure to remove previous markings
            imshow(discImg);
            hold on;
            xlim([xlimmin xlimmax]);
            ylim([ylimmin ylimmax]);

%             try
%                 delete(fp_1)
%                 delete(hh)
%             catch %take no action but don't crash
%             end


            n = 0;
            cptn = 'Select consecutive points that define the Tear - right
click to select final point, d to delete previous points';
            ttl = 'Tear Periphery';
            h1 = msgbox(cptn , ttl, 'CreateMode', 'modal');
            uiwait(h1);

            but=1;
            while (but ~= 3)%left mouse button has been clicked, but = 3 =
right mouse click
                [xi,yi,but] = ginput(1);
                n = n+1;
                hh(n) = plot(xi,yi,'rx');
                TGxy(:,n) = [xi;yi];

                %Costi March 28 2016 - allow user to delete a point by
pressing D or d
                if ((but==68||but==100) && n > 1) % 'typed D or d AND there
is at least one point
                    delete(hh(n-1:n));
                    n = n-2;
                    TGxy = TGxy(:,1:n);
                end
            end     %right mouse button has been clicked


            % Interpolate with a spline curve, finer spacing, and plot
            t = 1:n;            ts = 1: 0.01: n;
            TGxys = pchip(t, TGxy, ts)';    %tear geometry is less
consistant, so pchip is safer than spline
            cellTGclicks{i} = TGxy';%s;         %sa

            fp_1 = plot(TGxys(:,1),TGxys(:,2),'b-');
            pause(1)

            if debugy == 1
                TGxClick{i} = TGxy(1,:)'
                TGyClick{i} = TGxy(2,:)'
            end
```

```
        end
    otherwise
        cellTGclicks = {0, 0, 0};
end


if debugy == 1
    for i=1:rpts
        figure;
        plot(cellDPclicks{i}(:,1),cellDPclicks{i}(:,2),'o',...
            cellNPclicks{i}(:,1),cellNPclicks{i}(:,2),'o'); hold on
        plot(DPxClick{i},DPyClick{i},'x',...
            NPxClick{i},NPyClick{i},'x'); hold on
        if strcmp(IsTear,'Yes')
            plot(cellTGclicks{i}(:,1),cellTGclicks{i}(:,2),'o'); hold on
            plot(TGxClick{i},TGyClick{i},'x'); hold on
        end
    end
end


%% Calculate Centroid and Areas
DPcentroid = zeros(rpts, 2);
for i = 1:rpts
    DPxys = cellDPclicks{i};

    %find averaged centroid
    [x,y] = centroid(polyshape(DPxys));
    DPcentroid(i, :) = [x, y];

end
centr= [mean(DPcentroid(:, 1)), mean(DPcentroid(:, 2))];

%translate plotted point to new centroid into
cellDPtrans = cell(1, rpts);
cellNPtrans = cell(1, rpts);
cellTGtrans = cell(1, rpts);

for i=1:rpts
    cellDPtrans{i} = [cellDPclicks{i}(:,1)-centr(1), cellDPclicks{i}(:,2)-
centr(2)];
    cellNPtrans{i} = [cellNPclicks{i}(:,1)-centr(1), cellNPclicks{i}(:,2)-
centr(2)];
    switch IsTear
        case 'Yes'
            cellTGtrans{i} = [cellTGclicks{i}(:,1)-centr(1),
cellTGclicks{i}(:,2)-centr(2)];
    end
end

%% Scale datapoints
%xlim([xlimfull(1) xlimfull(2)]);   %zoom out to full size
%ylim([ylimfull(1) ylimfull(2)]);

theta  = -pi:stp:pi;    %list of radian measures evenly spaced in a circle
theta_ = -pi:stp:(pi - stp);    %theta without a repeated point
```

```
cellDPtr_s = cellfun(@(x) x*meanimgscale, cellDPtrans, 'un', 0);
cellNPtr_s = cellfun(@(x) x*meanimgscale, cellNPtrans, 'un', 0);
cellTGtr_s = cellfun(@(x) x*meanimgscale, cellTGtrans, 'un', 0);

%convert to polar coodinates
%preallocations
DPpolsArray = zeros(rpts, length(theta_));
NPpolsArray = zeros(rpts, length(theta_));
tgRad1 = zeros(1,3);
tgRad2 = zeros(1,3);

        thci = cell(1,3);
        rci = cell(1, 3);


for i = 1:rpts

    [thc,rc] = cart2pol(cellDPtr_s{i}(1:end-1,1),cellDPtr_s{i}(1:end-1,2));

    %--------
    [val,index] = maxk(thc,2);
    thc(end+1:end+2)=thc(index)-2*pi;
    rc(end+1:end+2)=rc(index);

    [val,index] = mink(thc(1:end-2),2);
    thc(end+1:end+2)=thc(index)+2*pi;
    rc(end+1:end+2)=rc(index);
    %--------

    DPpol_s = pchip(thc, rc, theta_); %use non repeated theta to prevent
average error
    DPpolsArray(i,:) = DPpol_s;

    if debugy==1
        figure
        polarplot(thc,rc,'x',theta_,DPpol_s); hold on
    end


    [thc,rc] = cart2pol(cellNPtr_s{i}(1:end-1,1),cellNPtr_s{i}(1:end-1,2));

    %--------
    [val,index] = maxk(thc,2);
    thc(end+1:end+2)=thc(index)-2*pi;
    rc(end+1:end+2)=rc(index);

    [val,index] = mink(thc(1:end-2),2);
    thc(end+1:end+2)=thc(index)+2*pi;
    rc(end+1:end+2)=rc(index);
    %--------

    NPpol_s = pchip(thc, rc, theta_);
    NPpolsArray(i,:) = NPpol_s;

    if debugy==1
        polarplot(thc,rc,'x',theta_,NPpol_s); hold on
    end
```

```
    %Tear geometry points cannot be uniformly spaced until all ranges are
    %known. Collect end points, and complete averaging in separate loop.
    switch IsTear
        case 'Yes'
            [thc,rc] = cart2pol(cellTGtr_s{i}(:, 1),cellTGtr_s{i}(:,2));
            %ensure that tear series end points are consistantly assigned
            %to same variables regardless of click order

            thci{i}=thc;
            rci{i} = rc;

            tgRad1(i) = min([thc(1), thc(end)]);
            tgRad2(i) = max([thc(1), thc(end)]);
            tgmid(i) = mean(thc);

            if debugy==1
                polarplot(thc,rc,'x',theta_,NPpol_s); hold on
            end

    end
end

switch IsTear
    case 'Yes'

        % Range of circle is -pi:pi. Construction of tg_thetaR array may
loop
        % past pi and need to be reset to the inverse.
        % Need to check if tg_thetaR crosses the -pi:pi boundary

        %data may transition from tg1 to tg2 in either positive(Clockwise)
        % or negative (CCW) direct. Result array MUST correct to use
        % positive steps.

        %truthtable = Clockwise? Tg1>0? Tg>0?
        %tthtble options...
        %note that tg1 is minimum
            %000  ==> CW, tg1<0, tg2<0, passes pi
            %001  ==> CW, tg1<0, tg2>0,  passes pi
            %010  Impossible value
            %011  ==> CW, tg1>0, tg2>0, passes pi

            %100  ==> CCW, tg1<0, tg2<0, does not pass pi
            %101  ==> CCW, tg1<0, tg2>0, does not pass pi
            %110  Impossible value
            %111  ==> CCW, tg1>0, tg2>0, does not pass pi
        tg1 = mean(tgRad1);
        tg2 = mean(tgRad2);
        tgm = mean(tgmid);

        D = tg2-tg1;      %Radial distane between end pointd
        R = 2*pi - D;     %Inverse radial distance

        if tgm > tg1 && tgm < tg2
            tg_theta = tg1:stp:tg2;
        else
            %construct array from zero and correct to original position
            tg_theta = [0:stp:R] + tg2;
```

```
            tg_theta = limitpimultiples(tg_theta);  %correct any range
exceeding -pi:pi
        end

%         % IN THIS CONFIG, ONLY CCW || CW matters
%         if  thc(2)<thc(1)
%              % option crossing -pi:pi (Anticlockwise)
%             tg_theta = [tg2:stp:pi, stp-pi:stp:tg1];
%         else
%             %not crossing boundary (Clockwise)
%             tg_theta = tg1:stp:tg2;
%         end
        thci = cell(1,3);
        rci = cell(1, 3);

        TGpolsArray = zeros(rpts, length(tg_theta));
        for i = 1:rpts
            thc = []; rc = [];   %clear arrays
            TGpol_s = [];
            [thc,rc] = cart2pol(cellTGtr_s{i}(:,1),cellTGtr_s{i}(:,2));
            thci{1,i} = thc;
            rci{1,i} = rc;
            %interpolate each run of defined tear onto uniform range and
spacing
            TGpolsArray(i,:) = spline(thc, rc, tg_theta);

            if debugy==1
                figure
                polarplot(thc,rc,'x',tg_theta,TGpolsArray(i,:)); hold on
            end

        end
end

%find mean of defined geometries
DPpols = zeros(1, length(DPpolsArray));
NPpols = zeros(1, length(NPpolsArray));
for i = 1:length(theta_)
    DPpols(i) = mean(DPpolsArray(:,i));
    NPpols(i) = mean(NPpolsArray(:,i));
end

switch IsTear
    case 'Yes'
        TGpolar = zeros(1, length(TGpolsArray));
        for i = 1:length(tg_theta)
            TGpolar(i) = mean(TGpolsArray(:,i));
        end
end

% add repeated point to close diagram. Use 'theta' for repeat point
DPpolar = [DPpols , DPpols(1)];
NPpolar = [NPpols , NPpols(1)];
% DPpolar = DPpols;
% NPpolar = NPpols;

%% Rotate Plots
% Align discs to show AN at top, PL at base of graph.
close all
```

```
theta = -pi:stp:pi;    %list of radian measures evenly spaced in a circle
theta_ = -pi:stp:(pi - stp);    %theta without a repeated point

[M, I] = min(DPpolar);  %get indices of posterior concave section (min
radial distance)
thetaRot = -theta(I);    %get rotation angle

if mod(thetaRot, pi) ~= 0
    thetaR = theta + thetaRot;
    thetaR_ = theta_ + thetaRot;
    switch IsTear
        case 'Yes'
            tg_thetaR = tg_theta + thetaRot;
    end
%     imshow(discImg)

    discImgR = imrotate(discImg, -rad2deg(thetaRot+pi/2), 'nearest');

%     xlim([xlimmin xlimmax]);
%     ylim([ylimmin ylimmax]);


end
%correct to ensure limits of -pi:pi
thetaR = limitpimultiples(thetaR);
thetaR_ = limitpimultiples(thetaR_);
switch IsTear
    case 'Yes'
        tg_thetaR = limitpimultiples(tg_thetaR);
end

%cartesian coordinates saved for convenience
[DPcartX, DPcartY] = pol2cart(thetaR,DPpolar);
[NPcartX, NPcartY] = pol2cart(thetaR,NPpolar);
switch IsTear
    case 'Yes'
        [TGcartX, TGcartY] = pol2cart(tg_thetaR,TGpolar);
end


%% Calc results
%Disc Width
DWidth = max(DPcartY)-min(DPcartY);
DDepth = max(DPcartX)-min(DPcartX);
DArea = polyarea(DPcartX, DPcartY);  %Disc Area
NPArea = polyarea(NPcartX, NPcartY); %NP Area

%Tear Length
TLng = 0;
switch IsTear
    case 'Yes'
        for i=2:length(TGcartX)
            TLng = TLng + sqrt((TGcartX(i)-TGcartX(i-1))^2 + ...
                (TGcartY(i)-TGcartY(i-1))^2);
        end
end

%Average Tear Depth
```

```
TDepth = [];    % average tear depth in AN region
IDepth = [];    % average depth in narrower Injection region
InjectDepth = [];   %Initialised

switch IsTear
    case 'Yes'
    depth = zeros(1, length(tg_thetaR)); %array for later averaging

    [d, I] = min(abs(thetaR - tg_thetaR(1))); %get starting theta indices
for tear

    for i=1:length(tg_thetaR)    %i is indices on tear
        j = i+I-1;               %j is indices on DP and NP
        if j > length(thetaR)
            j = 1;              %allows looping past array end
        end
        depth(i) = (DPpolar(j)-TGpolar(i)) / (DPpolar(j)-NPpolar(j));

        if abs(tg_thetaR(i)) >= 3*pi/4 %measure in anterior region
            TDepth(length(TDepth)+1) = depth(i);
            if abs(tg_thetaR(i)) >= 5*pi/6   %rate injection only in
forward 1/8th
                IDepth(length(IDepth)+1) = depth(i);
            end
        end
    end

    TearDepth = mean(TDepth);
    InjectDepth = mean(IDepth);
end

switch IsTear
    case 'Yes'
        format short
        dlgTitle    = strcat('Over Ride inject depth? (',
num2str(InjectDepth),'%)');
    case 'No'
        dlgTitle    = strcat('Manually set inject depth?');
end
dlgQuestion = 'Do you want to manually set injection depth estimate?';
OvrrdEst = questdlg(dlgQuestion,dlgTitle,'Yes','No', 'No');

switch OvrrdEst
    case 'Yes'
        InjectDepth = str2double(inputdlg('Enter injection depth as ratio
of depth to Annulue thickness'));
end

%Tear Radial Arc
switch IsTear
    case 'Yes'
        T_Arc_rad = (length(tg_thetaR)-1)*stp;
        T_Arc_deg = rad2deg(T_Arc_rad);
end

%variable for easy data copying
switch IsTear
    case 'Yes'
        AAA = {specNum, testRun, psi, dur, DWidth, DDepth, DArea, ...
```

```
            DArea/(DWidth*DDepth), NPArea, InjectDepth, IsTear, loc,
TLng,...
            TearDepth, T_Arc_rad, T_Arc_deg, OtherTears, preload,
1.5*preload/DArea};
    otherwise
        AAA = {specNum, testRun, psi, dur, DWidth, DDepth, DArea, ...
            DArea/(DWidth*DDepth), NPArea, InjectDepth, IsTear, loc, ...
            0, 1, 0, 0, OtherTears, preload, 1.5*preload/DArea};
end

%% plot results
clf
format bank
subplot(1,2,1);
imshow(discImgR);
% xlim([xlimmin xlimmax]);
% ylim([ylimmin ylimmax]);

h1 = msgbox('Next select two DIAGONAL points that define a box around the
disc periphery - use right click to select second point (type d to delete
last point)' ...
    ,'Image Calibration','CreateMode','modal');
uiwait(h1);

xydisc = [];
n = 0;

but = 1; %left mouse button
while but == 1 %left mouse button has been clicked
    % zoom on
    [xi,yi,but] = ginput(1);
    n = n+1;
    %plot(xi,yi,'rx');
    xydisc(:,n) = [xi;yi];
end

%redraw figure using the approximate disc coordinates to 'zoom in' for
better resolution when selecting the disc periphery
sz = size(xydisc);
s2 = sz(2);
if s2>=3 %sometimes more than 2 points could be clicked if user forgets to
right-click for the 2nd final point - remove all other points except for
1st and last points selected
    xydisc(:,2:s2-1)=[];
end

%now set xlim and ylim for the figure and redraw axes to zoom in to
calibration block
%first store the full image size xlim and ylim values for zooming back out
later
xlimfull = xlim;
ylimfull = ylim;

xlimmin = min(xydisc(1,:));
xlimmax = max(xydisc(1,:));
ylimmin = min(xydisc(2,:));
ylimmax = max(xydisc(2,:));

xlim([xlimmin xlimmax]);
ylim([ylimmin ylimmax]);
```

```
subplot(1,2,2);

switch IsTear
    case 'Yes'
        polarplot(thetaR,DPpolar,'-k', thetaR,NPpolar,'-b',
tg_thetaR,TGpolar,'-r', 'LineWidth',2)
        legend({'Disc periphery', 'NP periphery', 'Delamination'},
'Location', 'south')
    case 'No'
        polarplot(thetaR,DPpolar,'-k', thetaR,NPpolar,'-b', 'LineWidth',2)
        legend({'Disc periphery', 'NP periphery', 'Location', 'south'})
end
pax = gca;
pax.ThetaDir = 'clockwise';
pax.ThetaZeroLocation = 'bottom';

sgtitle({"Ovine Intervertebral Disc Cross Section - " + specNum , ...
        loc + " injection :" + num2str(dur)+ "s  at " + num2str(psi) + ...
        " psi (" +  num2str(round(psi*6.89476)) + " kPa)"},'fontsize',18);
%sgtitle(ttl);

answer = questdlg('Choose plot max radius', 'Plot Size', "18", "21", "24",
"18");
a = str2num(answer);
switch a
    case 15
        rlim([0 15])
        rticks([6 12]);
        rticklabels({'r = 6 mm','r = 12 mm'});%
    case 18
        rlim([0 18])
        rticks([9 12 15]);
        rticklabels({'r = 9 mm','r = 12 mm', 'r = 15 mm'});
    case 21
        rlim([0 21])
        rticks([6 12 18 ]);
        rticklabels({'r = 6 mm','r = 12 mm','r = 18 mm'});%

    case 24
        rlim([0 24])
        rticks([9 15 21]);
        rticklabels({'r = 9 mm','r = 15 mm','r = 21 mm'});%
end

switch IsTear
    case 'Yes'
        txt = {strcat('Tear Length :', num2str(TLng,'%.1f'), ' mm'), ...
            strcat('Needle depth :', num2str(InjectDepth*100,'%.1f'), '% of
AF'), ...
            strcat('Tear Arc :', num2str(T_Arc_deg,'%.1f'), ' degrees'),...
            strcat('Disc Area :', num2str(DArea, '%.1f'), ' mm','^{', '2',
'}')};
    otherwise
        txt = {strcat('Tear Length : NIL'), ...
            strcat('Disc Area :', num2str(DArea, '%.1f'), ' mm','^{', '2',
'}')};
end
```

```
annotation('textbox',[0.4,0.05,0.16,0.18],'String',txt,'EdgeColor','k','fon
tsize',14, 'FitBoxToText','on')

%figure
%plot(DPcartX,DPcartY,'-g', NPcartX,NPcartY,'-b', TGcartX,TGcartY,'-r')

%% save parameters to matlab file
save(paramfile);
savefig([specNum '_' num2str(testRun)]);
openvar('AAA')
msgbox('Disc digitisation complete, copy data to results.')


%% Fuctions
function A = limitpimultiples(V)
%for each element of vector, ensures corrects to single multiples of pi

for i = 1:length(V)
    if abs(V(i)) > pi
        %mult = ((abs(V(i)) - mod(abs(V(i)), pi)) / pi) + 1;
        if V(i) > pi
            V(i) = V(i) - 2*pi;
        elseif V(i) < -pi
            V(i) = V(i) + 2*pi;
        end
    end
end
A = V;
end
```

Apendix D SPSS Statistics Outputs

To analyse the results, it was necessary to compare the DV, delamination lengths (mm), to the IVs of injection pressure (psi) and injection duration. Two-way ANOVA comparisons were performed using SPSS software. ANOVA comparisons assume that;

1. The dependent variable (DV) is continuous
2. The independent variable (IV) has a least 2 groups
3. That there is independence of observations
4. That there are no significant outliers
5. That the dependent variable is normally distributed (for n >= 25)
6. That there is homogeneity of variance
7. That the groups are of relatively homogenous size

Full Data Set

Table D-1, Study groups pressure vs duration with unrestricted data

Injection Pressure (psi) * Injection Duration (s) Crosstabulation

Count

		Injection Duration (s)		
		15	60	Total
Injection Pressure (psi)	60	7	8	15
	80	5	9	14
	98	11	10	21
Total		23	27	50

A two way ANOVA was carried out on the full data set including 15 and 60-second injections, 60, 80, and 98 psi injections, and all hydration preloads cases. Delamination tear length (mm) was set as the DV. Pressure and injection duration were set as ordinal IV's. It should be noted that this was not a well-balanced study, with significant differences in group sizes shown in Table D-1.

Table D-2 shows that Levene's test failed to reject the null hypothesis ($P > 0.1$), confirming the assumption that error variance was homogenous between groups. However, Table D-3 showed that both the Kolmogorov-Smirnov and Shapiro-Wilk tests for normality of the residuals rejected the null hypothesis ($P < 0.001$), showing that the data is not normally distributed. Table D-4 also showed that skewness and kurtosis values both exceed the associated standard errors, indicating that the data is both skewed and highly variable

Table D-2, Levenes test, unrestricted, untransformed data

Levene's Test of Equality of Error Variances[a,b]

		Levene Statistic	df1	df2	Sig.
Delamination (mm)	Based on Mean	1.533	5	44	.199
	Based on Median	1.165	5	44	.341
	Based on Median and with adjusted df	1.165	5	39.625	.343
	Based on trimmed mean	1.461	5	44	.222

Tests the null hypothesis that the error variance of the dependent variable is equal across groups.

a. Dependent variable: Delamination (mm)

b. Design: Intercept + Pressure + Time + Pressure * Time

Table D-3, Normalcy of residuals for the full data range

Tests of Normality

	Kolmogorov-Smirnov[a]			Shapiro-Wilk		
	Statistic	df	Sig.	Statistic	df	Sig.
Standardized Residual for Length	.193	50	.000	.894	50	.000

a. Lilliefors Significance Correction

Table D-4, Length residual descriptives

Descriptives

			Statistic	Std. Error
Standardized Residual for Length	Mean		.0000	.13401
	95% Confidence Interval for Mean	Lower Bound	-.2693	
		Upper Bound	.2693	
	5% Trimmed Mean		-.0609	
	Median		-.2599	
	Variance		.898	
	Std. Deviation		.94761	
	Minimum		-1.20	
	Maximum		2.78	
	Range		3.98	
	Interquartile Range		1.02	
	Skewness		1.108	.337
	Kurtosis		.691	.662

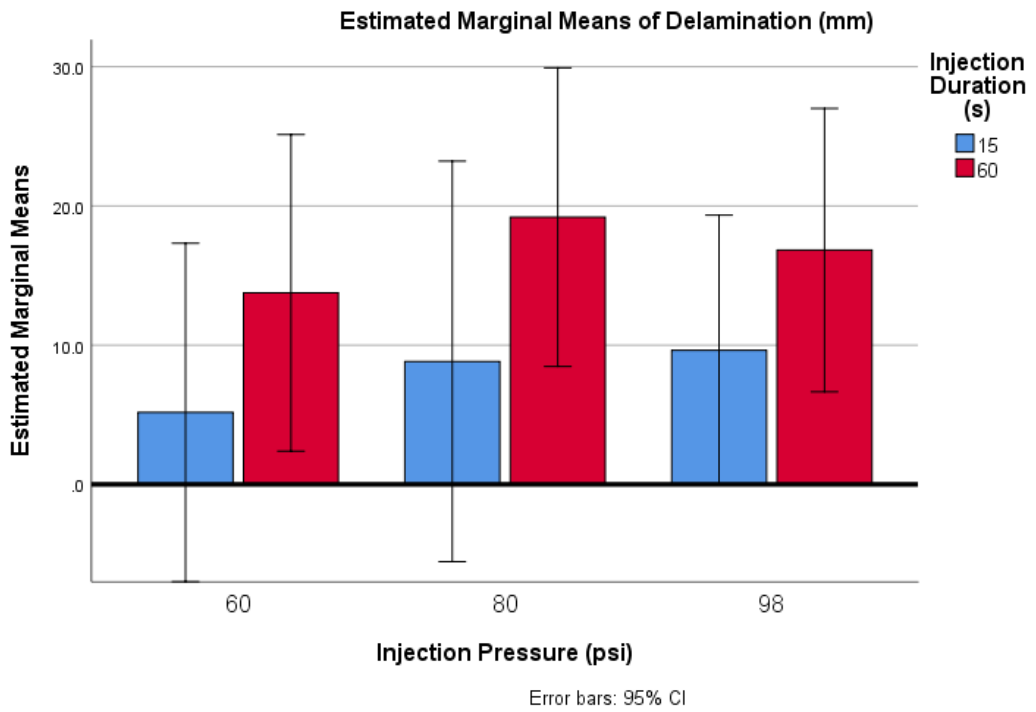

Figure D-1, Group Means for delamination, full data set untransformed

Table D-5, Test between-subject effects for delamination, unrestricted dataset

Tests of Between-Subjects Effects

Dependent Variable: Delamination (mm)

Source	Type III Sum of Squares	df	Mean Square	F	Sig.	Partial Eta Squared
Corrected Model	1134.392[a]	5	226.878	.891	.496	.092
Intercept	7001.754	1	7001.754	27.483	.000	.384
Pressure	176.067	2	88.033	.346	.710	.015
Time	888.161	1	888.161	3.486	.069	.073
Pressure * Time	20.207	2	10.103	.040	.961	.002
Error	11209.763	44	254.767			
Total	20471.122	50				
Corrected Total	12344.155	49				

a. R Squared = .092 (Adjusted R Squared = -.011)

Table D-6, Test between subjects for all loading cases

Table D-6 shows that the ANOVA did not show a significant interaction between the injection time and the injection pressure (P = .961). Similarly, the ANOVA did not appear to show a significant effect pressure (P = .710), and time was marginally significant (P = .069)

As the data was non-normal, the DV, delamination length was put through a standard transformation by adding 1 to remove zeros and taking the natural log

Equation 1, Data transformation equation

$$v = ln(DV + 1)$$

Where v is the transformed variable.

Table D-7, Lavene's Equality test, unrestricted transformed data

Levene's Test of Equality of Error Variances[a,b]

		Levene Statistic	df1	df2	Sig.
LogTrans	Based on Mean	2.194	5	44	.072
	Based on Median	.685	5	44	.637
	Based on Median and with adjusted df	.685	5	32.105	.638
	Based on trimmed mean	2.183	5	44	.073

Tests the null hypothesis that the error variance of the dependent variable is equal across groups.

a. Dependent variable: LogTrans

b. Design: Intercept + Pressure + Time + Pressure * Time

Equation 2, Normality tests, transformed unrestricted data

Tests of Normality

	Kolmogorov-Smirnov[a]			Shapiro-Wilk		
	Statistic	df	Sig.	Statistic	df	Sig.
Standardized Residual for LogTrans	.108	50	.200*	.942	50	.016

*. This is a lower bound of the true significance.

a. Lilliefors Significance Correction

The transformed data passed Levene's test for error variance (P = 0.72). The residuals of the transformed data all show negative Kurtosis and a skewness value less than the standard error. The Kolmogorov-Smirnova normality test showed a non-significant result, failing to reject the null hypothesis. The Shapiro-Wilk did test returned a significant result, indicating non-normal data. ANOVAs are known to be robust for violations of the normality assumption, so this was considered to be acceptable.

Equation 3, Descriptive stats, unrestricted tranformed data

Descriptives

			Statistic	Std. Error
Standardized Residual for LogTrans	Mean		.0000	.13401
	95% Confidence Interval for Mean	Lower Bound	-.2693	
		Upper Bound	.2693	
	5% Trimmed Mean		-.0167	
	Median		.0626	
	Variance		.898	
	Std. Deviation		.94761	
	Minimum		-1.40	
	Maximum		1.90	
	Range		3.30	
	Interquartile Range		1.57	
	Skewness		.058	.337
	Kurtosis		-1.130	.662

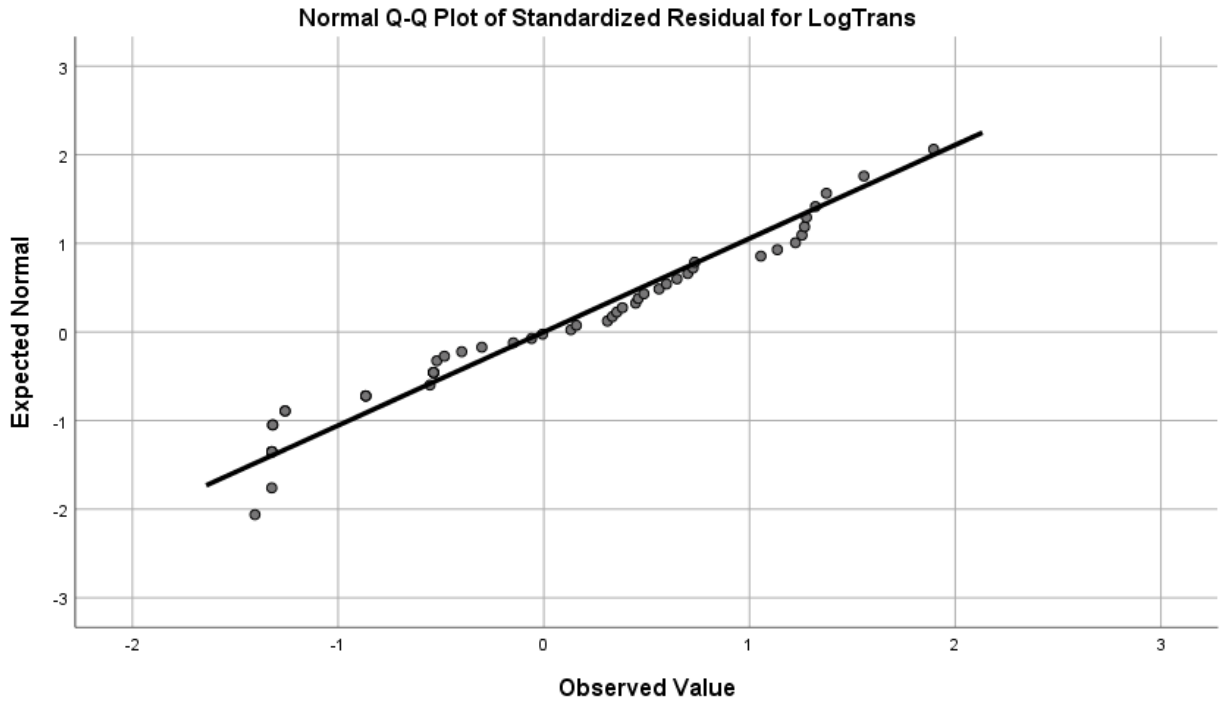

Figure D-2, Residual Q-Q Plot, transformed unrestricted data

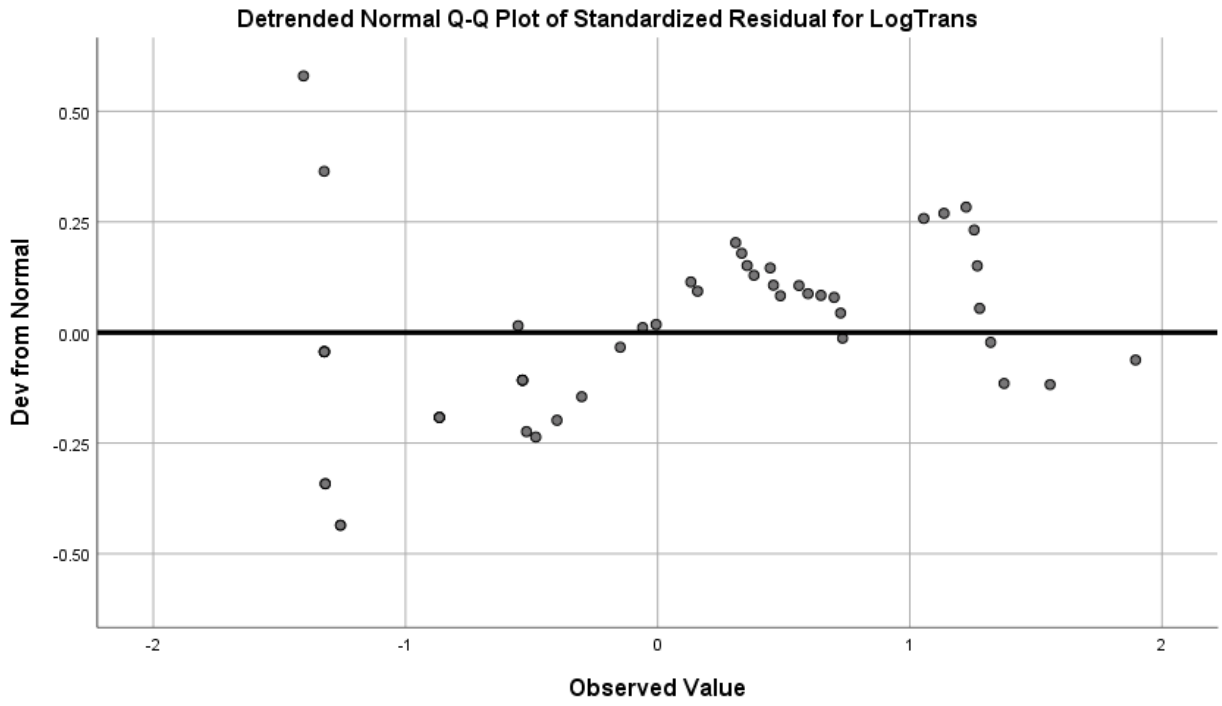

Figure D-3, Detrended Q-Q plot for transformed data (full dataset)

It should be noted that the Q-Q plots, shown in Figure D-2 and Figure D-3 show agreement albeit imperfect agreement with the normality assumption.

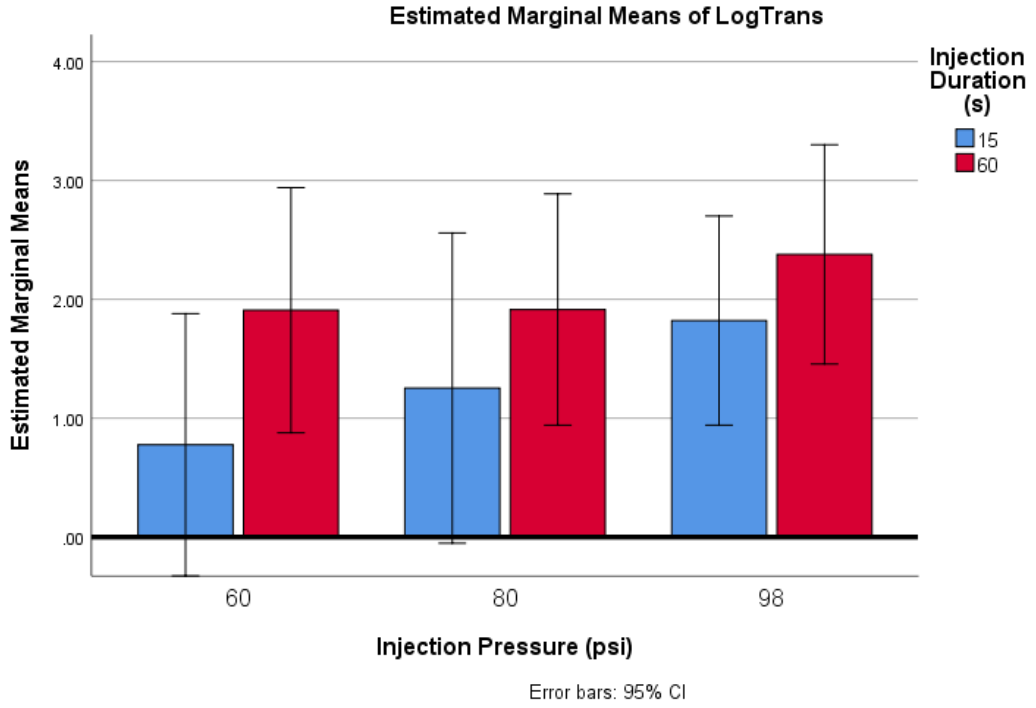

Figure D-4, Estimated means of transformed delamination results

Table D-8, ANOVA results for the full dataset

Tests of Between-Subjects Effects

Dependent Variable: LogTrans

Source	Type III Sum of Squares	df	Mean Square	F	Sig.	Partial Eta Squared
Corrected Model	12.304[a]	5	2.461	1.174	.337	.118
Intercept	131.216	1	131.216	62.600	.000	.587
Pressure	5.378	2	2.689	1.283	.287	.055
Time	7.170	1	7.170	3.421	.071	.072
Pressure * Time	.766	2	.383	.183	.834	.008
Error	92.229	44	2.096			
Total	259.429	50				
Corrected Total	104.534	49				

a. R Squared = .118 (Adjusted R Squared = .017)

The results of the two way ANOVA on the transformed data showed no significance for the effect of pressure on delamination length (P = 0.287), and no significance for interaction between pressure and injection duration (P = 0.834). The relationship of time to pressure was marginally significant (P < 0.1). Importantly the significance of the transformed data was consistent with the untransformed data, providing an indication that the result was reliable. Post hoc tests could not be performed on the time factor, as there were only two groups. It was not necessary to perform post-hoc tests on pressure, which returned an insignificant result.

The full data set was then subjected to an ANCOVA to test if covariant factors like disc size or hydration preload had a significant effect on the observed variations.

Table D-9, Full dataset Levene's Test

Levene's Test of Equality of Error Variances[a]

Dependent Variable: LogTrans

F	df1	df2	Sig.
2.457	5	44	.048

Tests the null hypothesis that the error variance of the dependent variable is equal across groups.

a. Design: Intercept + Preload + Area + Pressure + Time + Pressure * Time

Levene's test on the variance of error was significant (P = 0.48), indicating a lack of homogeneity between factors.

Tests of Between-Subjects Effects

Dependent Variable: LogTrans

Source	Type III Sum of Squares	df	Mean Square	F	Sig.	Partial Eta Squared
Corrected Model	13.125[a]	7	1.875	.861	.544	.126
Intercept	4.723	1	4.723	2.170	.148	.049
Preload	.781	1	.781	.359	.552	.008
Area	.018	1	.018	.008	.928	.000
Pressure	3.897	2	1.948	.895	.416	.041
Time	6.207	1	6.207	2.852	.099	.064
Pressure * Time	.857	2	.428	.197	.822	.009
Error	91.409	42	2.176			
Total	259.429	50				
Corrected Total	104.534	49				

a. R Squared = .126 (Adjusted R Squared = -.020)

The ANCOVA did not show a significant covariant effect for either hydration preload (P > 0.1) or for disc area (P > 0.1).

Restricted Data Set

As ANOVA tests are less sensitive to violations of assumptions in a balanced study, it was decided to run an ANOVA and ANCOVA with a balanced set. This was achieved by removing the smaller data groups associated with the 80 psi groups and the data low preload groups with a preload > 0.04 MPa.

Between-Subjects Factors

		Value Label	N
Injection Pressure (psi)	60	60	15
	98	98	16

Injection Duration (s)	15	15	16
	60	60	15

Table D-10, Descriptive Stats for restricted data set

Descriptive Statistics

Dependent Variable: Delamination (mm)

Injection Pressure (psi)	Injection Duration (s)	Mean	Std. Deviation	N
60	15	5.168	12.2086	7
	60	13.761	17.3987	8
	Total	9.750	15.3273	15
98	15	6.491	6.2832	9
	60	14.674	10.9796	7
	Total	10.071	9.3194	16
Total	15	5.912	9.0075	16
	60	14.187	14.2564	15
	Total	9.916	12.3727	31

As can be seen in Table D-10, the restricted data provided a well-balanced study.

Levene's Test of Equality of Error Variances[a,b]

		Levene Statistic	df1	df2	Sig.
Delamination (mm)	Based on Mean	2.363	3	27	.093
	Based on Median	.945	3	27	.433
	Based on Median and with adjusted df	.945	3	17.721	.440
	Based on trimmed mean	1.968	3	27	.143

Tests the null hypothesis that the error variance of the dependent variable is equal across groups.

a. Dependent variable: Delamination (mm)

b. Design: Intercept + Pressure + Time + Pressure * Time

Descriptives

			Statistic	Std. Error
Standardized Residual for Length	Mean		.0000	.17039
		Lower Bound	-.3480	

	95% Confidence Interval for Mean Upper Bound	.3480	
	5% Trimmed Mean	-.0631	
	Median	-.3285	
	Variance	.900	
	Std. Deviation	.94868	
	Minimum	-1.15	
	Maximum	2.29	
	Range	3.44	
	Interquartile Range	1.03	
	Skewness	1.226	.421
	Kurtosis	.996	.821

Tests of Normality

	Kolmogorov-Smirnov[a]			Shapiro-Wilk		
	Statistic	df	Sig.	Statistic	df	Sig.
Standardized Residual for Length	.207	31	.002	.864	31	.001

a. Lilliefors Significance Correction

Tests of Between-Subjects Effects

Dependent Variable: Delamination (mm)

Source	Type III Sum of Squares	df	Mean Square	F	Sig.	Partial Eta Squared
Corrected Model	540.093[a]	3	180.031	1.199	.329	.118
Intercept	3080.449	1	3080.449	20.524	.000	.432
Pressure	9.589	1	9.589	.064	.802	.002
Time	539.295	1	539.295	3.593	.069	.117
Pressure * Time	.323	1	.323	.002	.963	.000
Error	4052.434	27	150.090			
Total	7640.641	31				
Corrected Total	4592.528	30				

a. R Squared = .118 (Adjusted R Squared = .020)

Levene's test was not significant (P > 0.05), indicating that the assumption of homogeneity of variance had been met. However normality tests were significant (P > 0.05), and

skewness and kurtosis were both shown to be greater than the standard error, indicating that the normality assumption had been violated.

The comparison was run with the transformed data

Levene's Test of Equality of Error Variances[a,b]

		Levene Statistic	df1	df2	Sig.
LogTrans	Based on Mean	.354	3	27	.787
	Based on Median	.317	3	27	.813
	Based on Median and with adjusted df	.317	3	20.260	.813
	Based on trimmed mean	.371	3	27	.774

Tests the null hypothesis that the error variance of the dependent variable is equal across groups.

a. Dependent variable: LogTrans

b. Design: Intercept + Pressure + Time + Pressure * Time

Tests of Normality

	Kolmogorov-Smirnov[a]			Shapiro-Wilk		
	Statistic	df	Sig.	Statistic	df	Sig.
Standardized Residual for LogTrans	.093	31	.200*	.970	31	.506

*. This is a lower bound of the true significance.

a. Lilliefors Significance Correction

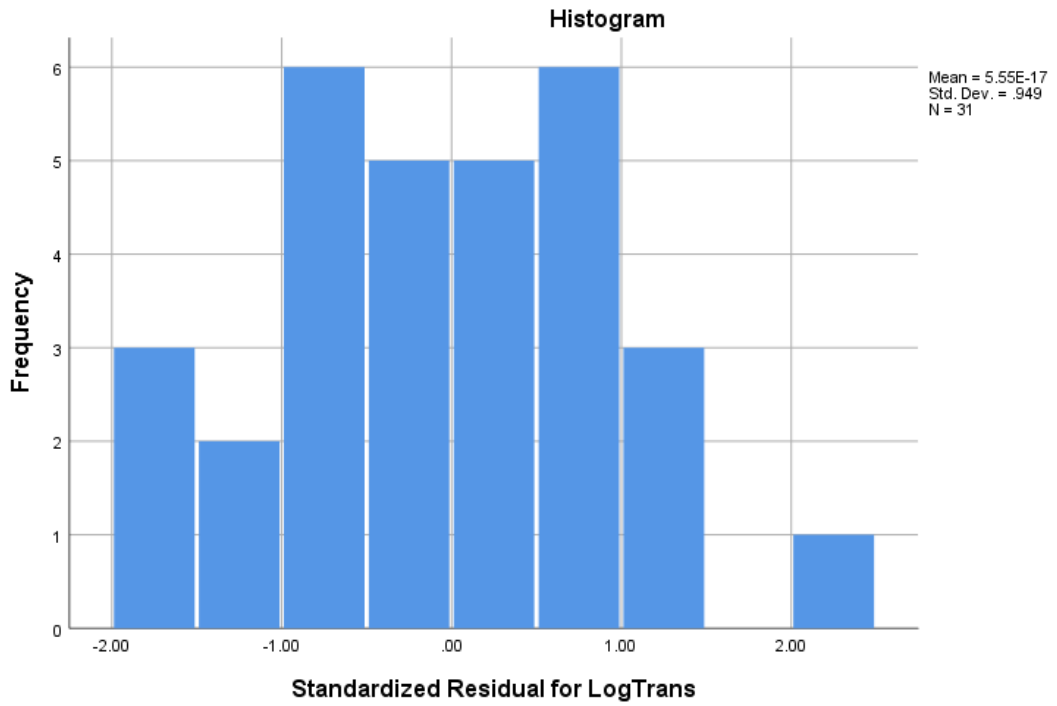

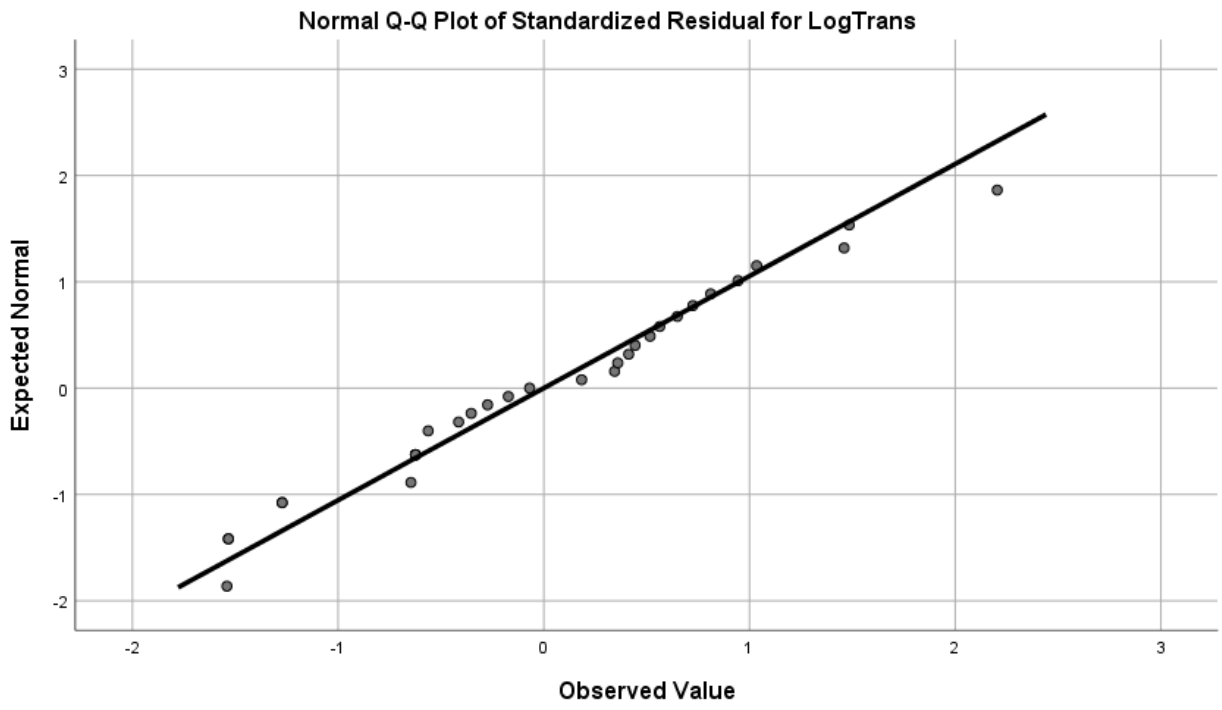
Normal Q-Q Plot of Standardized Residual for LogTrans
Expected Normal
Observed Value
3
2
1
0
-1
-2
-2
-1
0
1
2
3

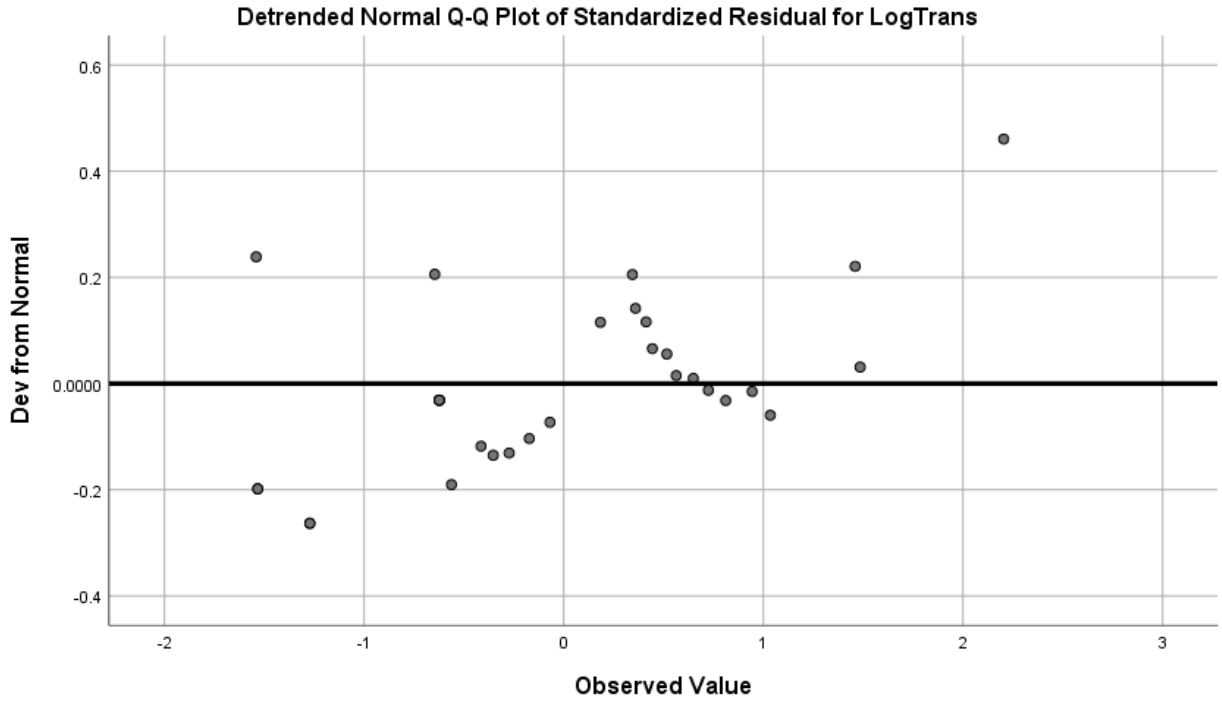
Detrended Normal Q-Q Plot of Standardized Residual for LogTrans
Dev from Normal
Observed Value
0.6
0.4
0.2
0.0000
-0.2
-0.4
-2
-1
0
1
2
3

Levene's returned a non-significant result, indicating that that homogeneity of variance assumptions had been met. Normality tests on the standardised residuals returned a non - significant results (P > 0.1) indicating that normality assumptions had been met. Examination of the residuals histogram reveals some platykurtosis, but the ANOVA is tolerant to violations of normality, particularly with a balanced design or N > 25.

Tests of Between-Subjects Effects

Dependent Variable: LogTrans

Source	Type III Sum of Squares	df	Mean Square	F	Sig.	Partial Eta Squared
Corrected Model	9.651[a]	3	3.217	2.076	.127	.187
Intercept	84.719	1	84.719	54.676	.000	.669
Pressure	3.137	1	3.137	2.025	.166	.070
Time	7.136	1	7.136	4.606	.041	.146
Pressure * Time	.215	1	.215	.139	.713	.005
Error	41.836	27	1.549			
Total	137.435	31				
Corrected Total	51.486	30				

a. R Squared = .187 (Adjusted R Squared = .097)

The transformed data showed a significant effect for the duration of injection (P < 0.05) but not for pressure (P >0.1) or for the interaction between pressure and time (P > 0.05).

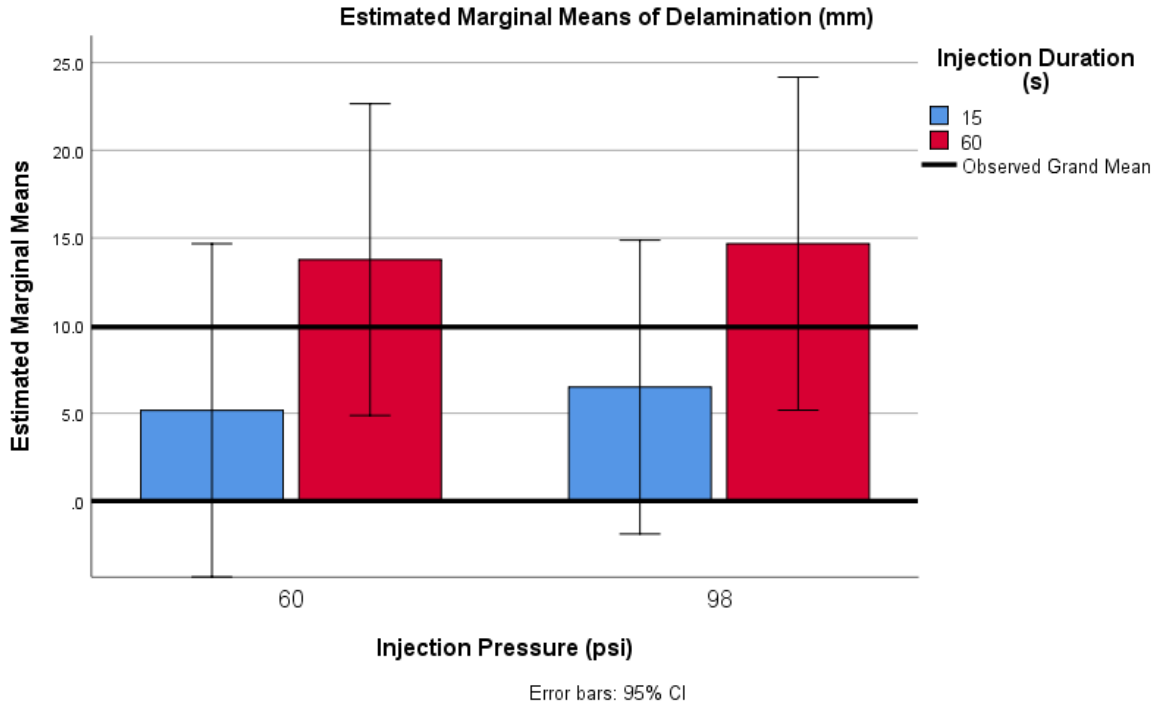

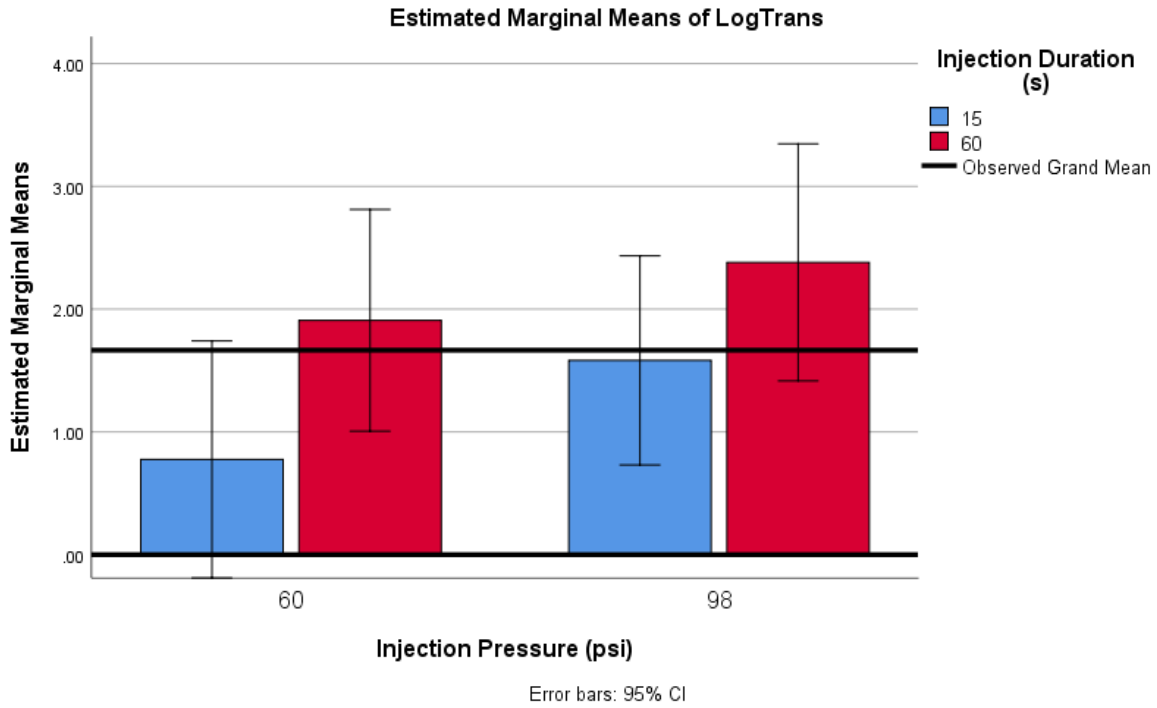

The ANCOVA was repeated for the restricted data set,

Levene's Test of Equality of Error Variances[a]

Dependent Variable: LogTrans

F	df1	df2	Sig.

.647	3	27	.592

Tests the null hypothesis that the error variance of the dependent variable is equal across groups.

a. Design: Intercept + Preload + Area + Pressure + Time + Pressure * Time

Tests of Between-Subjects Effects

Dependent Variable: LogTrans

Source	Type III Sum of Squares	df	Mean Square	F	Sig.	Partial Eta Squared
Corrected Model	11.180[a]	5	2.236	1.387	.263	.217
Intercept	.014	1	.014	.009	.927	.000
Preload	.190	1	.190	.118	.734	.005
Area	1.517	1	1.517	.941	.341	.036
Pressure	3.651	1	3.651	2.264	.145	.083
Time	7.386	1	7.386	4.581	.042	.155
Pressure * Time	.056	1	.056	.035	.854	.001
Error	40.306	25	1.612			
Total	137.435	31				
Corrected Total	51.486	30				

a. R Squared = .217 (Adjusted R Squared = .061)

The ANCOVA did not show a significant relationship for the covariants of hydration preload ($P > 0.1$) or for disc area ($P > 0.1$).

Comparison With Outliers Removed.

For the sake of comparison and discussion the means of data with outliers removed was considered.

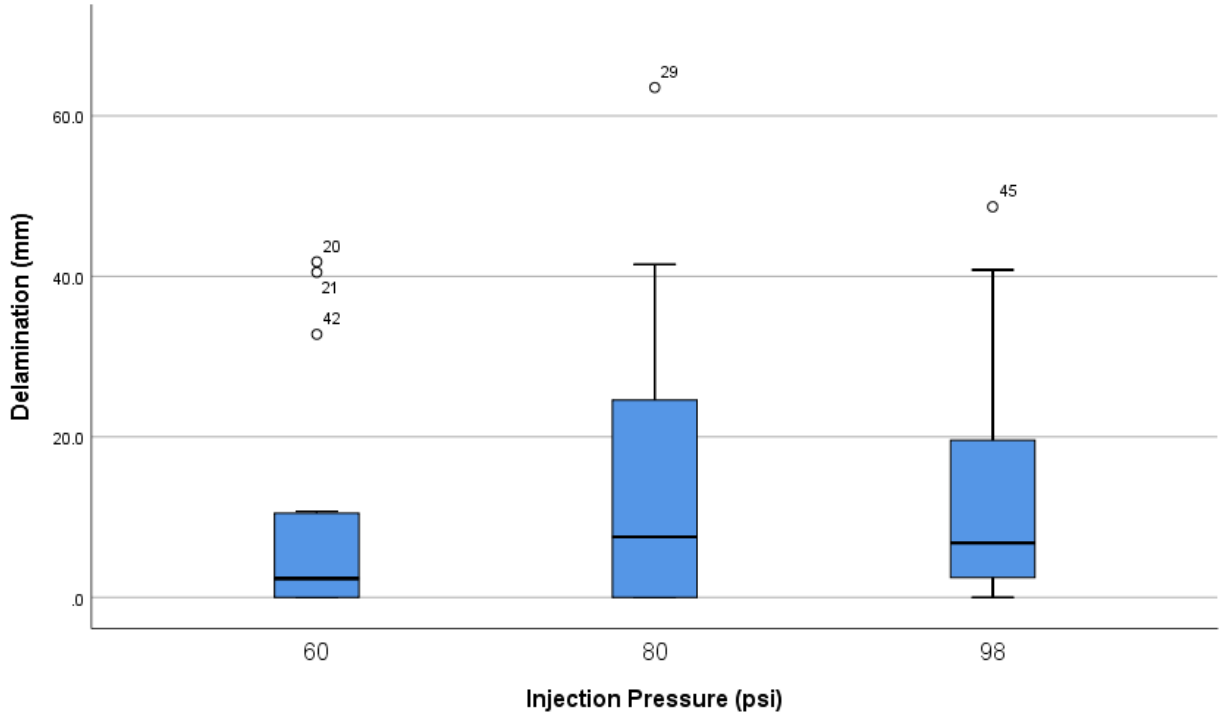

Figure D-5, Box chart with outliers marked

Levene's Test of Equality of Error Variances[a,b]

		Levene Statistic	df1	df2	Sig.
LogTrans	Based on Mean	5.257	5	39	.001
	Based on Median	1.796	5	39	.136
	Based on Median and with adjusted df	1.796	5	17.852	.165
	Based on trimmed mean	5.148	5	39	.001

Tests the null hypothesis that the error variance of the dependent variable is equal across groups.

a. Dependent variable: LogTrans

b. Design: Intercept + Pressure + Time + Pressure * Time

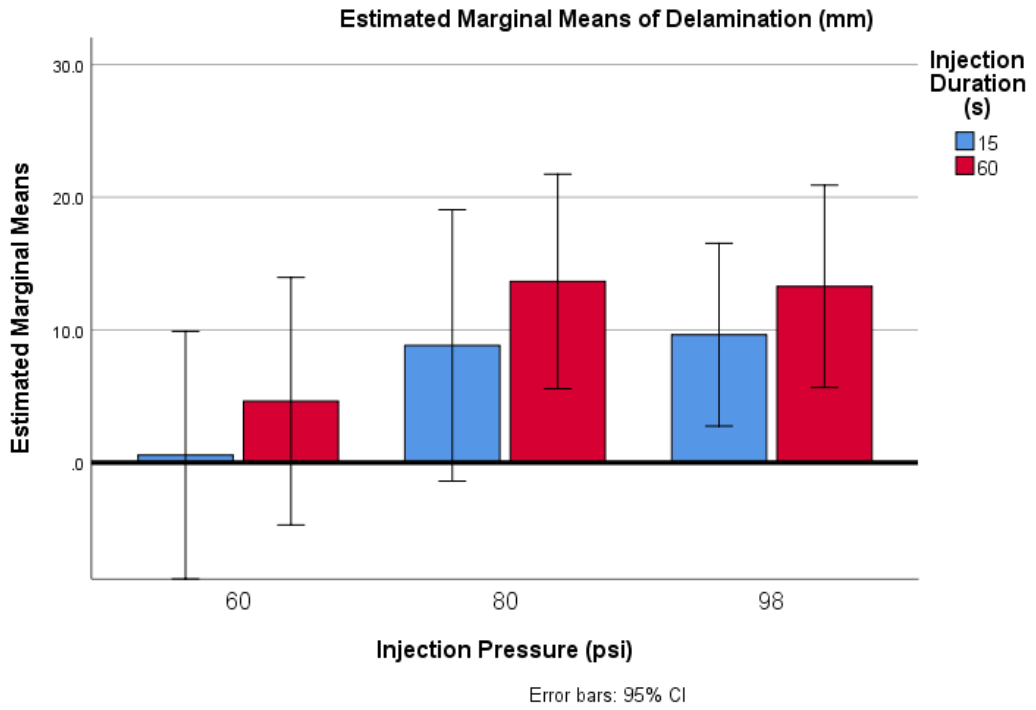

Figure D-6, Mean delamination with outliers removed

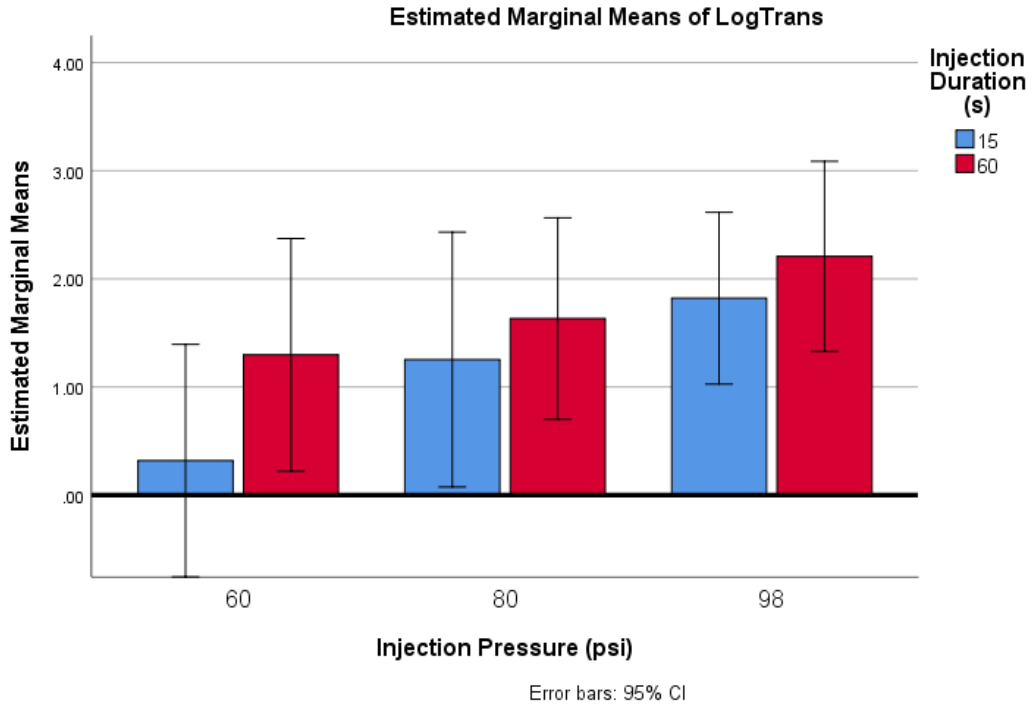

Apendix E Results and Geometry for All IVDs

Disc ID	Injection Pressure (psi)	Injection Duration (s)	Disc Width (mm)	Disc Depth (mm)	Disc Area (mm2)	DiscArea /Bounding box Ratio	NP Area (mm2)	Inject Depth)	Is Tear	Injection Region	Tear Length (mm)	Avg Tear Depth (% of AF)	Tear Arc (Rad)	Tear Arc (deg)	Other Tears Present	Preload (N)
S1L1	60	30	28.77	21.57	472.30	0.76	164.60	[]	No	AN	0.00	[]	0.00	0	No	31.85
S1L2	60	30	31.60	24.71	607.84	0.78	217.08	0.15	Yes	AN	2.54	0.15	0.22	12.42	Yes	151.08
S1L3	60	30	32.34	24.56	611.90	0.77	219.89	0.20	Yes	AN	20.68	0.20	1.60	91.89	Yes	36.29
S2L1	60	15	33.59	30.37	788.79	0.77	313.19	0.29	Yes	AN	22.53	0.28	1.64	94.23	No	162.64
S3L1	60	60	29.90	24.33	573.05	0.79	226.91	0.30	Yes	AN	3.83	0.30	0.35	20.07	No	133.94
S3L3	60	60	28.36	23.25	542.86	0.82	247.21	0.15	Yes	AN	4.65	0.15	0.40	23.04	Yes	24.03
S4L1	98	30	27.25	23.13	489.42	0.78	180.03	0.33	Yes	AN	7.36	0.33	0.74	42.66	Yes	9.8
S4L2	98	60	24.76	19.44	374.10	0.78	143.49	0.43	Yes	AN	0.41	0.43	0.06	3.24	No	9.8
S5L1	98	60	24.35	20.66	392.11	0.78	162.70	0.67	Yes	AN	48.66	0.65	4.97	284.7	Yes	9.8
S5L2	98	15	29.44	23.15	531.78	0.78	203.53	0.70	Yes	AN	40.80	0.69	3.84	219.8	Yes	9.8
S6L1	98	15	38.01	32.82	974.28	0.78	445.09	0.50	Yes	AN	6.77	0.50	0.53	30.42	Yes	9.8
S6L2	98	60	33.47	26.18	695.07	0.79	335.84	0.64	Yes	AN	16.47	0.64	1.61	92.52	No	9.8
S7L1	80	15	32.68	25.44	628.19	0.76	342.31	NaN	Yes	AN	5.41	NaN	0.44	25.38	Yes	9.8
S8L1	80	15	24.62	22.33	425.90	0.77	166.09	0.85	Yes	PL	2.02	NaN	0.21	11.79	No	9.8
S9L1	80	30	33.25	29.04	757.88	0.79	289.47	0.52	Yes	AN	13.39	0.52	1.24	71.1	No	9.8
S10L1	80	30	27.56	23.25	502.72	0.78	183.00	[]	No	AN	0.00	[]	0.00	0	No	9.8
S11L1	80	60	35.67	29.38	818.08	0.78	280.74	[]	No	AN	0.00	[]	0.00	0	No	9.8
S12L1	80	60	26.92	22.37	469.51	0.78	188.84	0.55	Yes	AN	34.09	0.53	3.39	194.2	No	9.8
S13L1	60	15	31.30	27.69	679.21	0.78	265.81	0.15	Yes	AN	1.04	0.15	0.08	4.5	No	39.72
S13L3	60	60	34.84	27.27	736.50	0.78	242.32	[]	No	PL	0.00	[]	0.00	0	Yes	43.2
S14L1	60	60	28.37	26.17	555.45	0.75	218.22	0.60	Yes	PL	0.53	NaN	0.05	2.61	No	26.48
S14L2	60	15	25.03	19.97	377.49	0.76	168.03	NaN	Yes	PL	3.49	NaN	0.27	15.75	No	26.48
S15L1	98	15	45.07	33.86	1173.20	0.77	394.16	0.69	Yes	AN	11.01	0.68	1.13	64.71	No	64.3
S16L1	98	30	29.91	23.93	534.14	0.75	240.49	[]	No	AN	0.00	[]	0.00	0	No	30.48
S16L2	98	15	29.41	24.34	560.11	0.78	206.68	0.67	Yes	AN	6.48	0.64	0.79	45.27	No	28.44
S17L1	98	60	29.55	27.37	617.00	0.76	230.08	0.61	Yes	AN	5.97	0.59	0.63	35.91	Yes	27.48
S17L2	98	30	27.85	25.93	554.76	0.77	174.33	[]	No	AN	0.00	[]	0.00	0	No	30.88
S19L1	80	60	30.53	25.94	620.68	0.78	216.64	[]	No	PL	0.00	[]	0.00	0	No	32.93
S19L2	80	30	32.49	26.15	666.44	0.78	247.23	[]	No	PL	0.00	[]	0.00	0	No	168.78
S19L3	80	30	26.50	21.67	440.05	0.77	170.54	0.60	Yes	PL	1.41	NaN	0.12	6.84	No	36.28
S21LX	80	60	36.80	27.45	796.06	0.79	337.08	0.76	Yes	AN	15.07	0.75	1.62	93.06	No	31.75
S22L1	80	60	32.66	27.12	702.75	0.79	197.35	[]	No	AN	0.00	[]	0.00	0	Yes	41.66
S22L2	80	15	33.95	27.11	735.96	0.80	262.29	[]	No	AN	0.00	[]	0.00	0	No	40.8
S23L1	80	15	29.80	23.03	525.53	0.77	179.01	[]	No	AN	0.00	[]	0.00	0	No	26.88
S29LX	80	15	31.61	28.99	729.96	0.80	246.65	0.50	No	AN	0.00	[]	0.00	0	No	34.84
S30LX	80	60	31.34	27.93	705.28	0.81	265.29	[]	No	AN	0.00	[]	0.00	0	No	30.88
S31TL	98	15	33.05	26.14	663.24	0.77	217.24	0.66	Yes	AN	5.12	0.66	0.53	30.15	No	28.5

S31L1	80	15	29.99	26.63	609.42	0.76	204.21	0.63	Yes	AN	19.58	0.61	2.07	118.8	Yes	30.88
S31L2	98	60	32.57	27.48	694.06	0.78	223.87	0.63	Yes	AN	20.81	0.62	2.05	117.3	Yes	30.86
S31L3	80	60	36.25	26.80	754.95	0.78	271.19	0.67	Yes	AN	18.61	0.66	1.86	106.5	No	33.81
S31L4	98	60	32.49	27.23	694.61	0.79	229.45	0.61	Yes	AN	28.69	0.59	2.78	159.4	No	33.92
S31L5	80	15	32.42	29.46	738.46	0.77	217.42	0.65	No	AN	0.00	[]	0.00	0	Yes	38.3
S32L2	98	15	38.46	31.72	934.69	0.77	317.67	0.69	Yes	AN	14.78	0.72	1.45	82.89	Yes	36.03
S33L1	98	60	32.35	26.75	669.69	0.77	254.34	0.88	Yes	AN	19.57	0.88	2.55	146.3	Yes	28.5
S33L2	98	60	29.13	23.46	525.40	0.77	206.63	1.10	No	AN	0.00	[]	0.00	0	No	27.71
S33L3	98	15	32.45	25.75	644.24	0.77	271.07	0.85	Yes	AN	16.66	0.85	1.98	113.7	No	26.5
S33L4	98	15	33.13	26.70	691.20	0.78	256.58	0.75	No	AN	0.00	[]	0.00	0	No	26.5
S34L1	98	60	36.87	32.21	903.21	0.76	355.25	0.48	Yes	AN	3.84	0.48	0.32	18.18	No	29.4
S34L2	98	15	33.70	27.44	737.26	0.80	308.67	0.60	Yes	AN	1.91	0.60	0.19	10.98	No	29.4
S35LX	60	15	41.04	30.99	972.38	0.76	411.50	0.50	Yes	AN	0.99	0.50	0.08	4.86	No	35.8
S36L1	60	15	31.58	26.30	629.68	0.76	261.48	[]	No	AN	0.00	[]	0.00	0	No	32.64
S36L2	60	60	32.15	26.46	650.59	0.76	274.71	[]	No	AN	0.00	[]	0.00	0	No	32.64
S37L1	60	15	28.04	23.35	528.39	0.81	215.25	0.67	Yes	AN	2.40	0.67	0.28	16.11	Yes	26
S37L2	98	15	31.94	26.91	682.75	0.79	268.48	0.49	Yes	AN	2.47	0.49	0.23	13.41	No	26.48
S37L3	60	15	34.93	27.24	756.04	0.79	322.20	[]	No	AN	0.00	[]	0.00	0	No	28.5
S37L4	60	60	38.30	27.83	847.74	0.80	371.27	0.59	Yes	AN	2.35	0.59	0.23	13.23	No	32.59
S37L5	60	60	32.97	27.42	726.16	0.80	310.15	0.61	Yes	AN	4.44	0.61	0.47	27	No	29.64
S38L1	98	60	29.63	23.74	557.40	0.79	212.84	0.57	Yes	AN	0.59	0.57	0.06	3.51	No	28.5
S38L2	60	15	35.85	29.89	859.11	0.80	286.24	0.53	Yes	AN	32.78	0.51	2.63	150.6	No	30.86
S38L3	60	60	34.61	28.10	784.73	0.81	281.36	0.62	Yes	AN	41.81	0.61	3.38	193.6	Yes	36.3
S39L1	98	15	31.29	25.26	619.48	0.78	195.54	[]	No	AN	0.00	[]	0.00	0	No	30.88
S39L2	80	60	30.92	27.69	677.57	0.79	233.49	[]	No	AN	0.00	1.00	0.00	0	Yes	26.8
S39L3	80	60	31.13	26.86	660.26	0.79	241.14	0.46	Yes	AN	63.53	0.45	4.89	280.4	No	27.8
S42L2	60	60	28.89	23.16	525.55	0.79	209.77	0.73	Yes	AN	10.72	0.72	1.36	77.85	No	29.4
S43L1	98	60	31.44	26.12	642.52	0.78	231.38	0.92	Yes	AN	23.26	0.91	2.81	161.1	No	30.88
S43L2	60	60	37.44	29.33	815.65	0.74	305.01	0.72	Yes	AN	10.27	0.72	1.12	64.44	Yes	35.8
S44L2	60	60	37.57	32.21	950.48	0.79	407.90	0.60	No	AN	0.00	[]	0.00	0	No	36.3
S44L3	60	15	32.24	26.95	674.26	0.78	292.86	1.10	No	AN	0.00	[]	0.00	0	Yes	36.3
S45L1	60	15	34.06	25.91	701.39	0.79	284.56	0.65	No	AN	0.00	[]	0.00	0	Yes	32.85
S45L2	80	60	35.17	27.70	726.36	0.75	215.85	0.87	Yes	AN	41.48	0.87	3.65	208.9	Yes	35.8
S45L3	80	15	32.98	25.78	679.39	0.80	223.88	0.71	Yes	AN	24.58	0.70	2.66	152.3	Yes	32.42
S46L1	60	15	31.87	25.73	642.44	0.78	261.12	0.50	No	AN	0.00	[]	0.00	0	No	36.3
S46L2	60	60	34.39	28.57	770.45	0.78	308.35	0.49	Yes	AN	40.50	0.48	3.22	184.5	No	38.33